

NASA
Technical
Paper
3310

May 1993

HZEFRG1:
An Energy-Dependent
Semiempirical Nuclear
Fragmentation Model

Lawrence W. Townsend,
John W. Wilson,
Ram K. Tripathi,
John W. Norbury,
Francis F. Badavi,
and Ferdous Khan

NASA
Technical
Paper
3310

1993

HZEFRG1:
An Energy-Dependent
Semiempirical Nuclear
Fragmentation Model

Lawrence W. Townsend
and John W. Wilson
Langley Research Center
Hampton, Virginia

Ram K. Tripathi
ViGYAN, Inc.
Hampton, Virginia

John W. Norbury
Rider College
Lawrenceville, New Jersey

Francis F. Badavi
Christopher Newport University
Newport News, Virginia

Ferdous Khan
Old Dominion University
Norfolk, Virginia

Symbols

A	nuclear mass number
b	impact parameter, fm
e	electric charge, C
F	fraction of nuclear volume sheared off by collision, given by equations (5), (11), (13), and (16)
m_0	nucleon rest mass, $939 \text{ MeV}/c^2$
N_i	number of particles of type i
P	parameter in equation (17) given by equations (4), (10), (12), and (15)
v	velocity, m/sec
Z	nuclear charge number
α	electromagnetic fine structure constant
ΔA	total number of abraded and ablated nucleons
Δ_{abr}	number of abraded nucleons
Δ_{abl}	number of ablated nucleons

Subscripts:

em	electromagnetic
F	fragment
n	neutron
P	projectile
p	proton
T	target
α	alpha particle

Abstract

Methods for calculating cross sections for the breakup of high-energy heavy ions by the combined nuclear and coulomb fields of the interacting nuclei are presented. The nuclear breakup contributions are estimated with an abrasion-ablation model of heavy ion fragmentation that includes an energy-dependent, mean free path. The electromagnetic dissociation contributions arising from the interacting coulomb fields are estimated by using Weizsäcker-Williams theory extended to include electric dipole and electric quadrupole contributions. The complete computer code (HZEFRG1) that implements the model is included as an appendix. Extensive comparisons of cross section predictions with available experimental data are made.

1. Introduction

As the era of human exploration of the solar system approaches, concern is mounting over assessing the risk to astronauts from galactic cosmic rays and adequate protection from their deleterious effects (refs. 1 through 8). To properly assess these biological risks, the particle fluence spectra at the organs of interest (e.g., ocular lens or bone marrow) must be known. These fluence spectra are estimated using charged particle transport codes that contain descriptions of all significant physical interactions that occur as the radiation fields propagate through bulk matter (ref. 6). Fragmentation cross section data bases are a major input into these transport codes and a significant source of uncertainty in the predicted output fluences (ref. 9). At present, there is neither an adequate experimental fragmentation cross section data base nor an adequate theory of nuclear fragmentation. Extrapolations to heavy targets (ref. 10) based on the model of Rudstam for hydrogen targets (ref. 11) are not adequate to define the necessary cross sections (ref. 12). In previous work (refs. 13 and 14), an energy-independent semiempirical model of high-energy, heavy ion fragmentation based upon a two-step abrasion-ablation formalism was presented. The abrasion step described removal of nucleons by direct knockout in the overlap region of the colliding nuclei. The abrasions were treated on a geometric basis and uniform, spherical nuclear density distributions were assumed. An impact-parameter-dependent average transmission factor was used for the projectile and target nuclei to account for the finite mean free path of nucleons in nuclear matter. The ablation step, as implemented by Bowman et al. (ref. 15), was treated as a single-nucleon emission for every 10 MeV of excitation energy. Fragmentation contributions

from electromagnetic dissociation (EMD) processes were limited to single-nucleon removal by electric dipole interactions (ref. 14) by using the Weizsäcker-Williams method of virtual quanta (refs. 16 and 17). Except for the EMD contributions to one-nucleon removal, the model was independent of the incident kinetic energy of the projectile nucleus.

In the present work, an energy-dependent semiempirical fragmentation model incorporating major improvements is reported. These improvements include (1) incorporating an explicit dependence on incident projectile kinetic energy through the use of an energy-dependent mean free path in the abrasion step, (2) replacing the simple parameterization for nuclear radii by their actual values obtained from electron scattering data, (3) extending the EMD model to include electric quadrupole contributions to one-nucleon removal cross sections, and (4) modifying the computational algorithm to use an interpolation rather than an iterative procedure in the abrasion step of the calculation. This last modification increases computational speed by more than a factor of 10 over the energy-independent model of reference 13.

Because the original energy-independent model has been replaced by the present model, this report will describe the current semiempirical model and its associated computer code. We begin by describing the semiempirical model in detail. This is followed by a description of the computer program. Then, extensive comparisons of the model with available high-energy, heavy ion fragmentation data are made. Some limitations on the use of the model are then discussed. Two appendices are included: (1) appendix A lists the computer code and (2) appendix B gives a sample input/output file. Note that

the abrasion-ablation methods apply only to nucleus-nucleus collisions. For projectiles fragmenting on hydrogen (proton) targets, the model of Rudstam (ref. 11) is used.

2. Theory

In the abrasion-ablation fragmentation model, the projectile nuclei, moving at relativistic speeds, collide with stationary target nuclei. In the abrasion step, those portions of the nuclear volumes that overlap are sheared away by the collision. The remaining projectile piece, called a prefragment or primary residue, continues its trajectory with essentially its pre-collision velocity. As a result of the dynamics of the abrasion process, the prefragment is highly excited and subsequently decays by the emission of gamma radiation and/or nuclear particles. This step is the ablation stage. The resultant isotope, sometimes referred to as a secondary product, is the nuclear fragment whose cross section is measured. The abrasion process can be analyzed with classical geometric arguments (refs. 15 and 18) or methods obtained from formal quantum scattering theory (refs. 19 and 20). The ablation stage can be analyzed from geometric arguments (ref. 15) or more sophisticated methods based upon Monte Carlo or intranuclear cascade techniques (refs. 18, 20, 21, and 22). Fragmentation cross sections can also be predicted with the approximate semiempirical parameterization formulas of Silberberg et al. (ref. 10).

2.1. Abrasion Description

The amount of nuclear material stripped away in the collision of two nuclei is taken as the volume of the overlap region times an average attenuation factor. The relevant formula for the number of abraded nucleons in the overlap volume (Δ_{abr}) for a projectile of mass A_P and radius R_P is given by the following formula:

$$\Delta_{\text{abr}} = F A_P \left[1 - \frac{1}{2} \exp\left(\frac{-C_P}{\lambda}\right) - \frac{1}{2} \exp\left(\frac{-C_T}{\lambda}\right) \right] \quad (1)$$

where C_P and C_T are the maximum chord lengths of the intersecting surface in the projectile and in the target (of radius R_T), respectively, and the expressions for F differ depending on the nature of the collision (peripheral versus central) and the relative sizes of the colliding nuclei. The energy-dependent mean free path λ in equation (1) is given in terms of the beam energy E (in MeV/nucleon) by

$$\lambda = \frac{16.6}{E^{0.26}} \quad (2)$$

which is an accurate parameterization of the phenomenological mean free paths obtained from experimental cross section measurements (ref. 23). In general, phenomenological values of λ are larger than the microscopic values estimated from

$$\lambda_{\text{micro}} = (\rho \sigma_{NN})^{-1} \quad (3)$$

where ρ is the nuclear number density and σ_{NN} is the free nucleon-nucleon cross section. It is interesting to note that the mean free path values estimated from equation (2) are nearly identical to those derived from nonlocal, optical-model calculations (ref. 24). Other differences may arise if nucleus-nucleus mean free paths are considered in future work.

For $R_T > R_P$, we have (ref. 18)

$$P = 0.125 (\mu \nu)^{1/2} \left(\frac{1}{\mu} - 2 \right) \left(\frac{1 - \beta}{\nu} \right)^2 - 0.125 \left[0.5 (\mu \nu)^{1/2} \left(\frac{1}{\mu} - 2 \right) + 1 \right] \left(\frac{1 - \beta}{\nu} \right)^3 \quad (4)$$

and

$$F = 0.75 (1 - \nu)^{1/2} \left(\frac{1 - \beta}{\nu} \right)^2 - 0.125 \left[3 (1 - \nu)^{1/2} - 1 \right] \left(\frac{1 - \beta}{\nu} \right)^3 \quad (5)$$

with

$$\nu = \frac{R_P}{R_P + R_T} \quad (6)$$

$$\beta = \frac{b}{R_P + R_T} \quad (7)$$

and

$$\mu = \frac{1}{\nu} - 1 = \frac{R_T}{R_P} \quad (8)$$

Equations (4) and (5) are valid when the collision is peripheral (i.e., the two nuclear volumes do not completely overlap). In this case, the impact parameter b is restricted such that

$$R_T - R_P \leq b \leq R_T + R_P \quad (9)$$

If the collision is central, then the projectile nucleus volume completely overlaps the target nucleus volume ($b < R_T - R_P$), and all the projectile nucleons are abraded. In this case, equations (4) and (5) are replaced by

$$P = -1 \quad (10)$$

and

$$F = 1 \quad (11)$$

and there is no ablation of the projectile, since it was destroyed by the abrasion.

For the case where $R_P > R_T$ and the collision is peripheral, equations (4) and (5) are replaced by (ref. 21)

$$P = 0.125(\mu\nu)^{1/2} \left(\frac{1}{\mu} - 2 \right) \left(\frac{1-\beta}{\nu} \right)^2 - 0.125 \left\{ 0.5 \left(\frac{\nu}{\mu} \right)^{1/2} \left(\frac{1}{\mu} - 2 \right) - \frac{\left[(1/\nu)(1-\mu^2)^{1/2} - 1 \right] [(2-\mu)\mu]^{1/2}}{\mu^3} \right\} \left(\frac{1-\beta}{\nu} \right)^3 \quad (12)$$

and

$$F = 0.75(1-\nu)^{1/2} \left(\frac{1-\beta}{\nu} \right)^2 - 0.125 \left\{ \frac{3(1-\nu)^{1/2}}{\mu} - \frac{\left[1 - (1-\mu^2)^{3/2} \right] \left[1 - (1-\mu)^2 \right]^{1/2}}{\mu^3} \right\} \left(\frac{1-\beta}{\nu} \right)^3 \quad (13)$$

where the impact parameter is restricted such that

$$R_P - R_T \leq b \leq R_P + R_T \quad (14)$$

For a central collision ($b < R_P - R_T$) with $R_P > R_T$, equations (12) and (13) are replaced by

$$P = \left[\frac{1}{\nu} (1-\mu^2)^{1/2} - 1 \right] \left[1 - \left(\frac{\beta}{\nu} \right)^2 \right]^{1/2} \quad (15)$$

and

$$F = \left[1 - (1-\mu^2)^{3/2} \right] \left[1 - \left(\frac{\beta}{\nu} \right)^2 \right]^{1/2} \quad (16)$$

2.2. Surface Distortion Excitation Energy

The surface distortion excitation energy of the projectile prefragment following the abrasion of m nucleons is calculated from the clean-cut abrasion formalism of references 15 and 18. For this model, the colliding nuclei are assumed to be uniform spheres of radii R_i ($i = P, T$). In the collision, the overlapping volumes shear off so that the resultant projectile prefragment is a sphere with a cylindrical hole gouged out of it. The excitation energy is then determined by calculating the difference in surface area between the misshapen sphere and a perfect

sphere of equal volume. This excess surface area ΔS is given by (ref. 18) as

$$\Delta S = 4\pi R_P^2 \left[1 + P - (1 - F)^{2/3} \right] \quad (17)$$

where the expressions for P and F , given in the previous section, differ depending upon the nature of the collision (peripheral versus central) and the relative sizes of the colliding nuclei.

The excitation energy E_s associated with surface energy is well-known to be 0.95 MeV/fm² for near equilibrium nuclei so that

$$E'_s = 0.95\Delta S \quad (18)$$

for small surface distortions. When large numbers of nucleons are removed in the abrasion process, equation (18) is expected to underestimate the actual excitation. We therefore introduce an excess excitation factor in terms of the number of abraded nucleons Δ_{abr} as

$$f = 1 + \frac{5\Delta_{\text{abr}}}{A_P} + \frac{25\Delta_{\text{abr}}^2}{A_P^2} \quad (19a)$$

when $R_T < R_P$ and $b < (R_P - R_T)$ and

$$f = 1 + \frac{5\Delta_{\text{abr}}}{A_P} \quad (19b)$$

otherwise. Note that f approaches 1 when Δ_{abr} is small but increases the excess excitation when large portions of the nucleus are removed in the collisions and when grossly misshapened nuclei are formed. The total excitation energy is then

$$E_s = E'_s f \quad (20)$$

which reduces to equation (18) for small Δ_{abr} . It is further assumed that all mass 5 fragments are unbound, that 90 percent of the mass 8 fragments are unbound, and that 50 percent of mass 9 fragments (⁹B) are unbound.

2.3. Excitation Energy Transfer

A secondary contribution to the excitation energy is the transfer of the kinetic energy of relative motion across the intersecting boundary of the two ions. The rate of energy loss of a nucleon passing through nuclear matter is taken as 13 MeV/fm, and it is assumed that the energy is symmetrically deposited about the azimuth so that 6.5 MeV/fm/nucleon at the interface is the average rate of transfer of kinetic energy into excitation energy. This energy is transferred in single-particle collision processes; in half of

the events, the energy is transferred to the excitation energy of the projectile, and the remaining half of the events leaves the projectile excitation energy unchanged. The first estimate of this contribution is the length of the longest chord C_l in the projectile surface interface. This chord length is the maximum distance traveled by any target constituent through the projectile interior. The number of other target constituents in the interface region may be found by estimating the maximum chord C_t transverse to the projectile velocity that spans the projectile surface interface. The total excitation energy from excess surface area and spectator interactions is then

$$E'_x = 13C_l + \frac{13}{3}C_l(C_t - 1.5) \quad (21)$$

where the second term only contributes if $C_t > 1.5$ fm. We have further assumed the effective longitudinal chord length for these remaining nucleons is one-third the maximum chord length.

2.4. Nuclear Ablation

The decay of highly excited nuclear states is dominated by particle emission. In the present model, we assume a nucleon is removed for every 10 MeV of excitation energy as

$$\Delta_{\text{abl}} = \frac{E_s + E_x}{10 \text{ MeV}} \quad (22)$$

In accordance with the previously discussed directionality of the energy transfer, E_x is double valued as

$$E_x = \begin{cases} E'_x & \left(P_x = \frac{1}{2} \right) \\ 0 & \left(P_x = \frac{1}{2} \right) \end{cases} \quad (23)$$

where P_x is the corresponding probability of occurrence of each value in collisions.

2.5. Nuclear Abrasion-Ablation

The total number of nucleons removed through the abrasion-ablation process is given as a function of impact parameter as

$$\Delta A = \Delta_{\text{abr}}(b) + \Delta_{\text{abl}}(b) \quad (24)$$

The nuclear fragmentation parameters herein are approximated according to the abrasion-ablation model of Bowman, Swiatecki, and Tsang (ref. 15). The cross section for removal of ΔA nucleons is estimated as

$$\sigma(\Delta A) = \pi b_2^2 - \pi b_1^2 \quad (25)$$

where b_2 is the impact parameter for which the volume of interaction of the projectile contains Δ_{abr} nucleons, and the resulting excitation energies release an additional Δ_{abl} nucleons such that

$$\Delta_{\text{abr}}(b_2) + \Delta_{\text{abl}}(b_2) = \Delta A - \frac{1}{2} \quad (26)$$

and similarly for b_1

$$\Delta_{\text{abr}}(b_1) + \Delta_{\text{abl}}(b_1) = \Delta A + \frac{1}{2} \quad (27)$$

The charge distributions of the final projectile fragments are strongly affected by nuclear stability. We expect that the Rudstam (ref. 11) charge distribution for a given $\sigma(\Delta A)$ to be reasonable such that

$$\sigma(A_F, Z_F) = F_1 \exp[-R|Z_F - SA_F + TA_F^2|^{3/2}] \sigma(\Delta A) \quad (28)$$

where $R = 11.8A_F^{-0.45}$, $S = 0.486$, $T = 3.8 \times 10^{-4}$ according to Rudstam, and F_1 is a normalizing factor such that

$$\sum_{Z_F} \sigma(A_F, Z_F) = \sigma(\Delta A) \quad (29)$$

The Rudstam formula for $\sigma(\Delta A)$ was not used because his ΔA dependence is too simple and breaks down for heavy targets (ref. 13).

The charge of the removed nucleons ΔZ is calculated according to charge conservation

$$Z_P = Z_F + \Delta Z \quad (30)$$

and is divided among the nucleons and alpha particles according to the following rules. The abraded nucleons are those removed from that portion of the projectile in the overlap region with the target. Therefore, the abraded nucleon charge is assumed to be proportional to the charged fraction of the projectile nucleus as

$$Z_{\text{abr}} = \frac{Z_P \Delta_{\text{abr}}}{A_P} \quad (31)$$

The charge release in the ablation is then given as

$$Z_{\text{abl}} = \Delta Z - Z_{\text{abr}} \quad (32)$$

which simply conserves the remaining charge.

It is well-known that the alpha particle is unusually tightly bound in comparison with other nucleon arrangements. Because of this unusually tight binding of the alpha particle, helium production is maximized in the ablation process

$$N_\alpha = \text{Int}(Z_{\text{abl}}/2) \quad (33)$$

where $\text{Int}(x)$ denotes the integer part of x . The number of protons produced is given by charge conservation as

$$N_p = \Delta Z - 2N_\alpha \quad (34)$$

Similarly, mass conservation requires the number of neutrons produced to be

$$N_n = \Delta A - N_p - 4N_\alpha \quad (35)$$

The mass 2 and 3 fragments are currently ignored.

The calculation is performed for $\Delta A = 1$ to $\Delta A = A_P - 1$, where the cross section associated with $\Delta A > A_P - 0.5$ is missed. These are, of course, the central collisions, for which it is assumed that the projectile disintegrates into single nucleons if $R_P < R_T$ as

$$N_p = Z_P \quad (36)$$

$$N_n = A_P - Z_P \quad (37)$$

and is ignored otherwise. Energetic target fragments and mesonic components are currently ignored.

Only the nuclear radii to be used in the model are yet to be defined. We compute the nuclear absorption cross section in millibarns using

$$\sigma(A_1, A_2) = 10\pi(R_1 + R_2 - 0.504)^2 \quad (38)$$

where the nuclear radii R_i ($i = 1, 2$) in units of fm are given by

$$R = 1.29R_{\text{rms}} \quad (39)$$

with the root-mean-square radius R_{rms} obtained directly from experiment (ref. 25) for $A_i \leq 26$. For $A_i > 26$, the experimental values are accurately parameterized by

$$R_{\text{rms}} = 0.84A_i^{1/3} + 0.55 \quad (40)$$

2.6. Electromagnetic Dissociation Cross Section

In electromagnetic dissociation (EMD) the virtual photon field of the target nucleus interacts electromagnetically with constituents of the projectile to cause excitation and eventual breakup. The electromagnetic theory has been extensively described elsewhere (refs. 26–29) and will only be briefly discussed here. We also limit the model to consideration of single-nucleon (proton or neutron) removal processes.

M multinucleon removal contributions will be incorporated when an adequate theory is developed for estimating their contributions to the fragmentation cross sections.

The total electromagnetic (EM) cross section for one-nucleon removal resulting from electric dipole (E1) and electric quadrupole (E2) interactions is written

$$\begin{aligned} \sigma_{\text{em}} &= \sigma_{E1} + \sigma_{E2} \\ &= \int [N_{E1}(E)\sigma_{E1}(E) + N_{E2}(E)\sigma_{E2}(E)]dE \end{aligned} \quad (41)$$

where the virtual photon spectra (of energy E) produced by the target nucleus are given by (ref. 26)

$$N_{E1}(E) = \frac{1}{E}\frac{2}{\pi}Z^2\alpha\frac{1}{\beta^2}\left[\xi K_0K_1 - \frac{1}{2}\xi^2\beta^2(K_1^2 - K_0^2)\right] \quad (42)$$

for the dipole field and by

$$\begin{aligned} N_{E2}(E) &= \frac{1}{E}\frac{2}{\pi}Z^2\alpha\frac{1}{\beta^4}\left[2(1 - \beta^2)K_1^2 \right. \\ &\quad \left. + \xi(2 - \beta^2)^2K_0K_1 - \frac{1}{2}\xi^2\beta^4(K_1^2 - K_0^2)\right] \end{aligned} \quad (43)$$

for the quadrupole field. The terms $\sigma_{E1}(E)$ and $\sigma_{E2}(E)$ are the corresponding photonuclear reaction cross sections for the fragmenting projectile nucleus. The terms K_0 and K_1 in the expressions for N_{E1} and N_{E2} are modified Bessel functions of the second kind and are also functions of the parameter ξ . The latter is given by

$$\xi = \frac{2\pi Eb_{\min}}{\gamma\beta hc} \quad (44)$$

where E is the virtual photon energy, b_{\min} is the minimum impact parameter below which the collision dynamics are dominated by nuclear interactions (rather than EM interactions), β is the speed of the target (measured from the projectile rest frame) as a fraction of the speed of light c , h is Planck's constant, and γ is the usual Lorentz factor from special relativity $\gamma = (1 - \beta^2)^{-1/2}$. The minimum impact parameter is given by

$$b_{\min} = (1 + x_d)b_c + \frac{\pi a_0}{2\gamma} \quad (45)$$

where $x_d = 0.25$ and

$$a_0 = \frac{Z_P Z_T e^2}{m_0 v^2} \quad (46)$$

allows for deviation of the trajectory from a straight line (ref. 30). The critical impact parameter for

single-nucleon removal is

$$b_c = 1.34 \text{ fm} \left[A_P^{1/3} + A_T^{1/3} - 0.75 \left(A_P^{-1/3} + A_T^{-1/3} \right) \right] \quad (47)$$

with A_P and A_T being the projectile and target nucleon numbers, respectively.

The photonuclear cross sections $\sigma_{E1}(E)$ and $\sigma_{E2}(E)$ are Lorentzian shaped and somewhat sharply peaked in energy. Therefore, they can be taken outside the integral of equation (41) to yield an approximate form given by (ref. 26)

$$\begin{aligned} \sigma_{\text{em}} \approx & N_{E1}(E_{\text{GDR}}) \int \sigma_{E1}(E) dE \\ & + N_{E2}(E_{\text{GQR}}) E_{\text{GQR}}^2 \int \sigma_{E2}(E) \frac{dE}{E^2} \end{aligned} \quad (48)$$

where E_{GDR} and E_{GQR} are the energies at the peaks of the $E1$ and $E2$ photonuclear cross sections. These integrals of the photonuclear cross sections over energy are evaluated with the following sum rules (ref. 26):

$$\int \sigma_{E1}(E) dE = 60 \frac{NZ}{A} \text{ MeV mb} \quad (49)$$

and

$$\int \sigma_{E2}(E) \frac{dE}{E^2} = 0.22 f Z A^{2/3} \frac{\mu b}{\text{MeV}} \quad (50)$$

In equations (49) and (50), N is the number of neutrons, Z is the number of protons, and A is the mass number of the projectile nucleus. The fractional exhaustion of the energy-weighted sum rule in equation (50) is (ref. 31)

$$f = \begin{cases} 0.9 & (A > 100) \\ 0.6 & (40 < A \leq 100) \\ 0.3 & (40 \leq A) \end{cases} \quad (51)$$

Note that equation (50) is the sum rule for the isoscalar $E2$ giant resonance. The isovector $E2$ resonance is not used, because it decays mainly by two-nucleon emission (ref. 26), which is not considered here.

In equation (48) E_{GDR} and E_{GQR} are the energies at the peaks of the $E1$ and $E2$ photonuclear cross sections. For the dipole term it is (ref. 31)

$$E_{\text{GDR}} = \frac{hc}{2\pi} \left[\frac{m^* c^2 R_0^2}{8J} \left(1 + u - \frac{1 + \varepsilon + 3u}{1 + \varepsilon + u} \varepsilon \right) \right]^{-1/2} \quad (52)$$

with

$$u = \frac{3J}{Q'} A^{-1/3} \quad (53)$$

and

$$R_0 = r_0 A^{1/3} \quad (54)$$

where $\varepsilon = 0.0768$, $Q' = 17 \text{ MeV}$, $J = 36.8 \text{ MeV}$, $r_0 = 1.18 \text{ fm}$, and m^* is $7/10$ of the nucleon mass. For the quadrupole term, it is simply given by

$$E_{\text{GQR}} = \frac{63}{A^{1/3}} \text{ MeV} \quad (55)$$

Finally, the single-proton or single-neutron removal cross sections are obtained from σ_{em} (eq. (48)) using proton and neutron branching ratios g_i ($i = p, n$) as

$$\sigma(i) = g_i \sigma_{\text{em}} \quad (i = p \text{ or } n) \quad (56)$$

The proton branching ratio has been parameterized by Westfall et al. (ref. 31) as

$$g_p = \min \left[\frac{Z}{A}, 1.95 \exp(-0.075Z) \right] \quad (57)$$

where Z is the number of protons, and the minimum value of the two quantities in square brackets is to be taken. This parameterization is satisfactory for heavier nuclei ($Z > 14$). For light nuclei, however, the following branching ratios are used instead:

$$g_p = \begin{cases} 0.5 & (Z < 6) \\ 0.6 & (6 \leq Z \leq 8) \\ 0.7 & (8 < Z < 14) \end{cases} \quad (58)$$

For neutrons, the branching ratio is given by

$$g_n = 1 - g_p \quad (59)$$

3. Program Description

The model described in section 2 has been programmed in the FORTRAN language. The complete package is fully commented. The main module and each function subprogram or subroutine begins with a brief description of what it is supposed to do. The program is approximately 1320 lines long and is written in FORTRAN 77. It was initially developed on the CDC® CYBER 750 mainframe under the NOS 2.3 level 617 operating system and requires a minimum of 12400_8 60-bit words of storage. The current version operates on a VAX-11/785 minicomputer using the VAX/VMS V5.3 operating system. The program size is approximately 32 kilowords. The VAX version also operates on personal computers with FORTRAN compilers.

The package is broken up into a main program (HZEFRAG), 7 function subprograms (FRAG, SNF, CROS, TEXP, TSQR, RADIUS, and XSEC) and 13 subroutines (YIELDEM, ASIGM, YIELDX, YIELDN, YIELDA, YELDT, YIELDH, GEODA, BSEARCH, LIMIT, GEOFR, BESSEL, and SORT). The main program (HZEFRAG) contains all the required inputs and outputs. The package is very fast and efficient. A complete calculation for a typical projectile-target combination usually takes less than a minute on the VAX. Appendix A gives a complete code listing. Appendix B lists a sample case.

3.1. Main Program HZEFRAG

HZEFRAG contains the one- and two-dimensional arrays that are used for storing and sorting the interactive inputs and outputs. The inputs are the projectile energy in MeV/nucleon and the masses and charges of the projectile and the target.

With proper inputs, HZEFRAG first calculates the electromagnetic dissociation cross sections and then begins the calculation for nuclear fragmentation by searching through a specific number of isotopes for any given charge number. Upon the completion of nuclear fragmentation calculations, HZEFRAG sorts through fragmentation results and writes the sorted output to TAPE7, in descending order, based on the charge number of the fragmented nucleus.

3.2. Function Subprogram FRAG

FRAG calculates the nuclear fragmentation probabilities for the range of charge numbers from $Z = Z_P$ to $Z = 1$, based on the methods of sections 2.1–2.5. It is the main module for all the subroutines and function subprograms except YIELDEM, BESSEL, and SORT. The inputs to FRAG are the projectile and target mass and charge numbers, arrays that store charge and corresponding isotopic mass numbers for a given charge number, and the incident energy of the projectile. The output is the nuclear fragmentation cross section probabilities. FRAG calls YIELDX, YIELDH, and ASIGM.

3.3. Function Subprogram SNF

SNF uses a nonlinear polynomial to relate mass and charge number on the nuclear stability curve. Input is the mass number for a given isotope. The output is the corresponding charge number.

3.4. Function Subprogram CROS

CROS calculates the Rudstam five-parameter formula (ref. 11), which describes the cross sections for

production of fragments from protons being bombarded by heavy ions. Inputs are the mass and charge numbers of the projectile and target, and the energy of the projectile in MeV/nucleon. The outputs are the cross section values for a hydrogen target.

3.5. Function Subprogram TEXP

The only purpose of TEXP is to calculate $\text{EXP}(x)$ for a given x . Since different computers have different domains for exponential calculations, TEXP was added to avoid possible CPU overflow and underflow warnings. The input is the argument of the exponential x . The output depends on the value of the argument x . If x is in the domain $-100 \leq x \leq 100$, $\text{TEXP}(x)$ is set equal to $\text{EXP}(x)$; otherwise x is set equal to the lower or upper value of the domain as appropriate.

3.6. Function Subprogram TSQR

TSQR calculates $\text{SQR}(y)$ for a given y while avoiding potential CPU overflow or underflow conditions for different computers. The input is the number y whose square root is to be calculated. The output is the positive value of the square root of y . If y is in the domain $1 \times 10^{-37} \leq y \leq 1 \times 10^{37}$, $\text{TSQR}(y)$ is set equal to $\text{SQR}(y)$, otherwise y is set equal to the upper or lower value of the domain as appropriate.

3.7. Function Subprogram RADIUS

RADIUS gives the radius of a nucleus of mass number A according to the methods detailed in section 2.5. The input is the mass number A of the nucleus whose radius is desired. The output is its radius in fm.

3.8. Function Subprogram XSEC

XSEC calculates microscopic total absorption cross sections in mb for any nucleus-nucleus or nucleon-nucleus collision. The nucleus-nucleus cross section is obtained from equation (38). The nucleon-nucleus cross section is from the parameterization of reference 32. The inputs are the masses of the colliding nuclei and the incident particle energy in MeV/nucleon. The output is the cross section.

3.9. Subroutine YIELDEM

YIELDEM calculates the EMD cross sections based on the methods in section 2.6. The inputs are the charge and mass numbers of the projectile and target and the kinetic energy of the projectile in MeV/nucleon. The outputs are the EMD cross sections for one-proton and one-neutron removal.

3.10. Subroutine ASIGM

ASIGM generates macroscopic ion-target cross sections in units of cm^{-1} for arbitrary ions with energies in MeV/nucleon. This subroutine multiplies the microscopic cross section from XSEC by the target number density to obtain the macroscopic cross section. Inputs are the energy, mass, and charge of the incident particle and two one-dimensional arrays that contain the target material constituent charges and number densities. The output is the macroscopic cross section.

3.11. Subroutine YIELDX

YIELDX is the main module for all the YIELD routines and decides which routine should be accessed by checking the mass number of the fragment A_F . For $A_F = 1$, YIELDN is called; for $A_F = 2$ or 3, YIELDT is called; for $A_F = 4$, YIELDA is called; and for $A_F > 4$, CROS is called. Inputs are the projectile and fragment charge and mass number and the energy of the projectile in MeV/nucleon. The output is the fragmentation cross section.

3.12. Subroutines YIELDN, YIELDA, YIELDT

YIELDN, YIELDA, and YIELDT are based on Bertini's method for proton, alpha, and mass 2 or mass 3 fragment production, with $A_F = 1$, $A_F = 4$, and $A_F = 2$ or 3 (ref. 33). Inputs to all three modules are the projectile and fragment charge and mass numbers and the energy of projectile in MeV/nucleon. The outputs are the fragmentation cross sections for $A_F = 1$, $A_F = 4$, and $A_F = 2$ or 3.

3.13. Subroutine YIELDH

YIELDH calculates fragmentation cross sections for a specific fragment. For a given fragment, it calls subroutine LIMIT to calculate the isotopic mass number above and below a given fragment charge number, and routine GEOFR and GEODA to calculate the normalization factor for Rudstam's charge distribution formula in section 2.5. Inputs are the projectile and fragment charge and mass numbers, and the target mass number. The output is the fragmentation cross section.

3.14. Subroutine GEODA

GEODA calculates the abrasion-ablation cross sections with and without final state interactions. It calls subroutine BSEACH and entry BSEEK to evaluate equations (4)–(16) in section 2.1. The inputs are the mass numbers of the projectile and the target. The output is abrasion-ablation and absorption cross sections.

3.15. Subroutine BSEARCH

BSEARCH uses the geometrical description of section 2.1 to find abrasion-ablation cross sections. Inputs are the projectile and fragment mass numbers, and projectile and target nuclear radii. The outputs are impact parameters and abrasion-ablation cross sections.

3.16. Subroutine LIMIT

LIMIT calculates the upper and lower limits of fragment mass numbers for a given fragment charge number. Inputs are fragment mass and charge numbers. Outputs are the integer values of the upper and lower limits for fragment mass numbers.

3.17. Subroutine GEOFR

GEOFR calculates the normalization factor for the Rudstam charge distribution formula, equation (28) in section 2.5. Inputs are the charge and mass numbers of the projectile and fragment, the mass of the target, and the upper and lower integer limits from subroutine LIMIT. The output is the normalization constant F_1 in equation (28).

3.18. Subroutine BESSEL

BESSEL evaluates $K_0(x)$ and $K_1(x)$, namely the modified Bessel function of the second kind. This calculation is carried out in subroutine BESSEL by using the polynomial approximations of reference 34, which are reliable for calculating the spectrum of any frequency. The input is the argument x . The outputs are values of $K_0(x)$ and $K_1(x)$.

3.19. Subroutine SORT

SORT contains the one- and two-dimensional arrays used for sorting the final cross sections in descending order based on the charge number of the fragments. The inputs are the unsorted two-dimensional arrays, which contain the mass and charge numbers of the nuclear and electromagnetic cross sections of the fragments. The outputs are the one-dimensional arrays, which contain the sorted fragments by charge number and corresponding mass number and fragmentation cross section. The final printout of the sorted result is carried out in the main module HZEFrag.

4. Comparisons With Experimental Data

To illustrate the predictive accuracy of the present model, we present comparisons with a representative sample of experimental cross section measurements.

Since cosmic ray nuclei heavier than iron make negligible contributions to astronaut exposures because of their scarcity, comparisons will be limited to fragmentation data for iron and lighter nuclei. In the earlier energy-independent model (ref. 13), comparisons between theory and experiment were limited to elemental production cross sections. In this report, we extend the scope of these comparisons to include isotope production cross sections from argon and oxygen projectile fragmentations.

The first comparisons are with recently published experimental results for iron nuclei at 1.57 GeV/nucleon (ref. 35). The elemental production cross sections for iron beams fragmenting in carbon, aluminum, copper, and lead targets are displayed in figures 1 through 4. Typically, the theoretical predictions overestimate the experimental data by approximately 20 percent.

Figures 5 through 11 show predictions from this model in comparison with experimental elemental production cross sections for iron beams at 1.88 GeV/nucleon fragmenting in carbon, sulphur, copper, silver, tantalum, lead, and uranium targets (ref. 31). Generally, the theoretical predictions appear to be in good agreement with the experimental measurements.

Recently, Tull measured elemental and isotopic production cross sections for 1.65 GeV/nucleon argon beams fragmenting in carbon and potassium chloride targets (ref. 36). Figure 12 displays theoretical elemental production cross sections and Tull's measurements for a carbon target. Measurement uncertainties are indicated by the vertical lines in figures 12 through 38. The theoretical predictions typically agree to within 25 percent of the experimental measurements, with many elements agreeing within 5 to 10 percent. The individual isotope production cross sections for each element are displayed in figures 13 through 25. From figure 13, it is apparent that the theoretical underestimate of chlorine ($Z = 17$) displayed in figure 12 mainly results from discrepancies for the ^{35}Cl and ^{39}Cl isotopes. Figure 14 indicates that the sulphur ($Z = 16$) underestimate displayed in figure 12 is the result of an overall underestimating of the data by the model. In general, however, these elemental and isotopic cross section predictions are in good agreement with the data. Figures 26 through 39 display the fragmentation cross section predictions for Ar on Ar collisions compared with Tull's Ar on KCl measurements. Using Ar as a target in our calculations, rather than KCl, results in a difference of less than 1 percent in any of the cross section predictions. The elemental production cross sections displayed in figure 26 show

good agreement between theory and experiment except for sulphur ($Z = 16$) and chlorine ($Z = 17$). Comparing figure 26 with figure 12 for the carbon target suggests that the trend in the KCl (fig. 26) experimental results appears to be inconsistent. Further confirmation of this data trend inconsistency is given by the iron beam results in figures 1 through 11. Figure 27 clearly shows that the apparent theoretical overestimate for the total chlorine cross section results mainly from the significant overestimate of the ^{36}Cl datum by the calculation. Comparing the ^{36}Cl datum of figure 27 with the same datum for the carbon target (fig. 13) suggests that this experimental measurement for the KCl target is probably in error. Overall, the predictions and measurements are in good agreement. Typical cross section differences are again within approximately 25 percent.

Finally, tables I and II display results for carbon and oxygen projectiles compared with the early measurements of Lindstrom et al. (ref. 37). Displayed are isotope production cross sections for 2.1 GeV/nucleon oxygen and 1.05 GeV/nucleon carbon beams fragmenting in various targets. The overall agreement is generally within 50 percent.

5. Limitations and Future Work

Although the model described herein is reasonably accurate and computationally fast, it does have limitations. Some of these include

1. The Rudstam charge dispersion formula (eq. (28)) is mainly applicable to nuclei with mass numbers less than 75 (ref. 11). Caution should be exercised if cross sections for heavier nuclei are desired. Future work should include investigating alternative dispersion formulations based upon experimental studies of heavy nuclei (e.g., ref. 38).
2. The neglect of fission processes also limits the validity of the model for nuclei heavier than Fe ($A = 56$). Prospective fission models are currently under investigation for future use in the code.
3. The treatment of light ion production is simplified, and mass 2 and 3 fragments are neglected. A comprehensive data base for alpha particle breakup is under development (ref. 39) and will eventually be incorporated into the current fragmentation model.
4. Although the single-nucleon removal cross sections for nuclei with $A \leq 56$ are well represented by the current model, there is a tendency for these cross sections to be *significantly* underestimated for heavy systems ($A > 100$). Since the EMD

cross section contributions are well described by the current formalism, the problem must result from the estimates of the hadronic cross section contribution. Recently, an accurate parameterization for the hadronic contributions to one-nucleon removal cross sections has been developed (refs. 40 and 41). Although it significantly improves the agreement between theory and experiment for systems of heavier mass, it yields mixed results when applied to the $A \leq 56$ nuclei considered in this work and has not yet been incorporated. Future work should focus on resolving these apparent discrepancies.

Overall, the current model generally agrees with experimental data to the extent that these data agree among themselves. Except for the above-mentioned improvements to the model for the breakup for heavy nuclei and production of light ions, future improvements will require additional, high-quality cross section data.

6. Concluding Remarks

An energy-dependent semiempirical fragmentation model for nucleus-nucleus collisions has been presented and its computer program described in some detail. Comparisons of cross section predictions with representative samples of recent and older experimental data have been presented. Limitations of the model have been discussed and suggestions for easing the limitations were made. Finally, a complete listing of the code and a sample test run have been included as appendices.

NASA Langley Research Center
Hampton, VA 23681-0001
April 5, 1993

7. References

1. Townsend, Lawrence W.; Nealy, John E.; Wilson, John W.; and Simonsen, Lisa C.: *Estimates of Galactic Cosmic Ray Shielding Requirements During Solar Minimum*. NASA TM-4167, 1990.
2. Simonsen, Lisa C.; Nealy, John E.; Townsend, Lawrence W.; and Wilson, John W.: *Radiation Exposure for Manned Mars Surface Missions*. NASA TP-2979, 1990.
3. Simonsen, Lisa C.; Nealy, John E.; Townsend, Lawrence W.; and Wilson, John W.: Space Radiation Dose Estimates on the Surface of Mars. *J. Spacecr. & Rockets*, vol. 27, July-Aug. 1990, pp. 353-354.
4. Simonsen, L. C.; Nealy, J. E.; Townsend, L. W.; and Wilson, J. W.: Martian Regolith as Space Radiation Shielding. *J. Spacecr. & Rockets*, vol. 28, Jan.-Feb. 1991, pp. 7-8.
5. Cucinotta, Francis A.; Katz, Robert; Wilson, John W.; Townsend, Lawrence W.; Nealy, John E.; and Shinn, Judy L.: *Cellular Track Model of Biological Damage to Mammalian Cell Cultures From Galactic Cosmic Rays*. NASA TP-3055, 1991.
6. Wilson, John W.; Townsend, Lawrence W.; Schimmerling, Walter; Khandelwal, Govind S.; Khan, Ferdous; Nealy, John E.; Cucinotta, Francis A.; Simonsen, Lisa C.; Shinn, Judy L.; and Norbury, John W.: *Transport Methods and Interactions for Space Radiations*. NASA RP-1257, 1991.
7. Townsend, Lawrence W.; Cucinotta, Francis A.; and Wilson, John W.: Interplanetary Crew Exposure Estimates for Galactic Cosmic Rays. *Radiat. Res.*, vol. 129, no. 1, 1992, pp. 48-52.
8. Townsend, L. W.; Wilson, J. W.; Cucinotta, F. A.; and Shinn, J. L.: Galactic Cosmic Ray Transport Methods and Radiation Quality Issues. *Nucl. Tracks Radiat. Meas.*, vol. 20, no. 1, 1992, pp. 65-72.
9. Townsend, Lawrence W.; Cucinotta, Francis A.; Shinn, Judy L.; and Wilson, John W.: *Effects of Fragmentation Parameter Variations on Estimates of Galactic Cosmic Ray Exposure-Dose Sensitivity Studies for Aluminum Shields*. NASA TM-4386, 1992.
10. Silberberg, R.; Tsao, C. H.; and Letaw, John R.: Improvement of Calculations of Cross Sections and Cosmic-Ray Propagation. *Composition and Origin of Cosmic Rays*, Maurice M. Shapiro, ed., D. Reidel Publ. Co., c.1983, pp. 321-336.
11. Rudstam, G.: Systematics of Spallation Yields. *Zeitschrift fur Naturforschung*, vol. 21a, no. 7, July 1966, pp. 1027-1041.
12. Wilson, John W.; Townsend, L. W.; Bidasaria, H. B.; Schimmerling, Walter; Wong, Mervyn; and Howard, Jerry: ^{20}Ne Depth-Dose Relations in Water. *Health Phys.*, vol. 46, no. 5, May 1984, pp. 1101-1111.
13. Wilson, John W.; Townsend, Lawrence W.; and Badavi, F. F.: A Semiempirical Nuclear Fragmentation Model. *Nucl. Instrum. & Methods Phys. Res.*, vol. B18, no. 3, Feb. 1987, pp. 225-231.
14. Badavi, Forooz F.; Townsend, Lawrence W.; Wilson, John W.; and Norbury, John W.: An Algorithm for a Semiempirical Nuclear Fragmentation Model. *Comput. Phys. Commun.*, vol. 47, 1987, pp. 281-294.
15. Bowman, J. D.; Swiatecki, W. J.; and Tsang, C. F.: *Abrasion and Ablation of Heavy Ions*. LBL-2908, Lawrence Berkeley Lab., Univ. of California, July 1973.
16. Williams, E. J.: Correlation of Certain Collision Problems With Radiation Theory. *Kgl. Danske Videnskab. Selskab Math.-Fys. Medd.*, vol. XIII, no. 4, 1935.
17. Jackson, John David: *Classical Electrodynamics*, Second ed. John Wiley & Sons, Inc., c.1975.

18. Gosset, J.; Gutbrod, H. H.; Meyer, W. G.; Poskanzer, A. M.; Sandoval, A.; Stock, R.; and Westfall, G. D.: Central Collisions of Relativistic Heavy Ions. *Phys. Review*, ser. C, vol. 16, no. 2, Aug. 1977, pp. 629–657.
19. Townsend, L. W.: Abrasion Cross Sections for ^{20}Ne Projectiles at 2.1 GeV/Nucleon. *Canadian J. Phys.*, vol. 61, no. 1, Jan. 1983, pp. 93–98.
20. Hüfner, J.; Schäfer, K.; and Schürmann, B.: Abrasion-Ablation in Reactions Between Relativistic Heavy Ions. *Phys. Review*, ser. C, vol. 12, no. 6, Dec. 1975, pp. 1888–1898.
21. Morrissey, D. J.; Marsh, W. R.; Otto, R. J.; Loveland, W.; and Seaborg, G. T.: Target Residue Mass and Charge Distributions in Relativistic Heavy Ion Reactions. *Phys. Review*, ser. C, vol. 18, no. 3, Sept. 1978, pp. 1267–1274.
22. Guthrie, Miriam P.: *EVAP-4: Another Modification of a Code To Calculate Particle Evaporation From Excited Compound Nuclei*. ORNL-TM-3119 U.S. Atomic Energy Commission, Sept. 10, 1970.
23. Dymarz, R.; and Kohmura, T.: *The Mean Free Path of Protons in Nuclei and the Nuclear Radius*. Ref: 58/82, Nuclear Physics Lab., Oxford Univ., 1982.
24. Negele, J. W.; and Yazaki, K.: Mean Free Path in a Nucleus. *Phys. Review Lett.*, vol. 47, no. 2, July 13, 1981, pp. 71–74.
25. De Vries, H.; De Jager, C. W.; and De Vries, C.: Nuclear Charge-Density-Distribution Parameters From Elastic Electron Scattering. *At. Data & Nucl. Data Tables*, vol. 36, no. 3, May 1987, pp. 495–536.
26. Bertulani, Carlos A.; and Baur, Gerhard: Electromagnetic Processes in Relativistic Heavy Ion Collisions. *Phys. Rep.*, vol. 163, nos. 5 & 6, June 1988, pp. 299–408.
27. Norbury, John W.: Nucleon Emission Via Electromagnetic Excitation in Relativistic Nucleus-Nucleus Collisions: Reanalysis of the Weizsäcker-Williams Method. *Phys. Review C*, third ser., vol. 40, no. 6, Dec. 1989, pp. 2621–2628.
28. Norbury, John W.: Electric Quadrupole Excitations in the Interactions of ^{89}Y With Relativistic Nuclei. *Phys. Review C*, third ser., vol. 41, no. 1, Jan. 1990, pp. 372–373.
29. Norbury, John W.: Electric Quadrupole Excitations in Relativistic Nucleus-Nucleus Collisions. *Phys. Review C*, third ser., vol. 42, no. 2, Aug. 1990, pp. 711–715.
30. Aleixo, A. N. F.; and Bertulani, C. A.: Coulomb Excitation in Intermediate-Energy Collisions. *Nucl. Phys.*, vol. A505, no. 2, Dec. 11, 1989, pp. 448–470.
31. Westfall, G. D.; Wilson, Lance W.; Lindstrom, P. J.; Crawford, H. J.; Greiner, D. E.; and Heckman, H. H.: Fragmentation of Relativistic ^{56}Fe . *Phys. Review*, ser. C, vol. 19, no. 4, Apr. 1979, pp. 1309–1323.
32. Letaw, John R.; Silberberg, R.; and Tsao, C. H.: Proton-Nucleus Total Inelastic Cross Sections: An Empirical Formula for $E > 10$ MeV. *Astrophys. J.*, Suppl. ser., vol. 51, no. 3, Mar. 1983, pp. 271–276.
33. MECC-7 *Intranuclear Cascade Code, 500-MeV Protons on O-16. I4C Analysis Codes* (Programmed for H. W. Bertini). Available from Radiation Shielding Information Center, Oak Ridge National Lab., 1968.
34. Abramowitz, Milton; and Stegun, Irene A., eds.: *Handbook of Mathematical Functions With Formulas, Graphs, and Mathematical Tables*. NBS Appl. Math. Ser. 55, U.S. Dep. of Commerce, June 1964.
35. Cummings, J. R.; Binns, W. R.; Garrard, T. L.; Israel, M. H.; Klarmann, J.; Stone, E. C.; and Waddington, C. J.: Determination of the Cross Sections for the Production of Fragments From Relativistic Nucleus-Nucleus Interactions. I. Measurements. *Phys. Review C*, third ser., vol. 42, no. 6, Dec. 1990, pp. 2508–2529.
36. Tull, C. E.: *Relativistic Heavy Ion Fragmentation at HISS*. LBL-29718 (Contract No. DE-AC03-76SF00098), Lawrence Berkeley Lab., Univ. of California, Oct. 1990.
37. Lindstrom, P. J.; Greiner, D. E.; Heckman, H. H.; Cork, Bruce; and Bieser, F. S.: *Isotope Production Cross Sections From the Fragmentation of ^{16}O and ^{12}C at Relativistic Energies*. LBL-3650 (NGR-05-003-513), Lawrence Berkeley Lab., Univ. of California, June 1975.
38. Cummings, J. R.; Binns, W. R.; Garrard, T. L.; Israel, M. H.; Klarmann, J.; Stone, E. C.; and Waddington, C. J.: Determination of the Cross Sections for the Production of Fragments From Relativistic Nucleus-Nucleus Interactions. II. Parametric Fits. *Phys. Review C*, third ser., vol. 42, no. 6, Dec. 1990, pp. 2530–2545.
39. Cucinotta, Francis A.; Townsend, Lawrence W.; and Wilson, John W.: *Description of Alpha-Nucleus Interaction Cross Sections for Cosmic Ray Shielding Studies*. NASA TP-3285, 1993.
40. Benesh, C. J.; Cook, B. C.; and Vary, J. P.: Single Nucleon Removal in Relativistic Nuclear Collisions. *Phys. Review C*, third ser., vol. 40, no. 3, Sept. 1989, pp. 1198–1206.
41. Norbury, John W.; and Townsend, Lawrence W.: Single Nucleon Emission in Relativistic Nucleus-Nucleus Reactions. *Phys. Review C*, third ser., vol. 42, no. 4, Oct. 1990, pp. 1775–1777.

Table I. Isotope Production Cross Sections for 2.1 GeV/Nucleon Oxygen Beams Fragmenting in Various Targets

Isotope produced	Cross section for target nucleus, mb							
	Carbon		Copper		Silver		Lead	
	Present model	Experimental (ref. 37)	Present model	Experimental (ref. 37)	Present model	Experimental (ref. 37)	Present model	Experimental (ref. 37)
¹⁵ O	57.7	42.9 ± 2.3	87.2	74.0 ± 7.8	110	99 ± 13	164	135 ± 22
¹⁴ O	0.62	1.67 ± 0.12	0.83	2.14 ± 0.42	0.91	2.20 ± 0.58	1.0	2.8 ± 1.5
¹⁵ N	58.1	54.2 ± 2.9	93.5	98.2 ± 9.6	125	121 ± 15	199	202 ± 26
¹⁴ N	64.6	41.8 ± 3.3	86.6	72 ± 14	94.5	68 ± 23	108	71 ± 22
¹³ N	7.71	8.06 ± 0.42	10.6	14.7 ± 1.6	11.8	18.6 ± 2.2	13.3	17.0 ± 3.2
¹² N	0.38	0.73 ± 0.07	0.54	0.42 ± 0.18	0.59	1.11 ± 0.34	0.68	
¹⁴ C	11.4	4.71 ± 0.31	15.3	7.76 ± 0.92	16.7	7.5 ± 1.3	19	12.3 ± 2.2
¹³ C	52.7	27.7 ± 1.4	72.8	35.8 ± 3.7	80.5	39.4 ± 5.1	91.2	45.4 ± 8.3
¹² C	46.9	65.1 ± 5.2	65.9	92 ± 14	73	104 ± 18	84	126 ± 25
¹¹ C	7.2	18.46 ± 0.92	10.4	27.0 ± 2.6	11.5	37.8 ± 3.8	13.2	36.9 ± 5.7
¹⁰ C	0.3	2.51 ± 0.16	0.4	4.45 ± 0.52	0.4	4.2 ± 1.2	0.5	7.2 ± 1.4
¹³ B	0.5	0.44 ± 0.05	0.6	0.82 ± 0.17	0.7	0.65 ± 0.28	0.8	0.7 ± 0.44
¹² B	5.0	2.44 ± 0.15	7.0	2.98 ± 0.38	7.8	4.04 ± 0.58	8.9	3.98 ± 0.75
¹¹ B	39	26.0 ± 1.3	56.3	35.9 ± 2.9	62.1	43.6 ± 3.9	71.4	52.9 ± 5.9
¹⁰ B	39.8	20.3 ± 1.6	57.9	35.2 ± 5.5	64.5	26.6 ± 6.3	74	35 ± 11
¹⁰ Be	2.4	3.98 ± 0.30	3.5	6.51 ± 0.86	3.9	5.65 ± 0.77	4.5	6.8 ± 1.1
⁹ Be	15.9	9.06 ± 0.51	23.6	12.3 ± 1.1	26.2	13.8 ± 1.5	30.3	15.3 ± 2.1
⁷ Be	8	22.3 ± 1.1	12.2	32.0 ± 2.5	13.6	36.4 ± 3.2	15.9	43.3 ± 6.4
⁷ Li	26.8	26.3 ± 1.3	41.2	38.7 ± 2.9	45.8	39.8 ± 3.5	53.4	39.7 ± 4.3
⁶ Li	32.5	35.9 ± 2.9	51.1	61.2 ± 7.9	57	49.4 ± 8.5	66	56 ± 13

Table II. Isotope Production Cross Sections for 1.05 GeV/Nucleon
Carbon Beams Fragmenting in Various Targets

Isotope produced	Cross section for target nucleus, mb							
	Aluminum		Copper		Silver		Lead	
	Present model	Experimental (ref. 37)	Present model	Experimental (ref. 37)	Present model	Experimental (ref. 37)	Present model	Experimental (ref. 37)
¹¹ C	67.4	57.8 ± 3.9	80.9	78.1 ± 8.1	95	98 ± 13	119	128 ± 22
¹⁰ C	0.54	5.06 ± 0.37	0.62	7.53 ± 0.70	0.7	7.7 ± 1.0	0.8	10.9 ± 1.7
¹¹ B	68.1	64.5 ± 5.3	83.7	80.1 ± 7.9	101	110 ± 15	132	149 ± 25
¹⁰ B	83.2	30.4 ± 3.5	95.8	36.4 ± 9.9	106	43 ± 12	121	51 ± 18
⁸ B	0.03	1.73 ± 0.16	0.03	2.29 ± 0.32	0.04	1.78 ± 0.38	0.04	2.70 ± 0.68
¹⁰ Be	5.03	6.49 ± 0.48	5.8	7.69 ± 0.61	6.4	8.4 ± 1.2	7.3	10.9 ± 1.8
⁹ Be	29.4	13.9 ± 0.9	34.2	14.3 ± 1.2	37.8	23.7 ± 2.7	43.5	22.2 ± 3.7
⁷ Be	13.3	19.9 ± 1.1	15.5	25.0 ± 1.9	17.3	21.6 ± 2.7	20	37.8 ± 4.7
⁸ Li	0.2	2.87 ± 0.27	0.2	3.99 ± 0.70	0.2	2.8 ± 1.2	0.3	4.9 ± 1.6
⁷ Li	44.6	28.5 ± 1.4	52.3	32.6 ± 1.9	58.1	42.1 ± 3.4	67.2	45.2 ± 4.8
⁶ Li	53.2	24.9 ± 2.9	62.2	33.1 ± 6.0	69.6	38.1 ± 7.6	80	51 ± 13

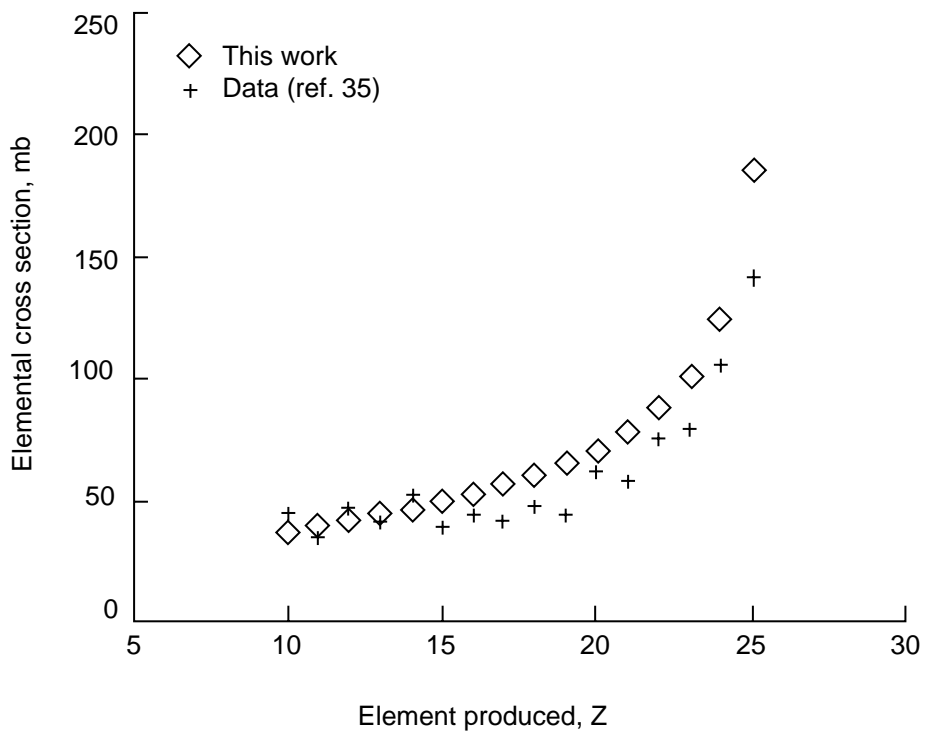


Figure 1. Element production cross sections as a function of fragment charge number. Fe on C at 1.55 GeV/nucleon.

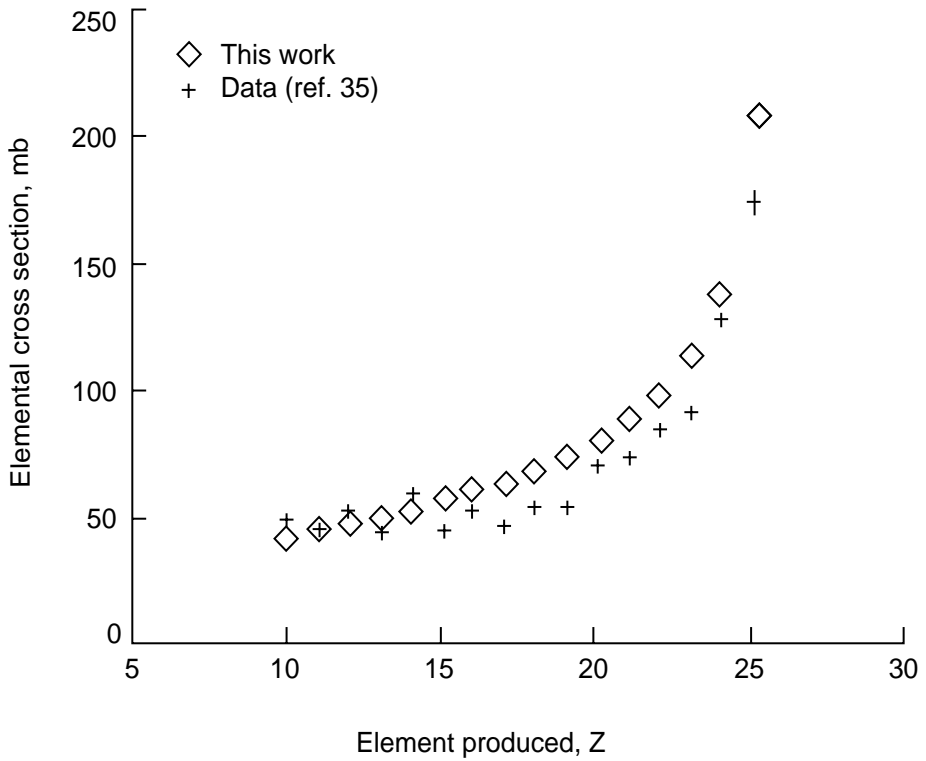


Figure 2. Element production cross sections as a function of fragment charge number. Fe on Al at 1.55 GeV/nucleon.

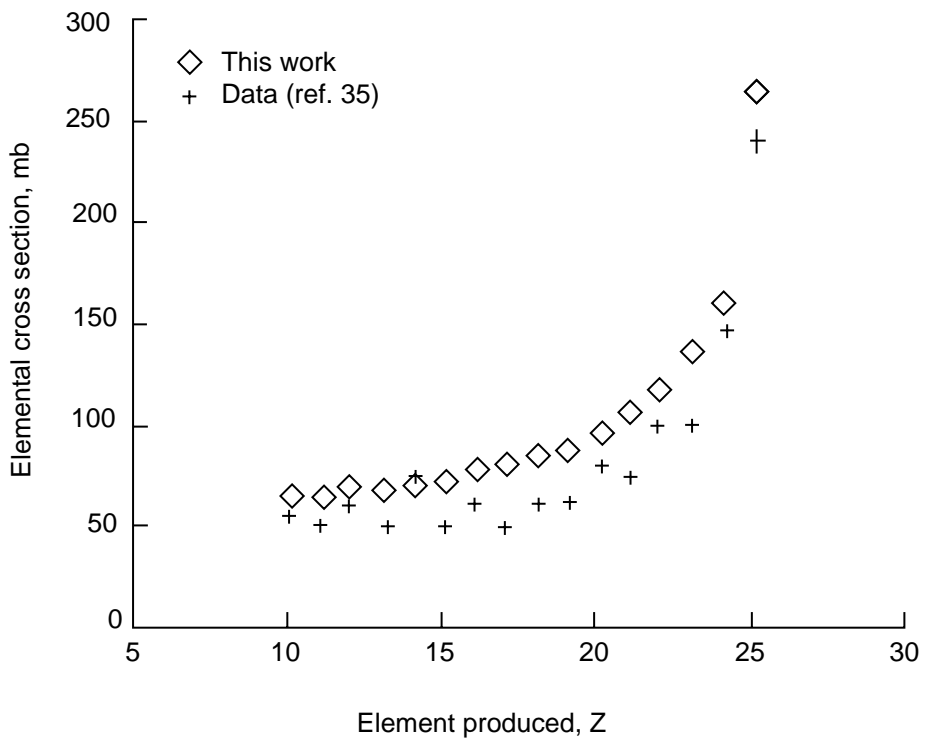


Figure 3. Element production cross sections as a function of fragment charge number. Fe on Cu at 1.55 GeV/nucleon.

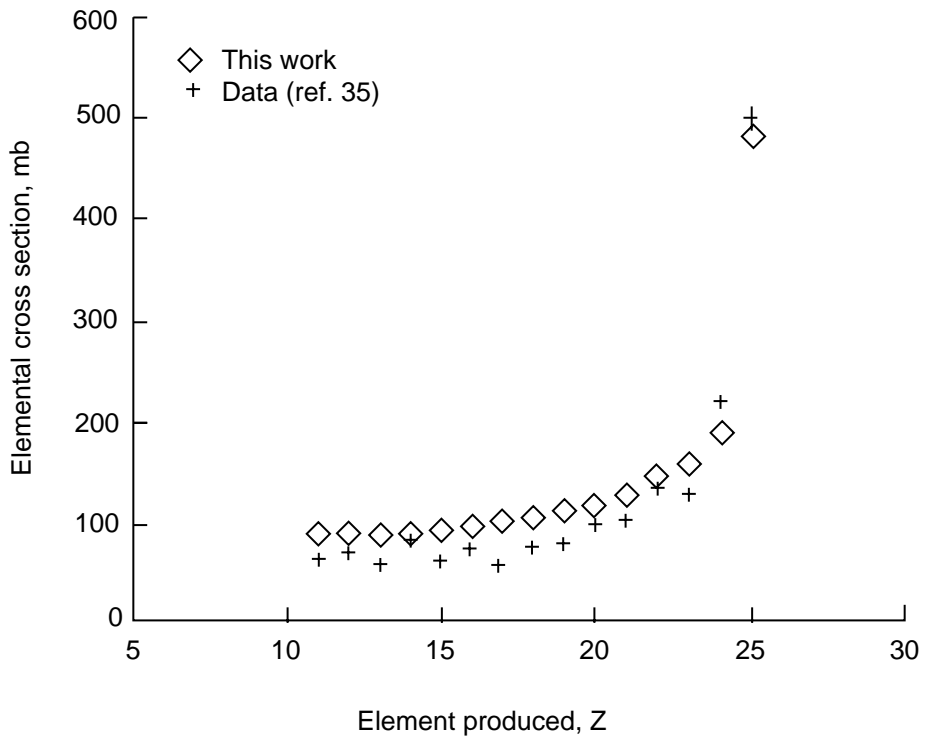


Figure 4. Element production cross sections as a function of fragment charge number. Fe on Pb at 1.55 GeV/nucleon.

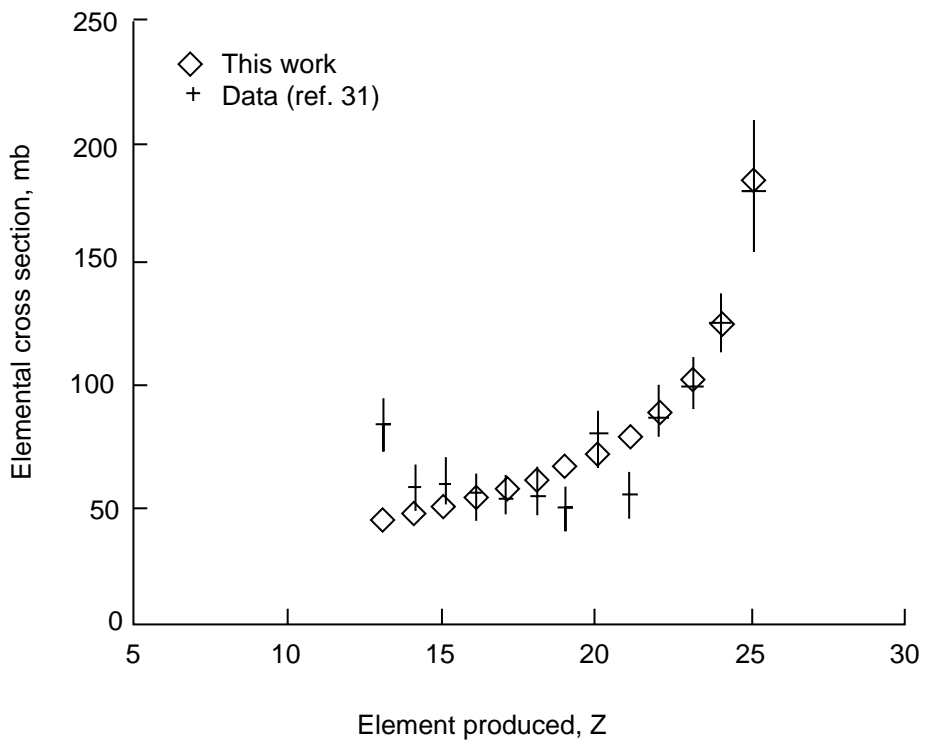


Figure 5. Element production cross sections as a function of fragment charge number. Fe on C at 1.88 GeV/nucleon.

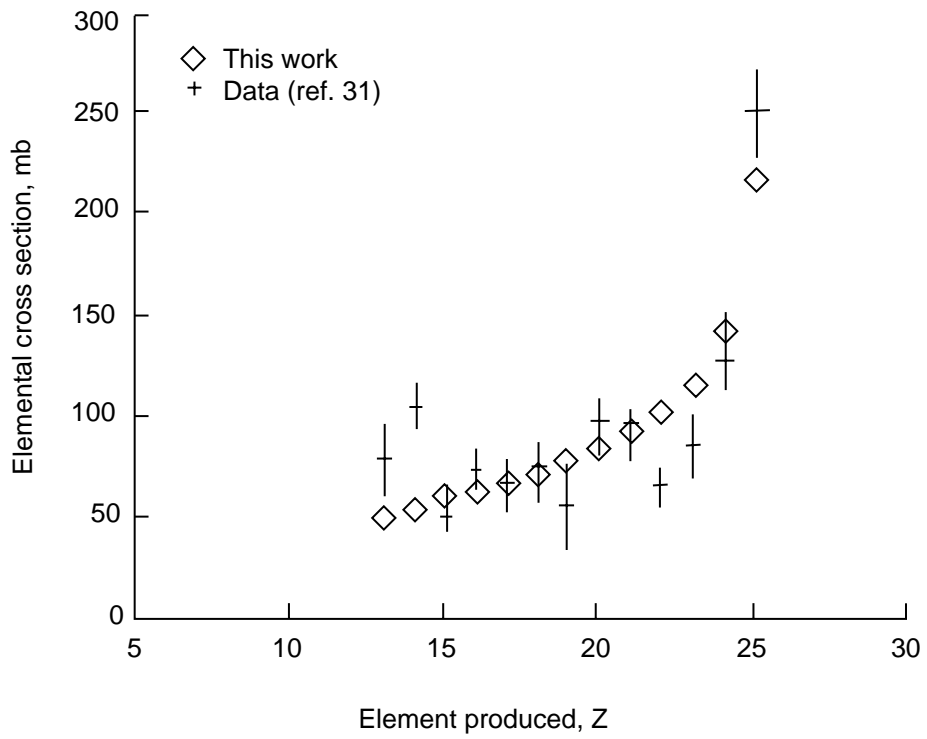


Figure 6. Element production cross sections as a function of fragment charge number. Fe on S at 1.88 GeV/nucleon.

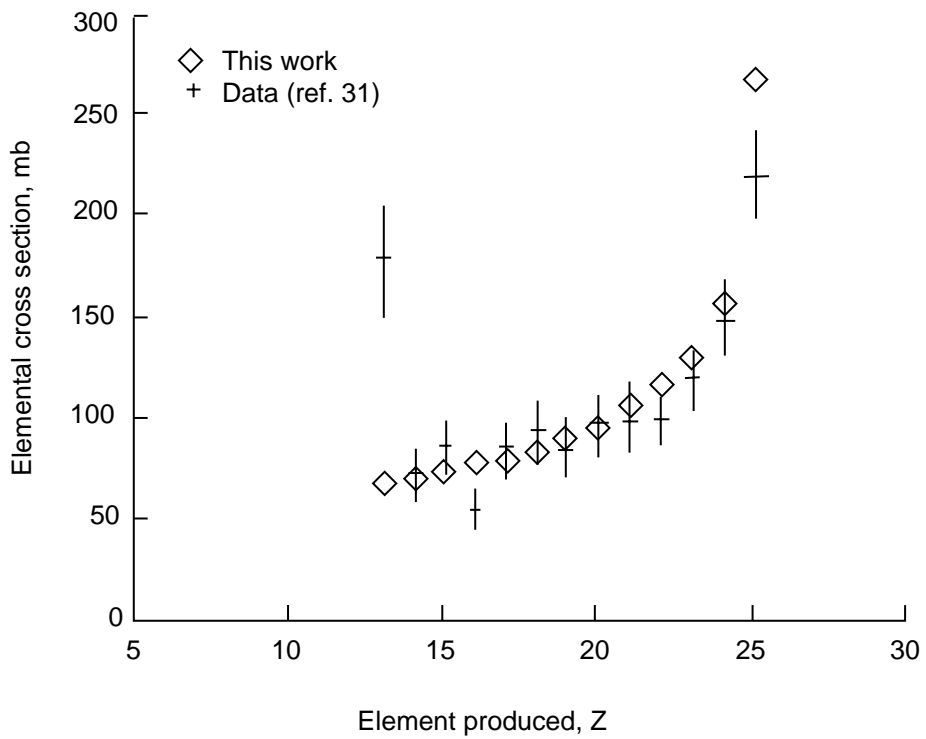


Figure 7. Element production cross sections as a function of fragment charge number. Fe on Cu at 1.88 GeV/nucleon.

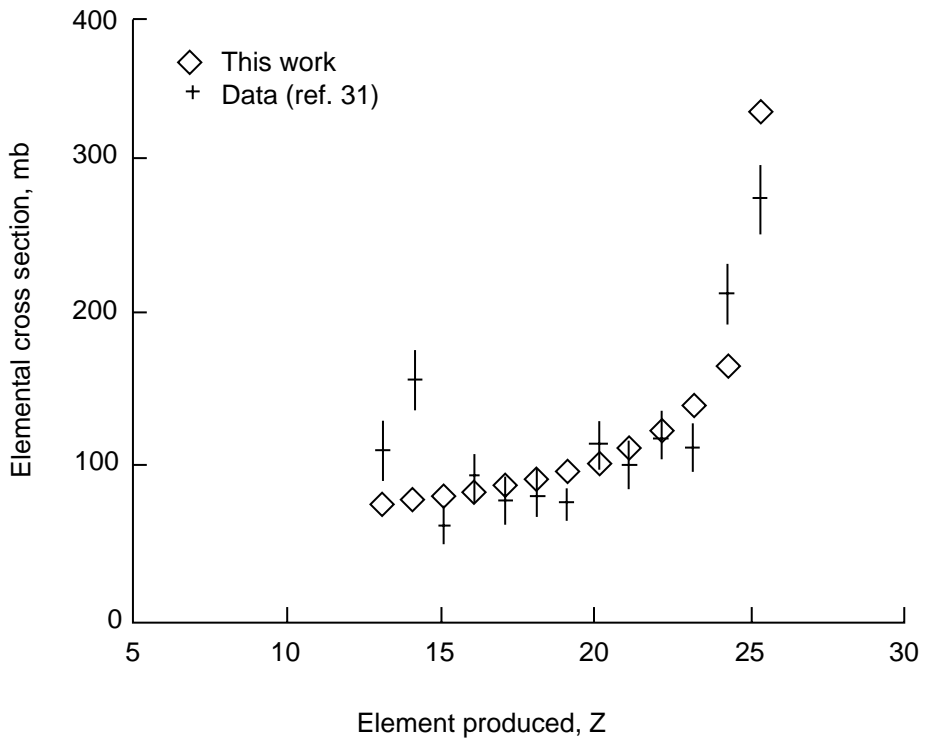


Figure 8. Element production cross sections as a function of fragment charge number. Fe on Ag at 1.88 GeV/nucleon.

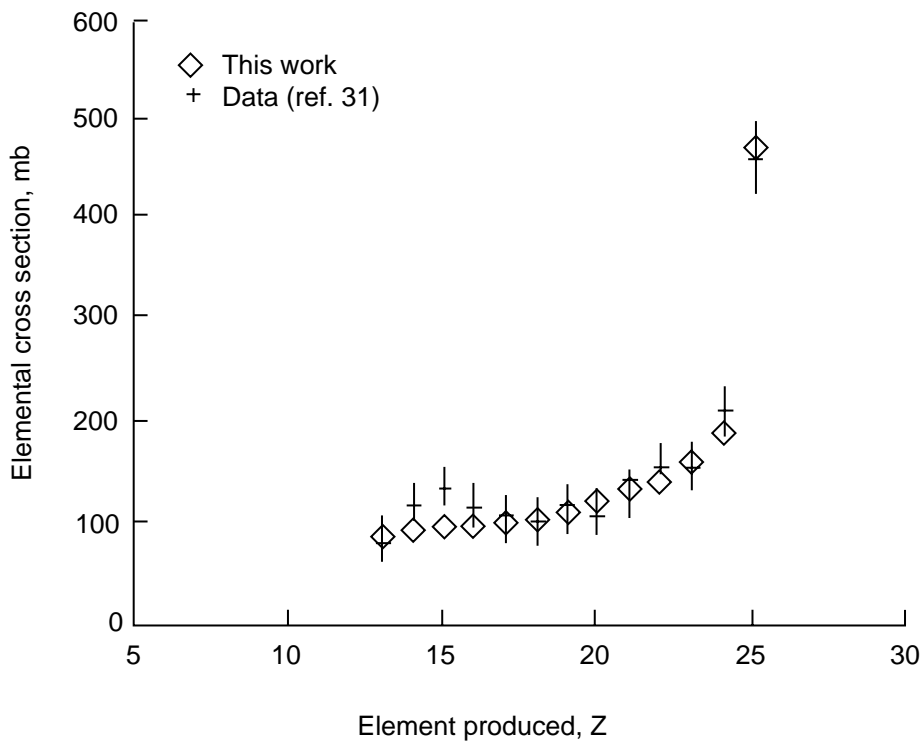


Figure 9. Element production cross sections as a function of fragment charge number. Fe on Ta at 1.88 GeV/nucleon.

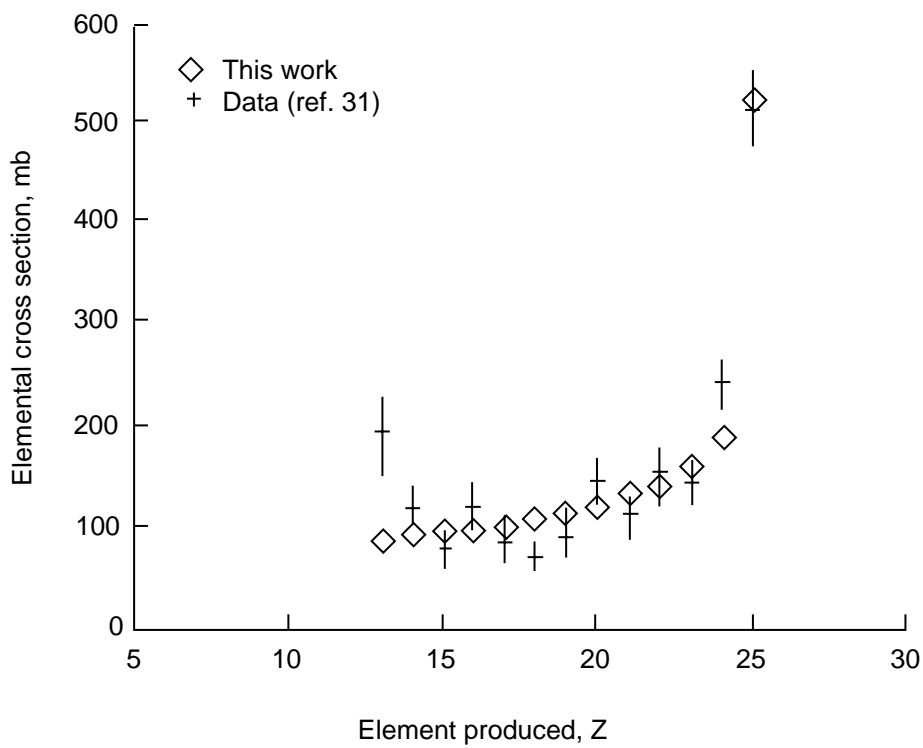


Figure 10. Element production cross sections as a function of fragment charge number. Fe on Pb at 1.88 GeV/nucleon.

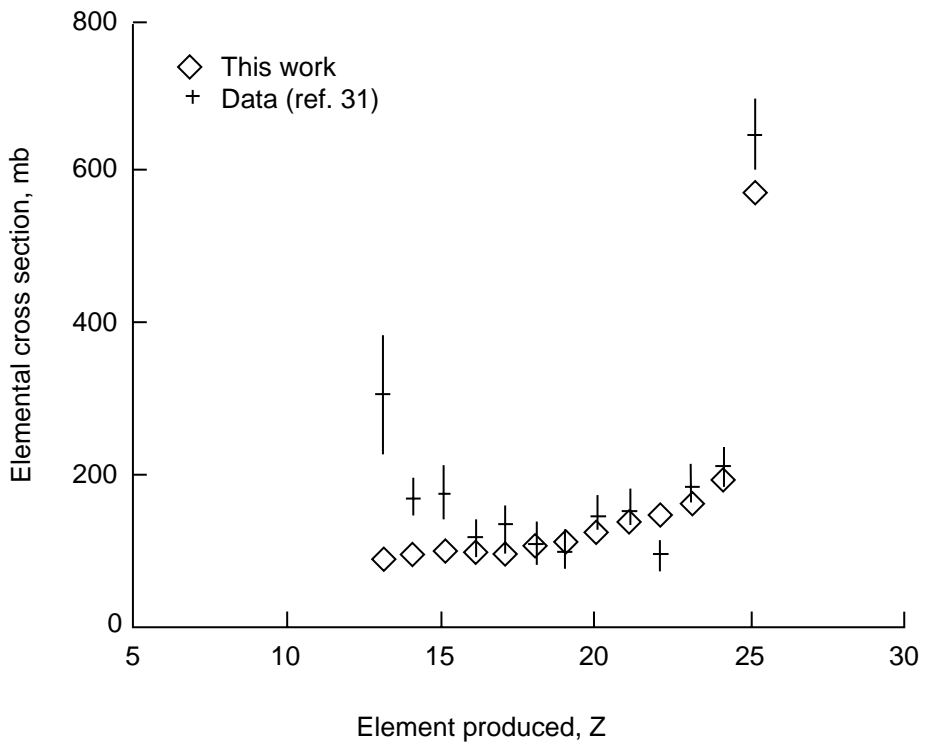


Figure 11. Element production cross sections as a function of fragment charge number. Fe on U at 1.88 GeV/nucleon.

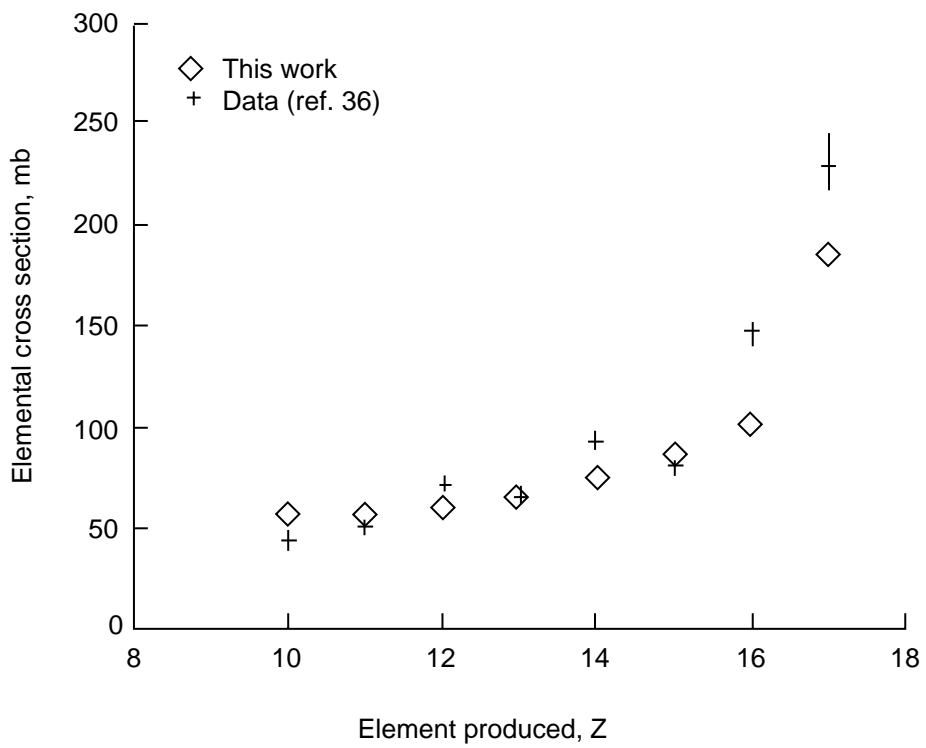


Figure 12. Element production cross sections as a function of fragment charge number. Ar on C at 1.65 GeV/nucleon.

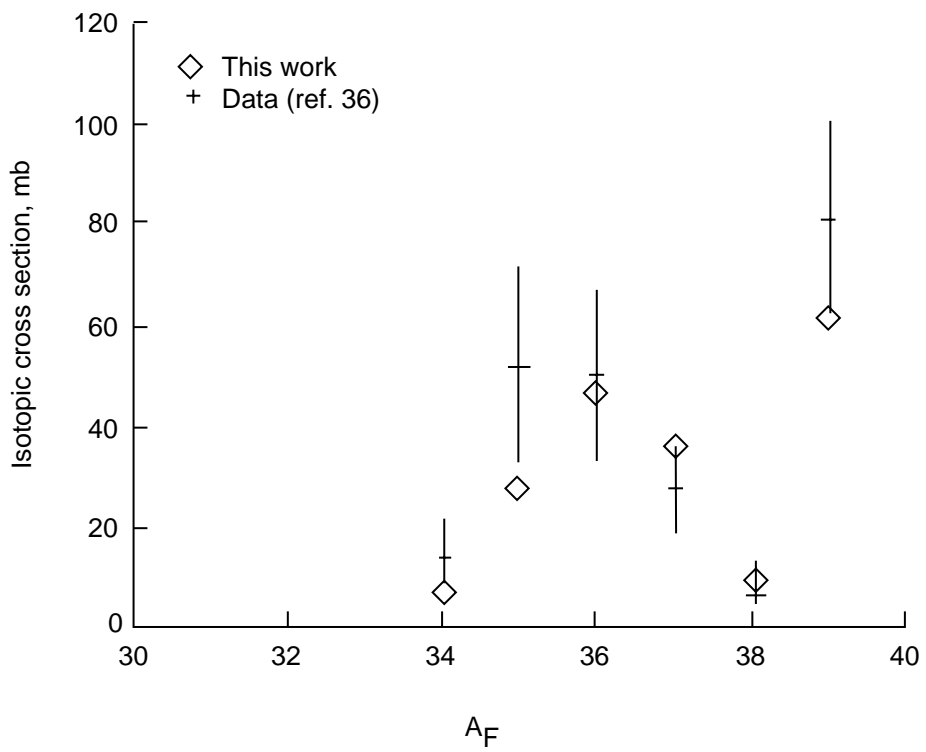


Figure 13. Isotope production cross sections for chlorine fragments. Ar on C at 1.65 GeV/nucleon.

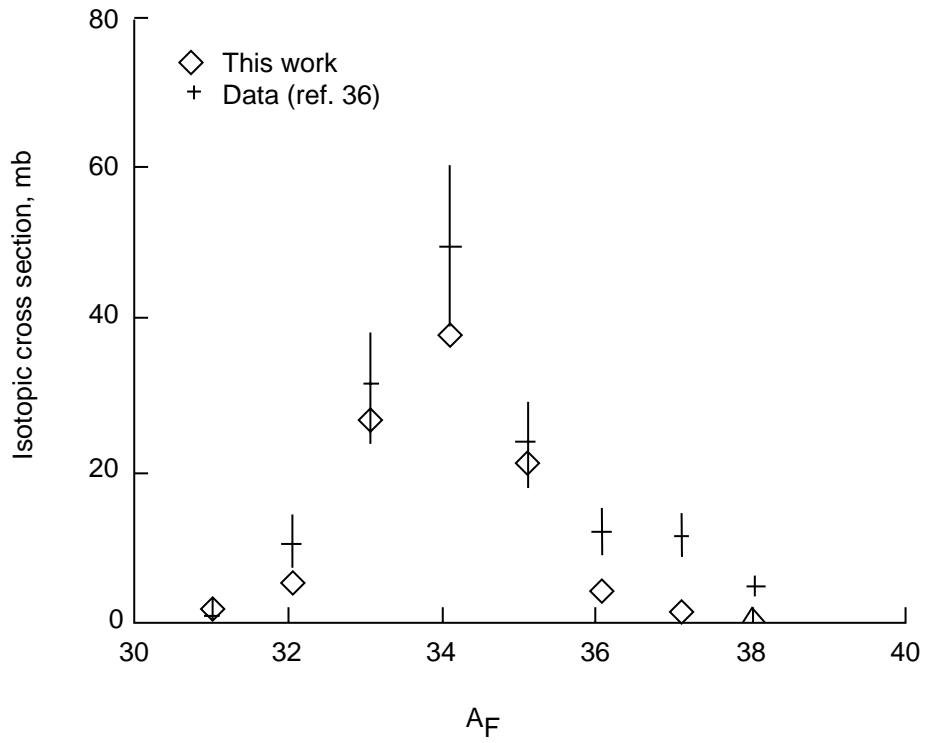


Figure 14. Isotope production cross sections for sulphur fragments. Ar on C at 1.65 GeV/nucleon.

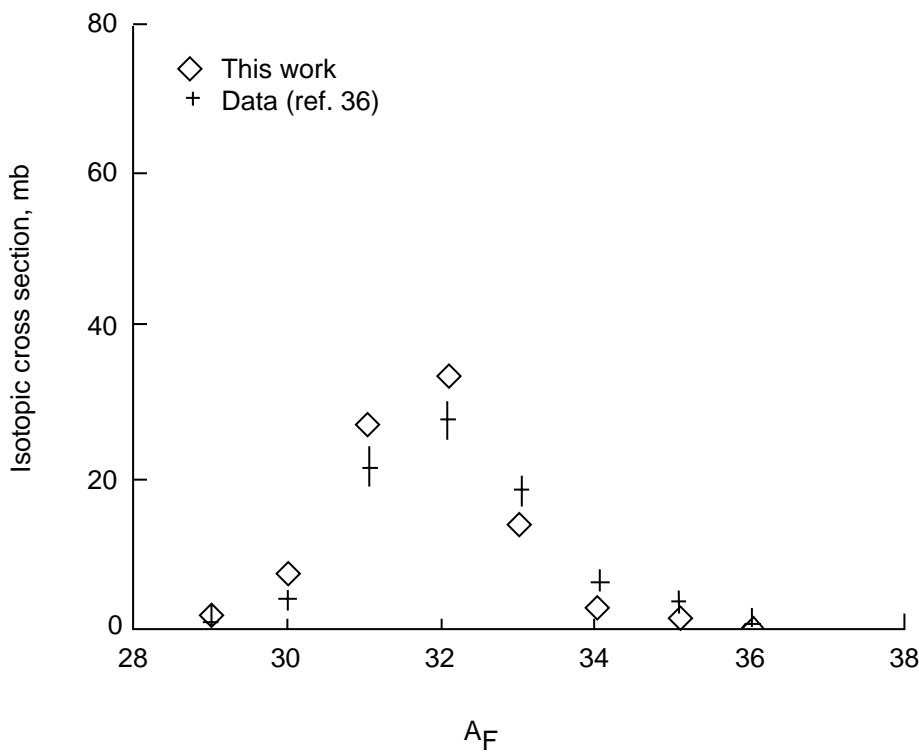


Figure 15. Isotope production cross sections for phosphorous fragments. Ar on C at 1.65 GeV/nucleon.

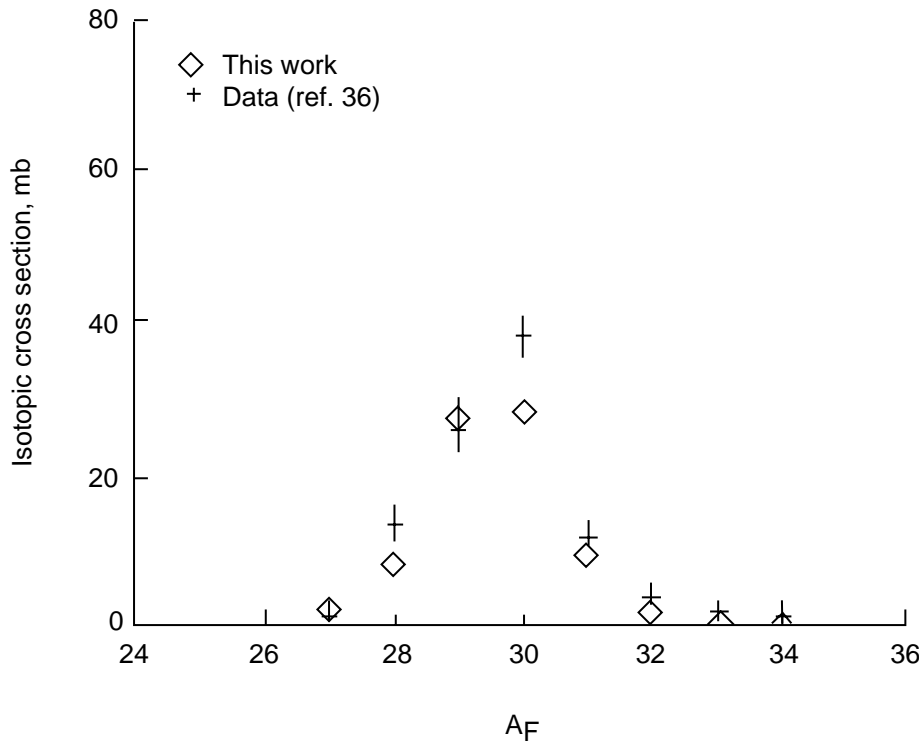


Figure 16. Isotope production cross sections for silicon fragments. Ar on C at 1.65 GeV/nucleon.

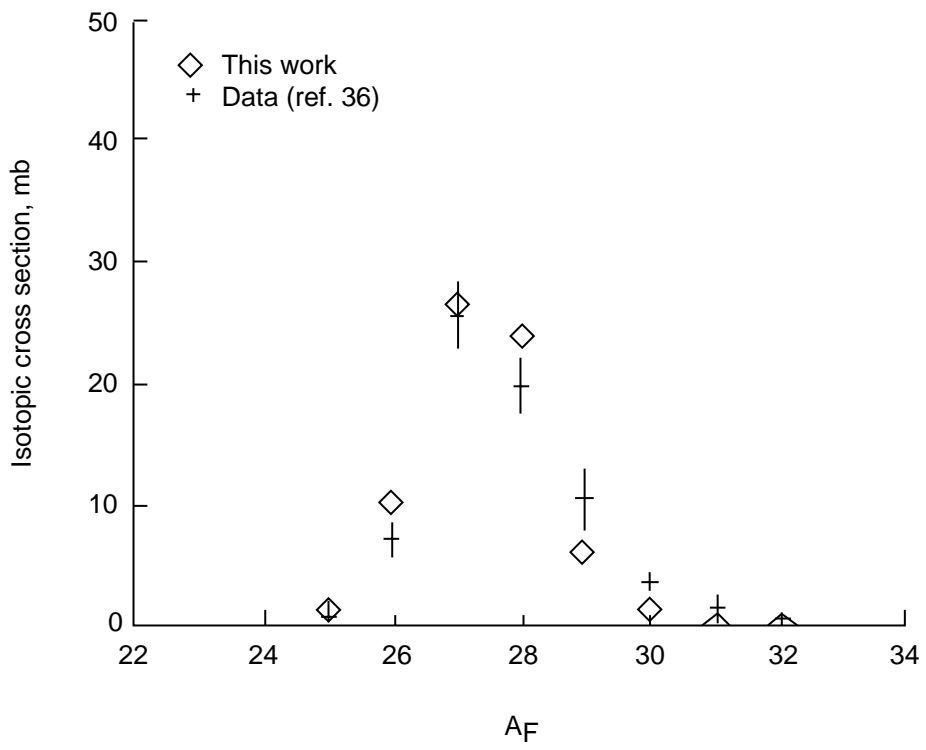


Figure 17. Isotope production cross sections for aluminum fragments. Ar on C at 1.65 GeV/nucleon.

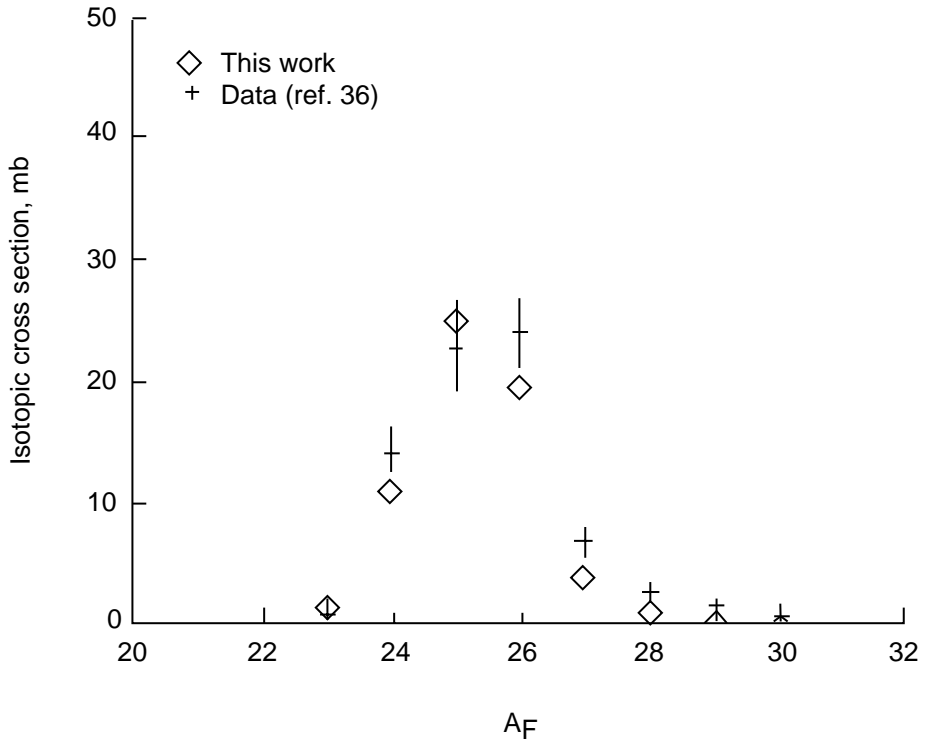


Figure 18. Isotope production cross sections for magnesium fragments. Ar on C at 1.65 GeV/nucleon.

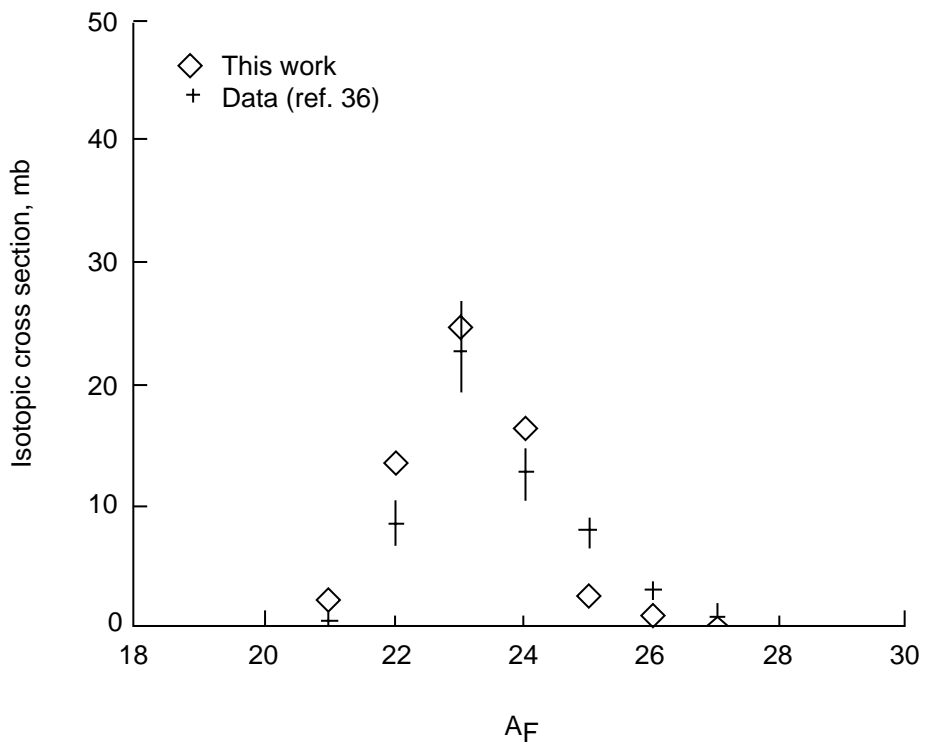


Figure 19. Isotope production cross sections for sodium fragments. Ar on C at 1.65 GeV/nucleon.

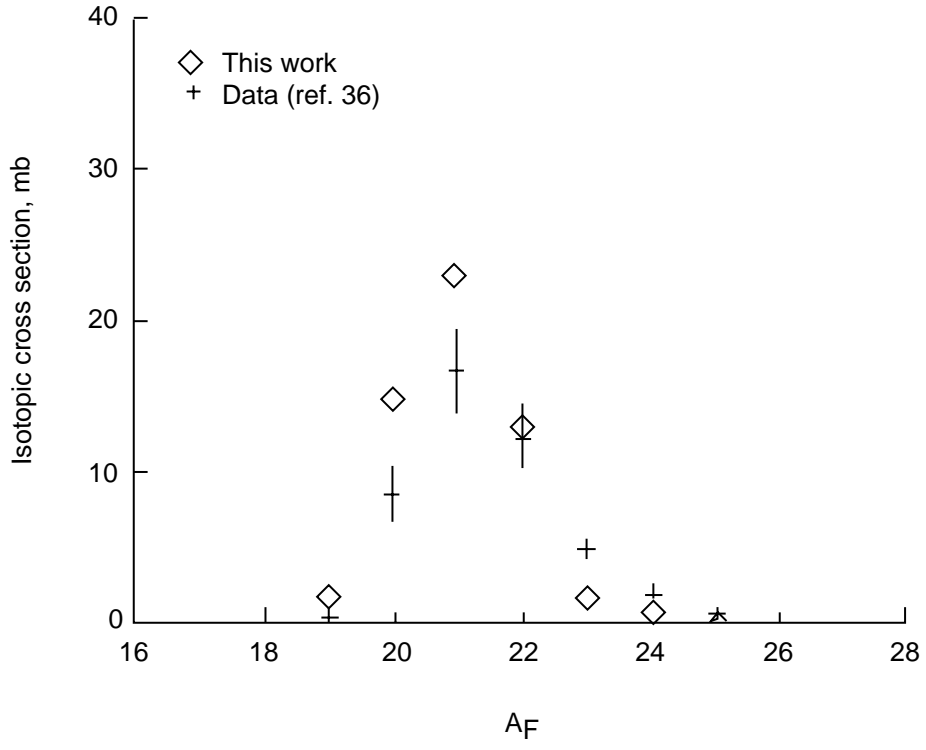


Figure 20. Isotope production cross sections for neon fragments. Ar on C at 1.65 GeV/nucleon.

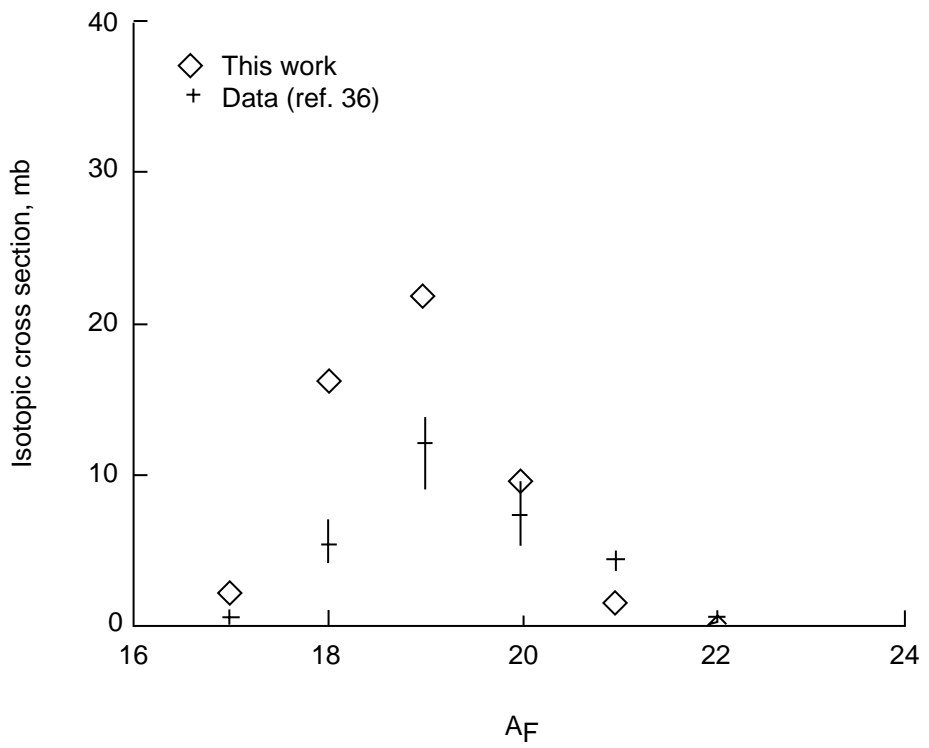


Figure 21. Isotope production cross sections for fluorine fragments. Ar on C at 1.65 GeV/nucleon.

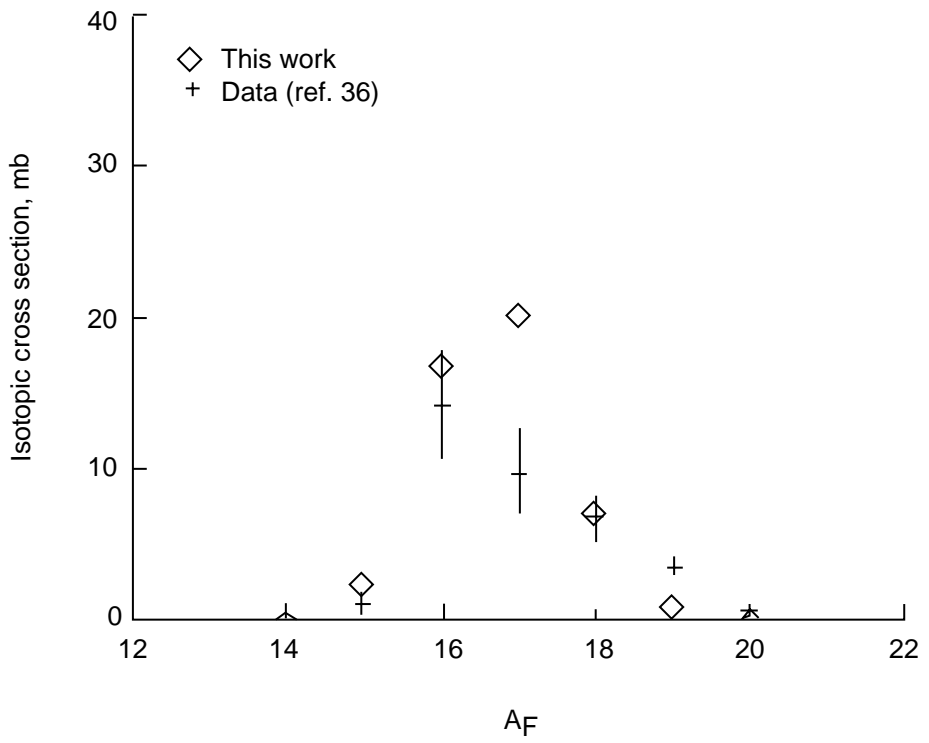


Figure 22. Isotope production cross sections for oxygen fragments. Ar on C at 1.65 GeV/nucleon.

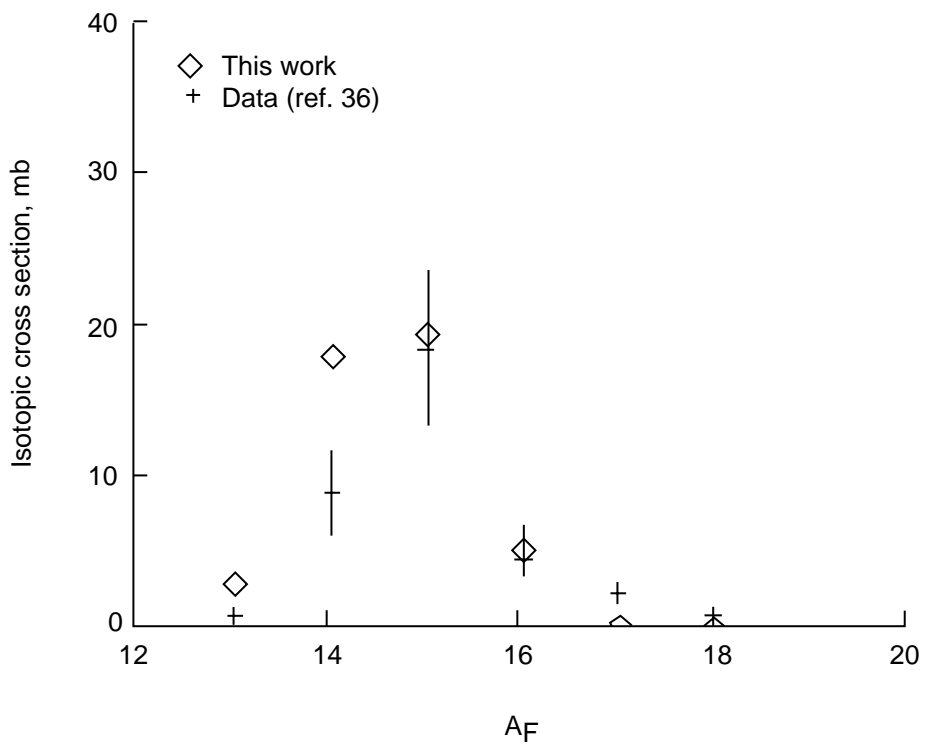


Figure 23. Isotope production cross sections for nitrogen fragments. Ar on C at 1.65 GeV/nucleon.

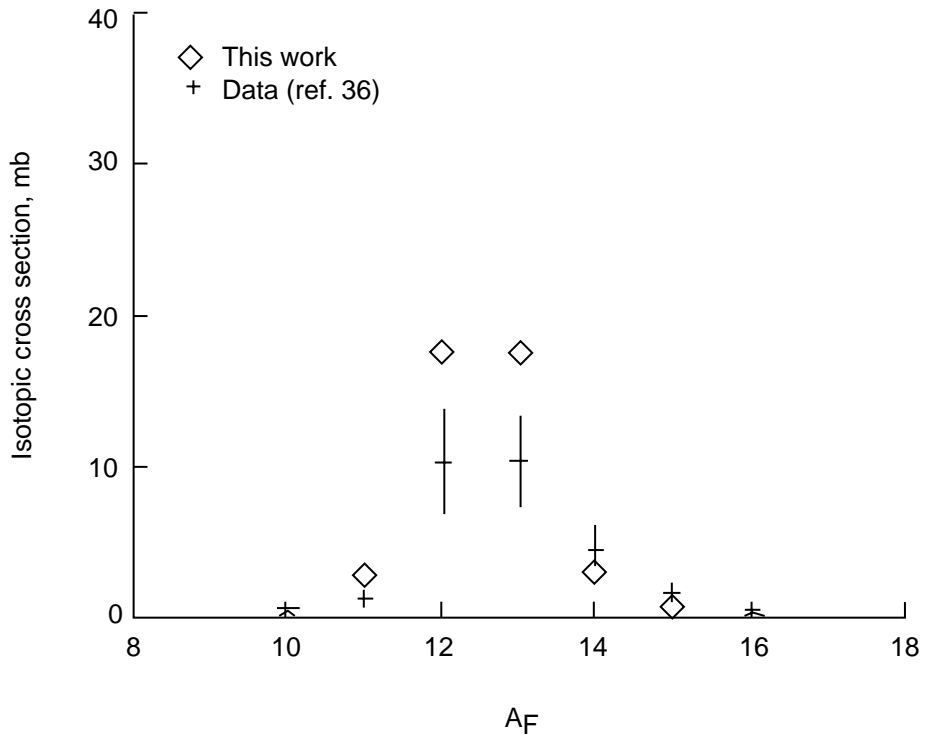


Figure 24. Isotope production cross sections for carbon fragments. Ar on C at 1.65 GeV/nucleon.

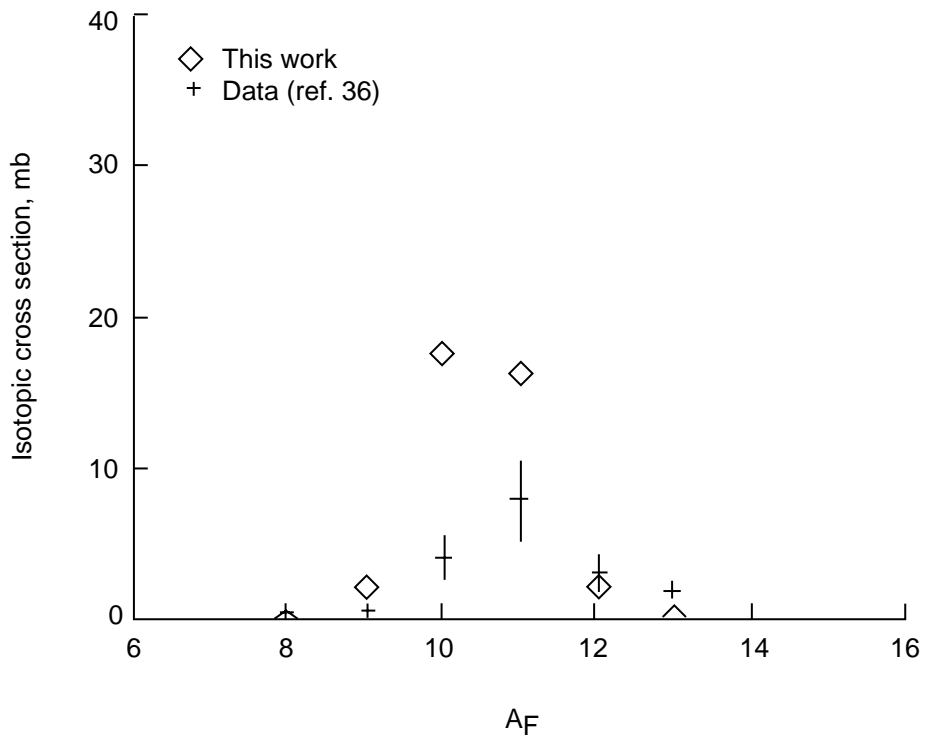


Figure 25. Isotope production cross sections for boron fragments. Ar on C at 1.65 GeV/nucleon.

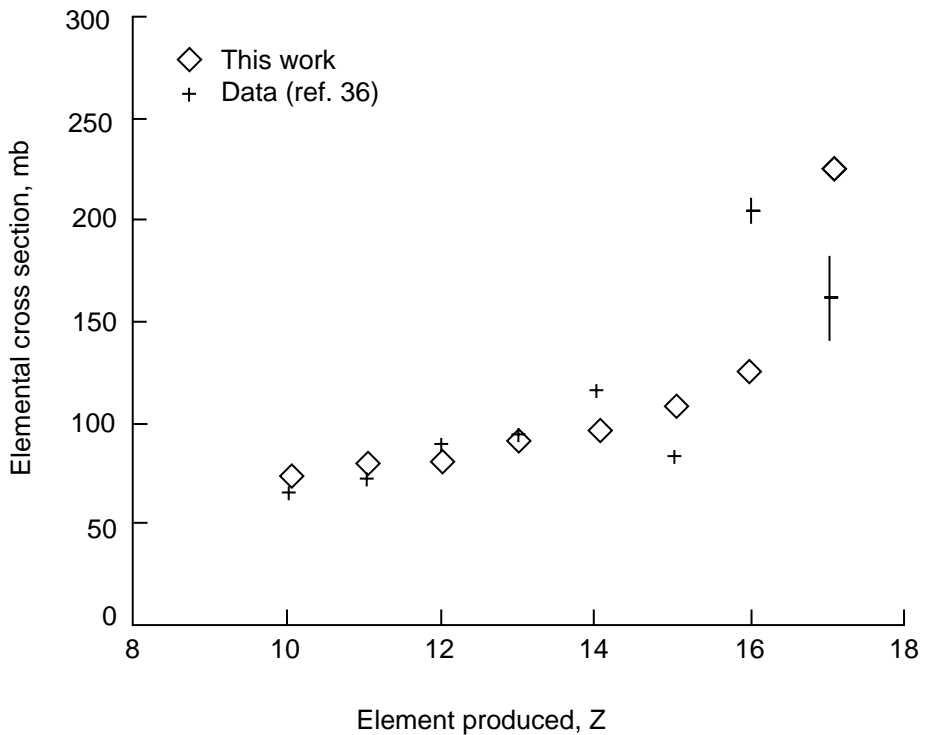


Figure 26. Element production cross sections as a function of fragment charge number. Ar on Ar at 1.65 GeV/nucleon.

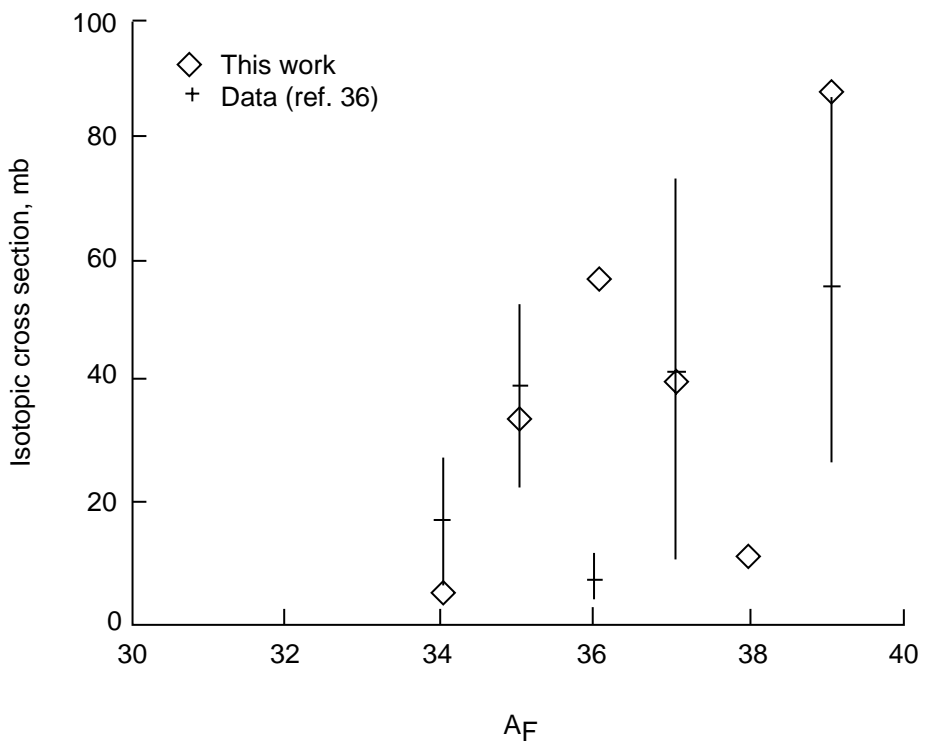


Figure 27. Isotope production cross sections for chlorine fragments. Ar on Ar at 1.65 GeV/nucleon.

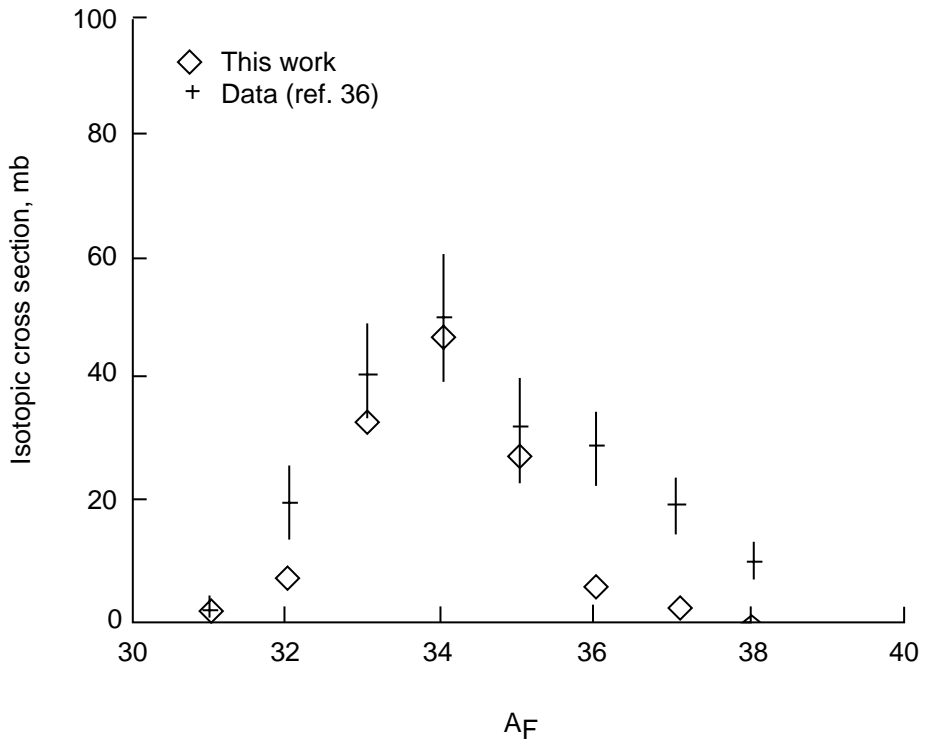


Figure 28. Isotope production cross sections for sulphur fragments. Ar on Ar at 1.65 GeV/nucleon.

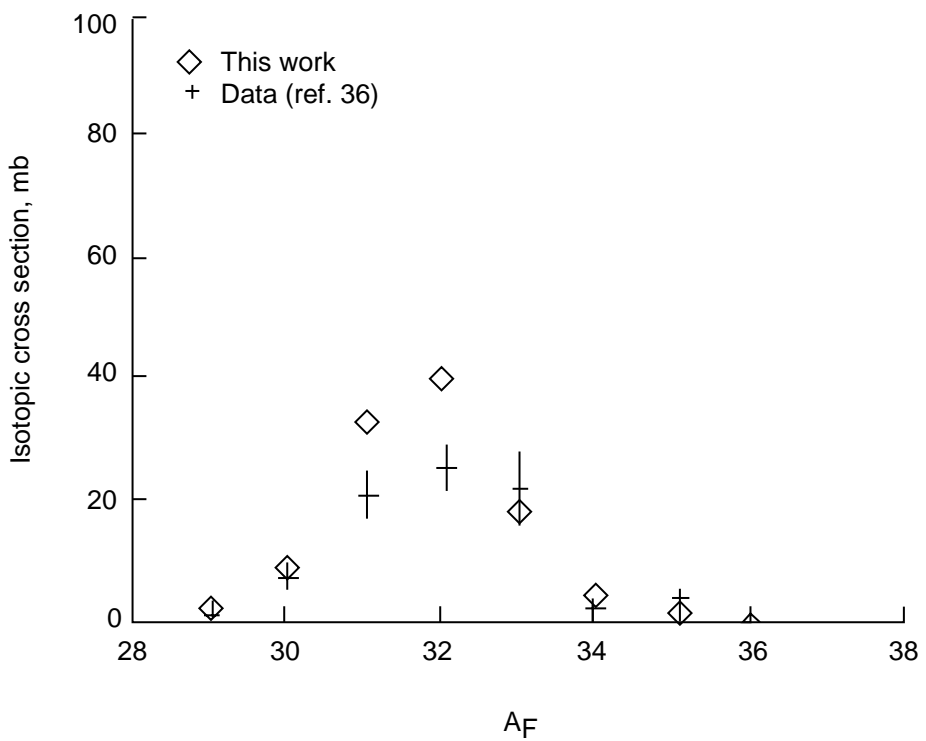


Figure 29. Isotope production cross sections for phosphorous fragments. Ar on Ar at 1.65 GeV/nucleon.

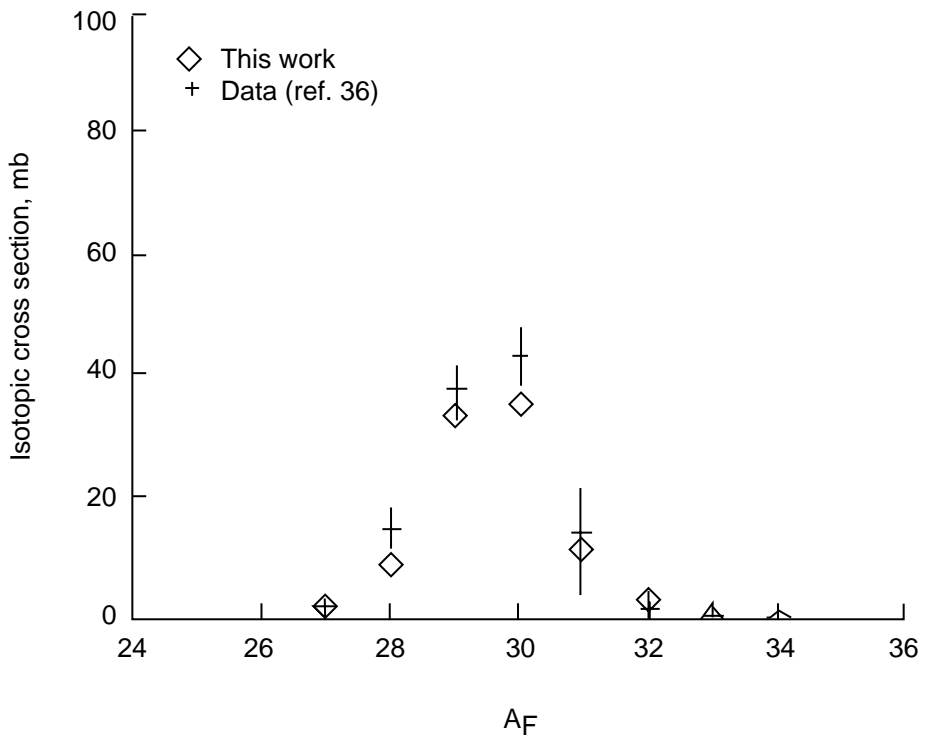


Figure 30. Isotope production cross sections for silicon fragments. Ar on Ar at 1.65 GeV/nucleon.

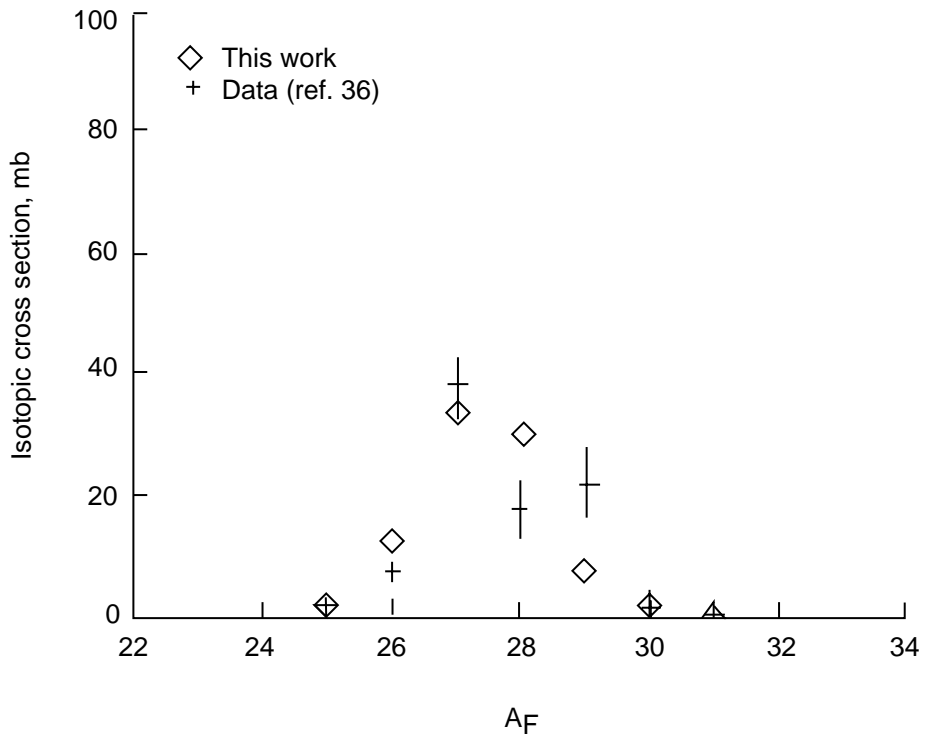


Figure 31. Isotope production cross sections for aluminum fragments. Ar on Ar at 1.65 GeV/nucleon.

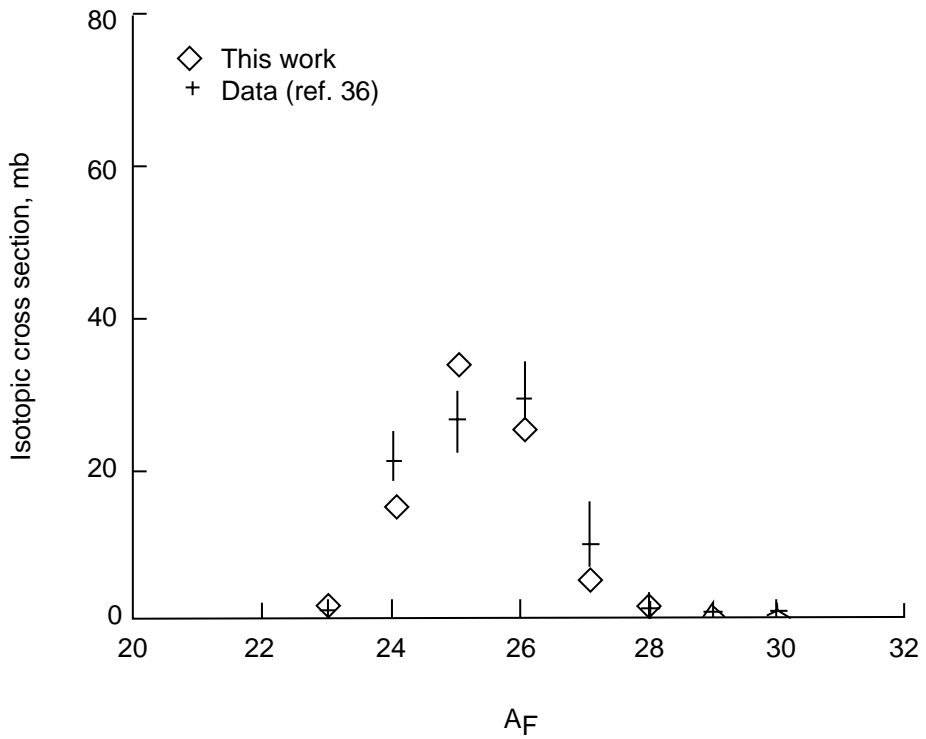


Figure 32. Isotope production cross sections for magnesium fragments. Ar on Ar at 1.65 GeV/nucleon.

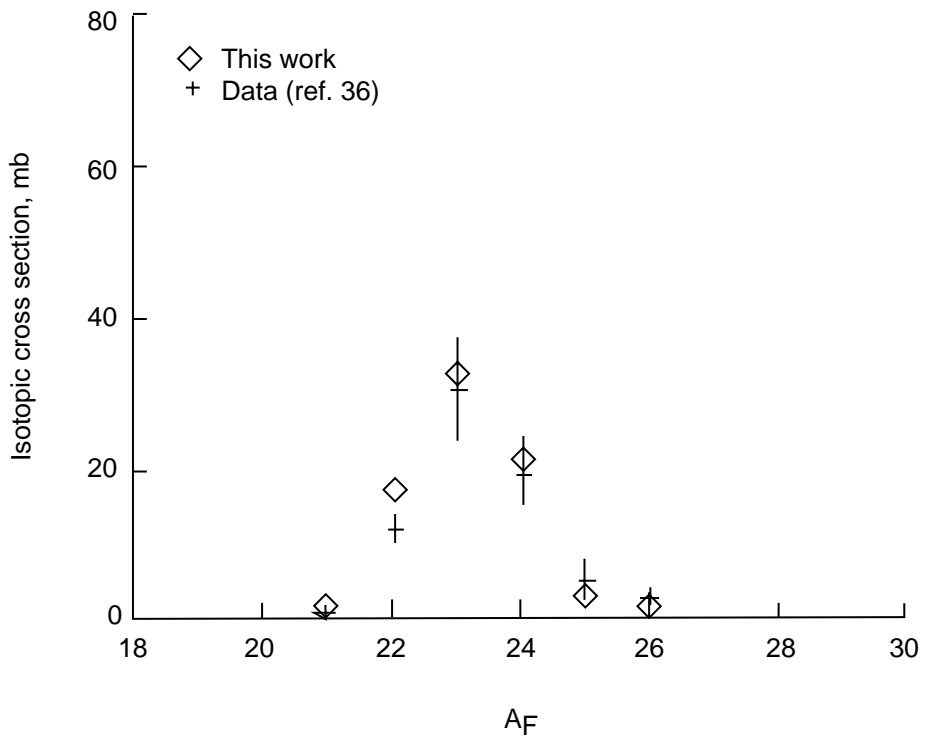


Figure 33. Isotope production cross sections for sodium fragments. Ar on Ar at 1.65 GeV/nucleon.

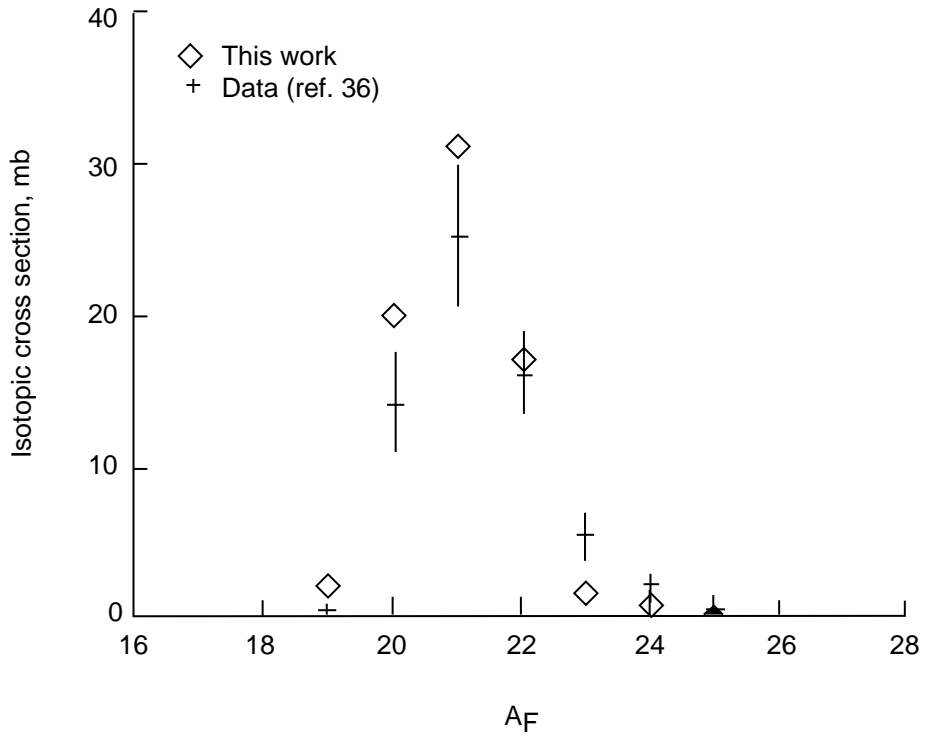


Figure 34. Isotope production cross sections for neon fragments. Ar on Ar at 1.65 GeV/nucleon.

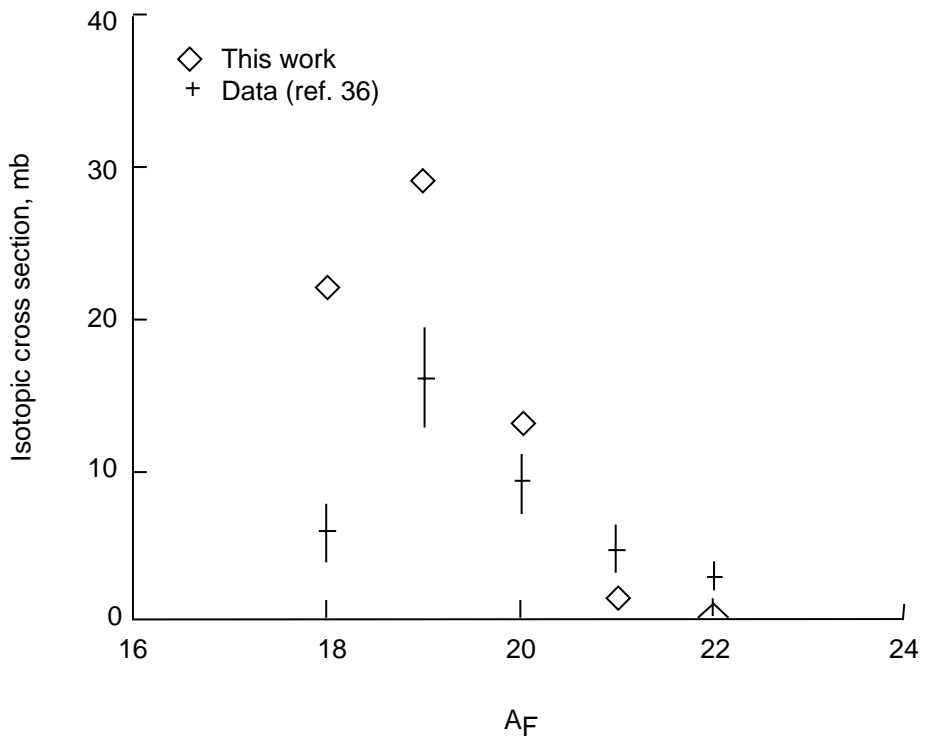


Figure 35. Isotope production cross sections for fluorine fragments. Ar on Ar at 1.65 GeV/nucleon.

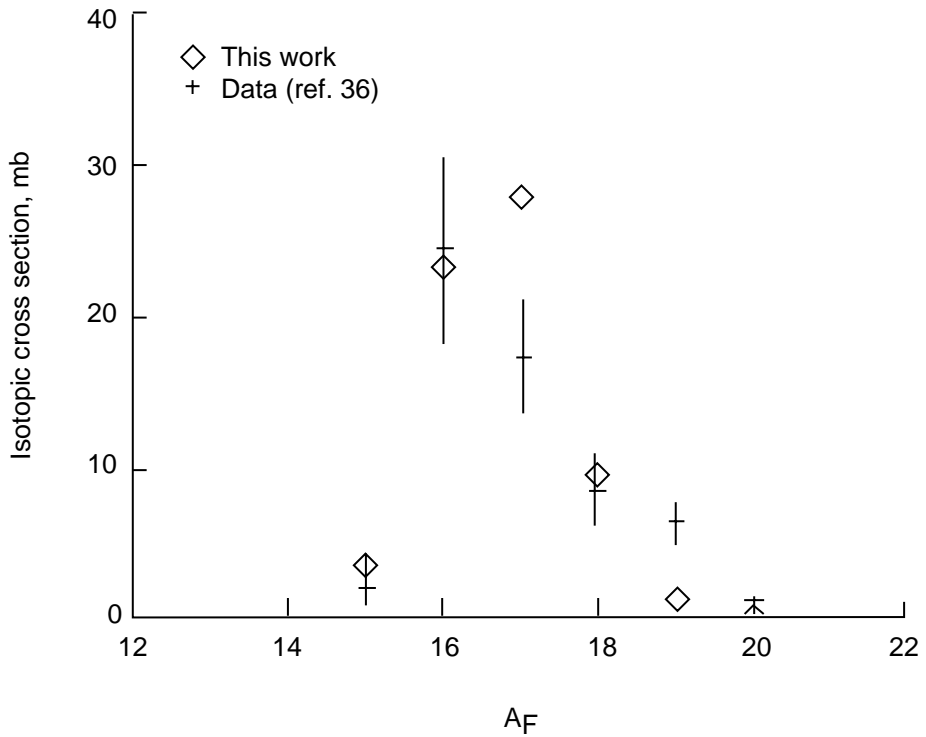


Figure 36. Isotope production cross sections for oxygen fragments. Ar on Ar at 1.65 GeV/nucleon.

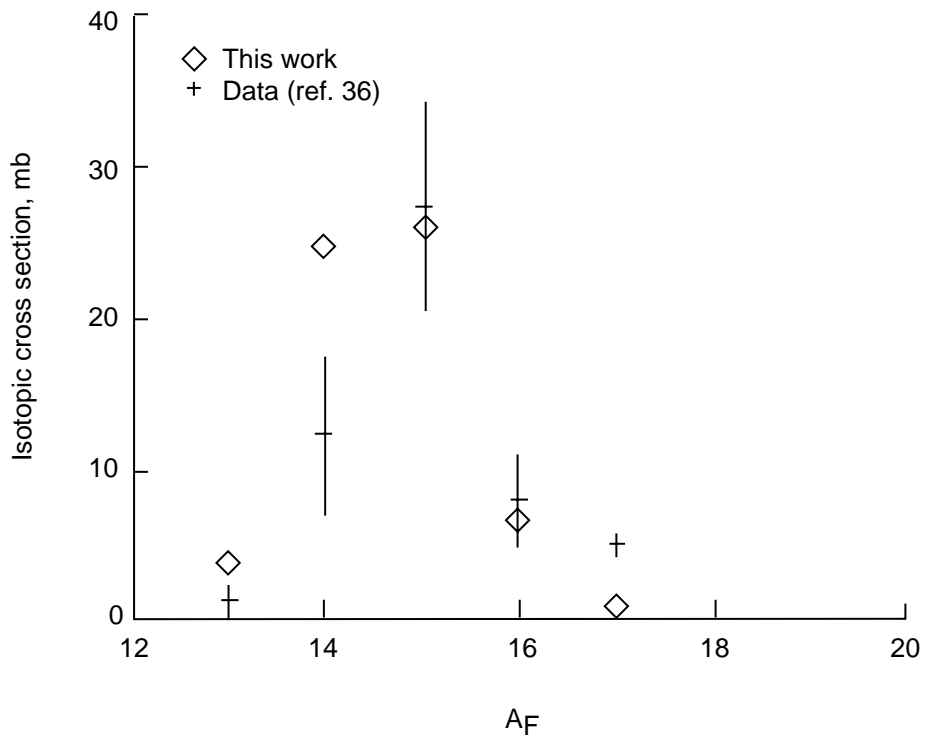


Figure 37. Isotope production cross sections for nitrogen fragments. Ar on Ar at 1.65 GeV/nucleon.

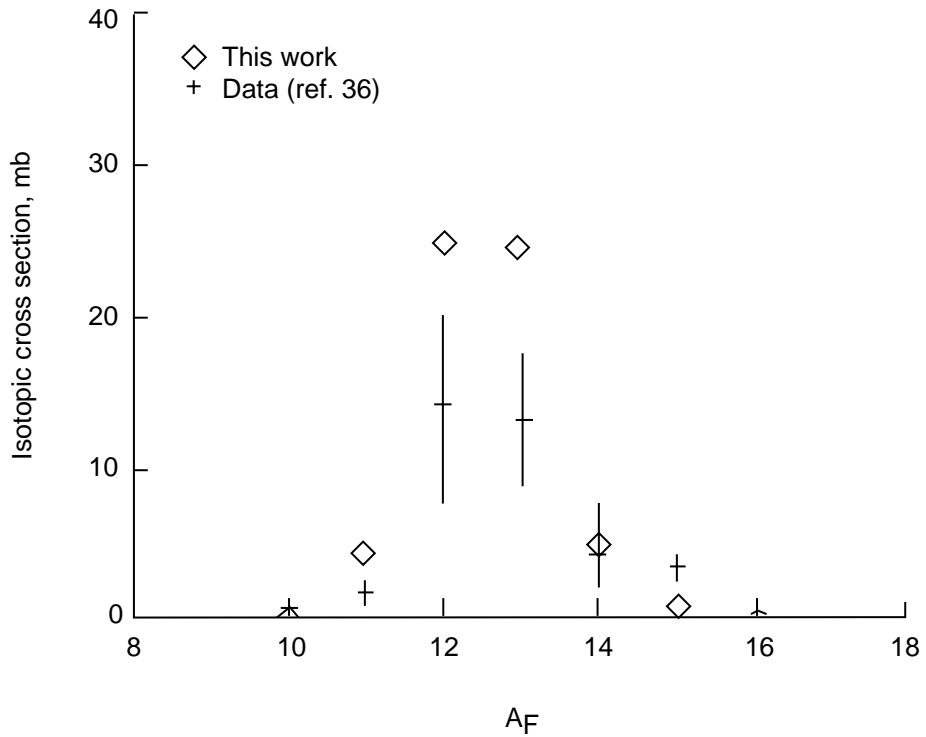


Figure 38. Isotope production cross sections for carbon fragments. Ar on Ar at 1.65 GeV/nucleon.

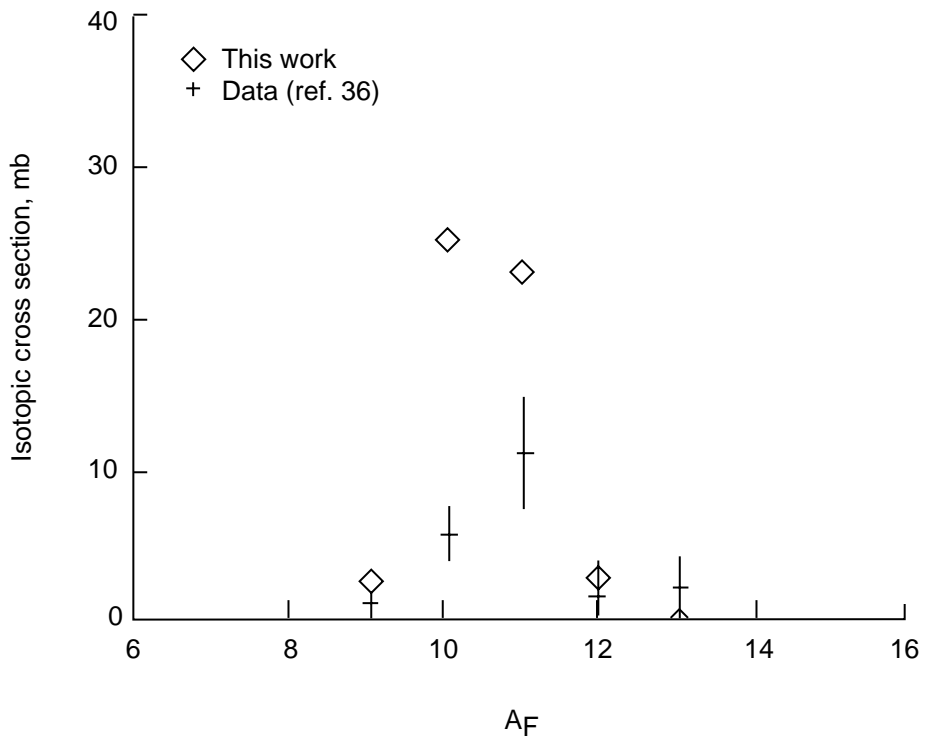


Figure 39. Isotope production cross sections for boron fragments. Ar on Ar at 1.65 GeV/nucleon.

Appendix A

Program Listing of Semiempirical Nuclear Fragmentation Program HZEFRG1

Appendix A contains the program listing of the semiempirical nuclear fragmentation program HZEFRG1, which consists of the main program (HZEFRAG), 7 function subprograms (FRAG, SNF, CROS, TEXP, TSQR, RADIUS, and XSEC), and 13 subroutines (YIELDEM, ASIGM, YIELDX, YIELDN, YIELDA, YIELDT, YIELDH, GEODA, BSEACH, LIMIT, GEOFR, BESSEL, and SORT).

```
C PROGRAM HZEFRG1(INPUT,OUTPUT,TAPE5=INPUT,TAPE6=OUTPUT,TAPE7)
C
C PURPOSE
C MAIN PROGRAM TO CALCULATE FRAGMENTATION CROSS SECTIONS OF PROJECTILE
C WITH PARTICULAR EMPHASIS ON COSMIC RAYS ENERGIES AND NUCLEI
C
C DESCRIPTION OF PARAMETERS
C IM - MAXIMUM MASS NUMBER OF PROJECTILE (CAN BE INCREASED TO HIGHER
C       VALUE IF NEEDED)
C ICH - MAXIMUM CHARGE NUMBER
C IEL - MAXIMUM ALLOWED NUMBER OF ISOTOPES FOR EACH ELEMENT
C IMM - MAXIMUM ONE DIMENSIONAL ARRAY USED FOR STORING NUCLEAR AND
C       ELECTROMAGNETIC CROSS SECTIONS
C A - ONE DIMENSIONAL ARRAY OF MASS NUMBERS FOR DIFFERENT CHARGES
C IZZ - TWO DIMENSIONAL ARRAY FOR STORING CHARGES OF EACH ISOTOPE
C IPP - TWO DIMENSIONAL ARRAY FOR STORING MASS NUMBER OF EACH ISOTOPE
C SIG - TWO DIMENSIONAL ARRAY FOR NUCLEAR CROSS SECTIONS
C SIGEM1 - TWO DIMENSIONAL ARRAY FOR STORING ELECTROMAGNETIC CROSS
C       SECTIONS FOR ONE NEUTRON REMOVAL FROM PROJECTILE
C SIGEM2 - TWO DIMENSIONAL ARRAY FOR STORING ELECTROMAGNETIC CROSS
C       SECTIONS FOR ONE PROTON REMOVAL FROM PROJECTILE
C IZZ2 - ONE DIMENSIONAL ARRAY FOR CHARGES OF ISOTOPES
C SIG2 - ONE DIMENSIONAL ARRAY FOR NUCLEAR CROSS SECTIONS OF ISOTOPES
C IPP2 - ONE DIMENSIONAL ARRAY FOR MASS NUMBERS OF ISOTOPES
C SIG3 - ONE DIMENSIONAL ARRAY FOR ELECTROMAGNETIC CROSS SECTIONS OF
C       ISOTOPES
C NLAY,XLAY,H - THESE OPTIONS ARE USEFUL FOR TRANSPORT CODES AND ARE
C       NOT USED HERE
C NAT - NUMBER OF TARGETS. PRESENT VERSION IS SET TO RUN FOR ONE
C       TARGET ONLY (NAT = 1)
C ATRG - MASS NUMBERS OF TARGETS (THIS OPTION IS USEFUL FOR TRANSPORT
C       CODES)
C ZTRG - CHARGES OF TARGETS (THIS OPTION IS USEFUL FOR TRANSPORT CODES)
C DENSTRG - DENSITY (WEIGHT FACTORS FOR DIFFERENT TARGETS (THIS OPTION
C       IS USEFUL FOR TRANSPORT CODES))
C
C TAPE7 IS THE OUTPUT
C
C PARAMETER(IM=257,ICH=103,IEL=5,IMM=IM*IEL)
C
C DIMENSION A(ICH),IZZ(IM,IEL),IPP(IM,IEL),SIG(IM,IEL)
C DIMENSION SIGEM1(IM,IEL),SIGEM2(IM,IEL)
C DIMENSION IZZ2(IMM),SIG2(IMM),IPP2(IMM),SIG3(IMM)
C COMMON/TARGET/NLAY,XLAY,H,NAT,ATRG(5),ZTRG(5),DENSTRG(5)
C
C DATA A/1.008,4.0026,6.941,9.012,10.81,12.011,14.007,15.999,
+18.998,20.18,22.99,24.31,26.98,28.09,30.974,32.07,35.453,
```

```

+39.948,39.10,40.08,44.96,47.88,50.94,52.,54.94,55.85,58.93,
+58.69,63.55,65.39,69.72,72.61,74.92,78.96,79.904,83.8,85.47,
+87.62,88.91,91.22,92.91,95.94,97.91,101.07,102.91,106.42,107.87,
+112.41,114.82,118.71,121.76,127.6,126.9,131.29,132.91,137.33,
+138.91,140.11,140.91,144.24,144.91,150.36,151.96,157.25,158.93,
+162.5,164.93,167.26,168.93,173.04,174.97,178.49,180.95,183.85,
+186.2,190.2,192.2,195.09,196.97,200.59,204.38,207.2,208.98,
+208.99,209.99,222.02,223.02,226.03,227.03,232.04,231.04,238.03,
+237.05,244.06,243.06,247.07,247.07,251.08,252.08,257.10,258.10,
+259.10,262.11/
C
C      DATA IZZ,IPP,SIG,SIGEM1,SIGEM2/IMM*0,IMM*0,IMM*0.,IMM*0.,IMM*0./
C      DATA IZZ2,SIG2,IPP2,SIG3/IMM*0,IMM*0.,IMM*0,IMM*0./
C
C      KOUNT=0
C      KOUNT2=0
C      KDUM1=0
C      KDUM2=0
C      SUM=0.
C      SUMNUC=0.
C      SUMEM=0.
C      ITRAP=0
C
C      PROJ. ENERGY IN MEV/NUCLEON
C
C      WRITE(6,1)
C      WRITE(7,1)
C      READ(5,*) ENG
C      WRITE(7,*) ENG
C
C      CHARGE AND MASS OF PROJ.
C
C      WRITE(6,12)
C      WRITE(7,12)
C      READ (5,*) ZZP,AZP
C      WRITE(7,*) ZZP,AZP
C      ICHARGE = ZZP
C
C      CHARGE AND MASS OF TARGET
C
C      WRITE(6,5)
C      WRITE(7,5)
C      READ (5,*) ZZT,AZT
C      WRITE(7,*) ZZT,AZT
C
C      FOLLOWING FOUR OPTIONS ARE MAINLY FOR TRANSPORT CODES
C
C      NAT=1
C      ATRG(1)=AZT
C      ZTRG(1)=ZZT
C      DENSTRG(1)=1.
C
C      CALCULATE ELECTROMAGNETIC CROSS SECTIONS
C
C      CALL YIELDDEM(AZP,ZZP,AZT,ZZT,AZP-1.,ZZP,ENG,DUM2)

```

```

CALL YIELDEM(AZP,ZZP,AZT,ZZT,AZP-1.,ZZP-1.,ENG,DUM1)
IPROJ=AZP
C
C   UPPER LIMIT OF LOOP 10 IS = IPROJ-1
C
C   ITOP=IPROJ-1
C
C   DO 10 J=1,ITOP
KOUNT=KOUNT+1
IP=IPROJ-J
AP=IP
IZ=AP/(1.+SNF(AP))+.5
IZM=IZ-3
C
DO 10 I=1,5
KOUNT2=KOUNT2+1
IZ=IZM+I
IZZ(J,I)=IZ
IPP(J,I)=IP
IF((IZ.GT.ICHARGE).OR.(IZ.LT.1))THEN
SIG(J,I)=-1.
GO TO 10
END IF
C
QQQJ=FRAG(ICLAGE,IPROJ,IZ,IP,ENG)
CALL ASTIGM(ENG,AZP,ZZP,SIGMA)
C
QQQJ=QQQJ*SIGMA*1.E27
SIG(J,I)=QQQJ
IF(IZ.EQ.ICLAGE.AND.KDUM1.EQ.0) THEN
SIGEM1(J,I)=DUM2
KDUM1=1
ELSE
SIGEM1(J,I)=0.0
END IF
IF(IZ.EQ.ICLAGE-1.AND.KDUM2.EQ.0) THEN
SIGEM2(J,I)=DUM1
KDUM2=1
ELSE
SIGEM2(J,I)=0.0
END IF
10 CONTINUE
C
CALL SORT(IZZ,IPP,SIG,SIGEM1,SIGEM2,KOUNT,KOUNT2,ICLAGE,
+IZZ2,SIG2,IPP2,SIG3)
C
WRITE(6,67)
WRITE(7,67)
C
DO 3 I=1,KOUNT2
IF((IZZ2(I).GT.ICLAGE).OR.(IZZ2(I).LT.1)) GO TO 3
IF(SIG2(I).EQ.-1.) GO TO 3
IF(ITRAP.NE.0) GO TO 34
WRITE(6,11)
WRITE(7,11)

```

```

34 CONTINUE
C
      WRITE(6,109) IZZ2(I),IPP2(I),SIG2(I),SIG3(I),SIG2(I)+SIG3(I)
      WRITE(7,109) IZZ2(I),IPP2(I),SIG2(I),SIG3(I),SIG2(I)+SIG3(I)
      SUM=SUM+SIG2(I)+SIG3(I)
      SUMNUC=SUMNUC+SIG2(I)
      SUMEM=SUMEM+SIG3(I)
      IF(IZZ2(I).NE.IZZ2(I+1)) WRITE(6,111) SUMNUC,SUMEM,SUM
      IF(IZZ2(I).NE.IZZ2(I+1)) WRITE(7,111) SUMNUC,SUMEM,SUM
      IF(IZZ2(I).NE.IZZ2(I+1)) WRITE(6,108)
      IF(IZZ2(I).NE.IZZ2(I+1)) WRITE(7,108)
      IF(IZZ2(I).NE.IZZ2(I+1)) THEN
         SUM=0.
         SUMNUC=0.
         SUMEM=0.
         END IF
      IF(IZZ2(I).EQ.IZZ2(I+1)) THEN
         ITRAP=1
         ELSE
         ITRAP=0
         END IF
3 CONTINUE
C
      1 FORMAT(' INPUT PROJ. ENERGY IN MEV/NUCLEON ?')
      5 FORMAT(' INPUT CHARGE AND MASS OF TARGET ?')
     11 FORMAT(1X,'CHARGE (ZF)',4X,'MASS (AF)',6X,'NUC.FRAG. CRS. (MB)',,
     +6X,'E1+E2 FRAG CRS (MB)',6X,'(NUC+E1+E2) FRAG CRS (MB)',/,,
     +1X,11('='),4X,9('='),2(6X,19('=')),6X,26('='),/)
     12 FORMAT(' INPUT CHARGE AND MASS OF PROJ. ?')
     67 FORMAT(/)
     108 FORMAT(/,106(''),/)
     109 FORMAT(5X,I3,10X,I3,3(10X,G16.8))
     111 FORMAT(31X,19(''),6X,19(''),6X,26(''),/,31X,
     +G16.8,10X,G16.8,9X,'TOTAL = ',G16.8)
         STOP
         END
C
C*****SUBROUTINE SORT(IZZ,IPP,SIG,SIGEM1,SIGEM2,KOUNT,KOUNT2,ICHARGE,
+C
+C PURPOSE
+C TO CONVERT TWO DIMENSIONAL ARRAYS OF IZZ,IPP,SIG,SIGEM1,SIGEM2 INTO
+C ONE DIMENSIONAL ARRAY OF IZZ2,IPP2,SIG2,AND SIG3 AND ARRANGE ONE
+C DIMENSIONAL ARRAYS IN DESCENDING ORDER OF IZZ2
+C
+C DESCRIPTION OF PARAMETERS
+C SAME AS IN MAIN PROGRAM
+C
+C USAGE
+C CALL SORT(IZZ,IPP,SIG,SIGEM1,SIGEM2,KOUNT,KOUNT2,ICHARGE,
+C
+C PARAMETER(IM=257,ICH=103,IEL=5,IDUM=IM*IEL)

```

```

C
DIMENSION IZZ(IM,IEL),IPP(IM,IEL),SIG(IM,IEL)
DIMENSION IZZ2(IDUM),SIG2(IDUM),IPP2(IDUM)
DIMENSION SIG3(IDUM),SIGEM1(IM,IEL),SIGEM2(IM,IEL)

C
DO 1 I=1,5

C
DO 2 J=1,KOUNT
IZZ2(J+(I-1)*KOUNT)=IZZ(J,I)
IPP2(J+(I-1)*KOUNT)=IPP(J,I)
SIG2(J+(I-1)*KOUNT)=SIG(J,I)
IF(SIGEM1(J,I).NE.0.) THEN
SIG3(J+(I-1)*KOUNT)=SIGEM1(J,I)
ELSE
SIG3(J+(I-1)*KOUNT)=SIGEM2(J,I)
END IF
2 CONTINUE

C
1 CONTINUE

C
DO 10 I=1,KOUNT2-1
N=I+1

C
DO 10 J=N,KOUNT2
IF(IZZ2(I).GE.IZZ2(J)) GO TO 10
TEMP=IZZ2(I)
IZZ2(I)=IZZ2(J)
IZZ2(J)=TEMP
TEMP=IPP2(I)
IPP2(I)=IPP2(J)
IPP2(J)=TEMP
TEMP=SIG2(I)
SIG2(I)=SIG2(J)
SIG2(J)=TEMP
TEMP=SIG3(I)
SIG3(I)=SIG3(J)
SIG3(J)=TEMP
10 CONTINUE

C
RETURN
END

C*****
C      NUCLEAR FRAGMENTATION OF LARC
C
FUNCTION FRAG(IZP,IAP,JZF,JAF,EN)

C
C      PURPOSE
C      FUNCTION FRAG CALCULATES FRAGMENTATION PROBABILITY FOR
C      MATERIAL FOR SPECIFIC ISOTOPE
C
C      DESCRIPTION OF PARAMETERS
C      IZP - CHARGE OF PROJECTILE
C      IAP - MASS NUMBER OF PROJECTILE

```

```

C   JZF - CHARGE OF FRAGMENT
C   JAF - MASS NUMBER OF FRAGMENT
C   EN - LAB ENERGY MEV/NUCLEON
C
C   USAGE
C   RESULT = FRAG(IZP,IAP,JZF,JAF,EN)
C
C           COMMON/TARGET/NLAY,XLAY,H,NAT,ATRG(5),ZTRG(5),DENSTRG(5)
C
C   IZ=IZP
C   ZP=IZ
C   AP=IAP
C   EJ=EN
C   IF(EJ.LT.10) EJ=10.
C   QTOT=0.
C
C   DO 1 I=1,NAT
C   JZT=ZTRG(I)
C   JAT=ATRG(I)
C   IF(JAT.EQ.1) CALL YIELDX(IZP,IAP,JZF,JAF,EJ,QJ)
C   AT=JAT
C   ZT=JZT
C   AP=IAP
C   ZP=IZP
C   ZF=JZF
C   AF=JAF
C   QTRG=QJ
C   IF(JAT.GT.2)CALL YIELDH(AP,ZP,AT,ZT,AF,ZF,EJ,QJ,SOG,SIGT)
C   QTOT=QTOT+DENSTRG(I)*QJ
1 CONTINUE
C
C   CALL ASIGM (EN,AP,ZP,SIGMA)
C   QTOT=QTOT*1.E-27/SIGMA
5 CONTINUE
FRAG=QTOT
IZP=IZ
RETURN
END
C
C*****
C
C   SUBROUTINE ASIGM(EN,A,Z,SIGMA)
C
C   PURPOSE
C   THIS SUBROUTINE GENERATES ION TARGET CROSS SECTIONS FOR ARBITRARY
C   ION TYPE AS A FUNCTION OF ENERGY IN MEV/NUCLEON
C   CROSS SECTIONS IN UNITS OF CM**-1
C
C   DESCRIPTION OF PARAMETRS
C   EN - LAB ENERGY MEV/NUCLEON
C   A - MASS OF ION
C   Z - CHARGE OF ION
C   SIGMA - CROSS SECTIONS IN UNITS OF CM**-1
C
C   USAGE

```

```

C CALL ASIGM(EN,A,Z,SIGMA)
C
C COMMON/TARGET/NLAY,XLAY,H,NAT,ATRG(5),ZTRG(5),DENSTRG(5)
C
C EP=EN
C SIGMA=0.
C
C DO 111 ITAR=1,NAT
C ZT=ZTRG(ITAR)
C AT=ATRG(ITAR)
C SIGMT=XSEC(A,Z,AT,ZT,EP)
C SIGMA=SIGMA+DENSTRG(ITAR)*SIGMT*1.E-27
111 CONTINUE
C
C RETURN
C END
C
C*****
C FUNCTION XSEC(A,Z,AT,ZT,E)
C
C PURPOSE
C FUNCTION XSEC IS TOTAL ABSORPTION CROSS SECTION (MB)
C
C DESCRIPTION OF PARAMETERS
C A - MASS OF ION
C Z - CHARGE OF ION
C AT - MASS OF TARGET
C ZT - CHARGE OF TARGET
C E - LAB ENERGY MEV/NUCLEON
C
C USAGE
C RESULT = XSEC(A,Z,AT,ZT,E)
C
C COMMON/PIE/PI
C
C XS(A1,A2)=10.*PI*(RADIUS(A1)+RADIUS(A2)-0.504)**2
C
C PI=3.1415927
C XXX=XS(A,AT)
C EK=E+1.E-7
C SHE=1.-.62*TEXP(-EK/200.)*SIN(10.9*EK**(-.28))
C IF(A.EQ.1.)XXX=45.*AT**.7*(1.+0.016*SIN(5.3-2.63* ALOG(AT)))*SHE
C IF(AT.EQ.1.)XXX=45.*A**.7*(1.+0.016*SIN(5.3-2.63* ALOG(A)))*SHE
C
C THE POST FACTOR PLACES A 10 MEV THRESHOLD IN XSEC
C
C XSEC=XXX/(1.+TEXP(-2.*(E-10.)))
C
C IF(A*AT.GT.1.) RETURN
C
C THE NUCLEON-NUCLEON INELASTIC EVENTS NOT YET INCLUDED
C
C IF(Z*ZT.EQ.1.) XSEC=0.
C IF(Z*ZT.EQ.0.) XSEC=0.

```

```

RETURN
END
C
C*****SUBROUTINE YIELDEM(AP,ZP,AT,ZT,AF,ZF,TLAB,QJ)
C
C PURPOSE
C CALCULATES ELECTROMAGNETIC DISSOCIATION CROSS SECTIONS FOR ONE
C NUCLEON REMOVAL
C
C DESCRIPTION OF PARAMETERS
C AP - MASS OF PROJECTILE
C ZP - CHARGE OF PROJECTILE
C AT - MASS OF TARGET
C ZT - CHARGE OF TARGET
C AF - MASS OF FRAGMENT
C ZF - CHARGE OF FRAGMENT
C TLAB - LAB ENERGY MEV/NUCLEON
C QJ - ELECTROMAGNETIC CROSS SECTION FOR ONE NUCLEON REMOVAL
C
C USAGE
C CALL YIELDEM(AP,ZP,AT,ZT,AF,ZF,TLAB,QJ)
C
      REAL MNCSQ,II,INT,INTD,INTQ,K0,K1,NDIP,NQUAD,NP,NT,MSTAR,JAY,NU
C
      XDEE=.25
      IF(AF.NE.AP-1.) RETURN
      NT=AT-ZT
      NP=AP-ZP
      PI=3.141592653589793238D0
      FSC=0.00729735D0
      HBARC=197.32858D0
      MNCSQ=938.95D0
C
C DIPOLE PARAMETERS
C
      JAY=36.8
      RZERO=1.18*AP**(.D0/3.D0)
      QPRIM=17.0
      EPS=0.0768
      MSTAR=0.7*MNCSQ
      UU=3.0*JAY/(QPRIM*AP**(.D0/3.D0))
      XFF=(1.0+EPS+3.0*UU)/(1.0+EPS+UU)
      EGDR=HBARC/SQRT(MSTAR*RZERO**2*(1.0+UU-XFF*EPS)/(8.0*JAY))
      FTRK=1.0
C
C QUADRUPOLE PARAMETERS
C
      IF(AP.GT.100.0) FEWSR=0.9
      IF(AP.LE.100.0) FEWSR=0.6
      IF(AP.LE.40.0) FEWSR=0.3
      EGQR=63.0/AP**(.D0/3.D0)
C
      IF(ZP.GE.14.0) GP=1.95*EXP(-0.075*ZP)

```

```

IF(ZP.LT.14.0) GP=0.7
IF(ZP.LE.8.0) GP=0.6
IF(ZP.LT.6.0) GP=0.5
C
GAMMA=1.0+TLAB/MNCSQ
VEL=SQRT(1.0-1.0/GAMMA**2)
HL=1.0/3.0
HLL=-HL
BMIN=1.34*(AP**HL+AT**HL-0.75*(AP**HLL+AT**HLL))
DEEHILL=XDEE*BMIN
C
C DEEHILL IS THE ONLY 'FUDGE' FACTOR IN THE CODE
C
BMIN=BMIN+DEEHILL
REDMAS=(AP*AT/(AP+AT))*MNCSQ
C
C NOW APPLY BERTULANI LOW ENERGY CORRECTION TO BMIN
C
BMIN=BMIN+PI*ZT*ZP*FSC*HARC/(2.*GAMMA*REDMAS*VEL**2)
C
SIGD=60.*NP*ZP/AP
SIGQ=FEWSR*0.00022*ZP*AP**(.3.)
ECUTOF=HARC*GAMMA*VEL/BMIN
GD=EGDR/ECUTOF
GQ=EGQR/ECUTOF
CALL BESSEL(GD,K0,K1)
C
NDIP=((2.0*ZT**2*FSC)/(EGDR*PI*VEL**2))*
+(GD*K0*K1-0.5*VEL**2*GD**2*(K1**2-K0**2))
CALL BESSEL(GQ,K0,K1)
NQUAD=((2.0*ZT**2*FSC)/(EGQR*PI*VEL**4))*
+(2.0*(1.0-VEL**2)*K1**2 + GQ*(2.0-VEL**2)**2*K0*K1
+-0.5*VEL**4*GQ**2*(K1**2-K0**2))
INTD=SIGD*NDIP
INTQ=SIGQ*NQUAD*EGQR**2
TOT=INTD+INTQ
IF(ZP.EQ.ZF+1.) QJ=GP*TOT
IF(ZP.EQ.ZF) QJ=(1.-GP)*TOT
C
RETURN
888 CONTINUE
STOP
END
C
*****
C SUBROUTINE BESSEL(G,K0,K1)
C
C PURPOSE
C CALCULATES MODIFIED BESSEL FUNCTION OF SECOND KIND
C
C DESCRIPTION OF PARAMETERS
C G - INPUT ARGUMENT
C K0 - OUTPUT K0(G)
C K1 - OUTPUT K1(G)

```

```

C   A - ARRAY OF COEFFICIENTS OF APPROXIMATING POLYNOMIALS
C   B - ARRAY OF COEFFICIENTS OF APPROXIMATING POLYNOMIALS
C
C   USAGE
C   CALL BESSEL(G,K0,K1)
C
C       DIMENSION A(30),B(27)
C
C       REAL IO,I1,K0,K1
C
C       DATA (A(I),I=1,30)/
+3.5156229,3.0899424,1.2067492,.2659732,.0360768,.0045813,
+.39894228,.01328592,.00225319,.00157565,.00916281,.02057706,
+.02635537,.01647633,.00392377,.87890594,.51498869,.15084934,
+.02658733,.00301532,.00032411,.39894228,.03988024,.00362018,
+.00163801,.01031555,.02282967,.02895312,.01787654,.00420059/
        DATA (B(I),I=1,27)/
+.57721566,.42278420,.23069756,.0348859,.00262698,.0001075,
+.0000074,1.25331414,.07832358,.02189568,.01062446,.00587872,
+.00251540,.00053208,.15443144,.67278579,.18156897,.01919402,
+.00110404,.00004686,1.25331414,.23498619,.03655620,.01504268,
+.00780353,.00325614,.00068245/
C
T=G/3.75
IF(G.LE.3.75) THEN
  IO=1.+A(1)*T**2+A(2)*T**4+A(3)*T**6+A(4)*T**8+A(5)*T**10
  ++A(6)*T**12
  I1=G*(.5+A(16)*T**2+A(17)*T**4+A(18)*T**6+A(19)*T**8
  ++A(20)*T**10+A(21)*T**12)
ELSE
  IO=1./SQRT(G)*EXP(G)*(A(7)+A(8)/T+A(9)/T**2-A(10)/T**3
  ++A(11)/T**4-A(12)/T**5+A(13)/T**6-A(14)/T**7+A(15)/T**8)
  I1=1./SQRT(G)*EXP(G)*(A(22)-A(23)/T-A(24)/T**2+A(25)/T**3
  +-A(26)/T**4+A(27)/T**5-A(28)/T**6+A(29)/T**7-A(30)/T**8)
END IF
S=G/2.
IF(G.LE.2.) THEN
  K0=-ALOG(S)*IO-B(1)+B(2)*S**2+B(3)*S**4+B(4)*S**6+B(5)*S**8
  ++B(6)*S**10+B(7)*S**12
  K1=ALOG(S)*I1+1./G*(1.+B(15)*S**2-B(16)*S**4-B(17)*S**6-
  +B(18)*S**8-B(19)*S**10-B(20)*S**12)
ELSE
  K0=1./SQRT(G)*EXP(-G)*(B(8)-B(9)/S+B(10)/S**2-B(11)/S**3
  ++B(12)/S**4-B(13)/S**5+B(14)/S**6)
  K1=1./SQRT(G)*EXP(-G)*(B(21)+B(22)/S-B(23)/S**2+B(24)/S**3
  +-B(25)/S**4+B(26)/S**5-B(27)/S**6)
END IF
RETURN
END
C
C*****
C
SUBROUTINE YIELDX(IZ, IA, JZ, JA, EJ, QJ)
C
C   PURPOSE

```

```

C CALLS VARIOUS SUBROUTINES DEPENDING ON MASS OF FRAGMENT
C AF = 1 : YIELDN
C AF = 2,3 : YIELDT
C AF = 4 : YIELDA
C AF > 4 : CROS
C
C DESCRIPTION OF PARAMETERS
C IZ - CHARGE OF PROJECTILE
C IA - MASS NUMBER OF PROJECTILE
C JZ - CHARGE OF FRAGMENT
C JA - MASS NUMBER OF FRAGMENT
C EJ - LAB ENERGY MEV/NUCLEON
C QJ - OUTPUT FRAGMENTATION CROSS SECTION
C
C USAGE
C CALL YIELDX(IZ, IA, JZ, JA, EJ, QJ)
C
    QJ = 0
    IF(IZ+1.LT.JZ) RETURN
    IF(IA.LT.JA) RETURN
    IF(JA.LE.0.OR.JZ.LT.0) RETURN
    IF(JA.EQ.1.AND.JZ*JZ.LE.1) CALL YIELDN(IZ,IA,JZ,JA,EJ,QJ)
    IF(JA.EQ.4) CALL YIELDA(IZ,IA,JZ,JA,EJ,QJ)
    IF(JA.EQ.2.OR.JA.EQ.3) CALL YIELDT(IZ,IA,JZ,JA,EJ,QJ)
    IF(JA.LE.4) RETURN
    AP=IA
    ZF=JZ
    AF=JA
    IF(IZ*IA.EQ.JZ*JA) RETURN
C
C IF FRAGMENTS MASS IS GREATER THAN 4 USE RUDSTAM
C
    QJ=CROS(AP,ZF,AF,EJ)
    IF((IA-JA).GT.1)GO TO 2001
    IF((IZ-JZ).GE.0.AND.(IZ-JZ).LE.1)QJ=0.04
2001 CONTINUE
    SIGMA=45.*AP**.7*(1.+0.016*SIN(5.3-2.62* ALOG(AP)))
    IF(EJ.GT.2000.) GO TO 2000
    SIGMA=SIGMA*(1.-62*TEXP(-EJ/200.)*SIN(10.6/EJ**.2))
2000 CONTINUE
    QJ=QJ*SIGMA
    IF(JA.EQ.8) QJ=QJ/10.
    RETURN
    END
C
C*****
C
C FUNCTION SNF(A)
C
C PURPOSE
C FUNCTION SNF RELATES MASS AND CHARGE ON NUCLEAR STABILITY CURVE
C
C DESCRIPTION OF PARAMETERS
C A - MASS OF NUCLEUS (OUTPUT IS THE CHARGE NUMBER)
C

```

```

C   USAGE
C   RESULT = SNF(A)
      SNF=1.011363617+A*(3.522612875E-3-A*5.340775146E-6)
      RETURN
      END
C
C ****
C
C   SUBROUTINE YIELDN(IZP,IAP,IZF,IAF,EJ,QJ)
C
C   PURPOSE
C   SUBROUTINE YIELDN IS BERTINI NUCLEON PRODUCTION IN COLLISION WITH
C   PROTONS
C
C   DESCRIPTION OF PARAMETERS
C   IZP - CHARGE OF PROJECTILE
C   IAP - MASS OF PROJECTILE
C   IZF - CHARGE OF FRAGMENT
C   IAF - MASS OF FRAGMENT
C   EJ - LAB ENERGY MEV/NUCLEON
C   QJ - OUTPUT FRAGMENTATION CROSS SECTION
C
C   USAGE
C   CALL YIELDN(IZP,IAP,IZF,IAF,EJ,QJ)
C
C   DIMENSION AT(10),AH(10,2),AL(10,2),CN(10,2)
C
C   DATA AT/1.,2.,3.,4.,5.,6.,12.,16.,27.,64./
C   DATA AH/0.,0.,0.,0.,.34,.42,.42,.54,.48,
C   +.34,.34,.34,0.,.39,.2,.2,.32,.56/
C   DATA AL/0.,0.,0.,0.,.33,.396,.407,.322,.411,
C   +0.,0.,0.,0.,.22,.24,.26,.387,.619/
C   DATA CN/0.,1.,1.5,1.,1.,1.29,1.42,1.71,4.19,
C   +2.,2.,2.,1.5,1.,1.,2.14,2.42,2.69,2.56/
C
C   N=IZF+1
C   AP=IAP
C   EN=EJ/AP
C   A3=AP**.6667
C   IF(IAP.GT.6) GO TO 10
C   SIG =45.*AP**.7*(1.+0.016*SIN(5.3-2.62* ALOG(AP)))
C   IF(EN.GT.2000.) GO TO 2000
C   SIG =SIG *(1-.62*TEXP(-EN/200.)*SIN(10.6/EN**.28))
2000 CONTINUE
      IF( EN.LT.400.) QJ=CN(IAP,N)*(EN/400.)**AL(IAP,N)
      IF( EN.GE.400.) QJ=CN(IAP,N)*(EN/400.)**AH(IAP,N)
      QJ=QJ*SIG
      RETURN
10 IF(IAP.GT.12) GO TO 12
      IAT=7
      A1=6.**.6667
      A2=12.**.6667
      GO TO 100
12 IF(IAP.GT.16) GO TO 16
      IAT=8

```

```

A1=12.**.6667
A2=16.**.6667
GO TO 100
16 IF(IAP.GT.27) GO TO 27
IAT=9
A1=16.**.6667
A2=27.**.6667
GO TO 100
27 IAT=10
A1=27.**.66667
A2=64.**.6667
100 IF(EN.GT.400.) GO TO 200
Q2=CN(IAT,N)*(EN/400.)**AL(IAT,N)
IAT=IAT-1
Q1=CN(IAT,N)*(EN/400.)**AL(IAT,N)
QJ=Q2+(Q1-Q2)*(A3-A2)/(A1-A2)
SIG =45.*AP**.7*(1.+016*SIN(5.3-2.62* ALOG(AP)))
IF(EN.GT.2000.) GO TO 2001
SIG =SIG *(1-.62*TEXP(-EN/200.)*SIN(10.6/EN**.28))
2001 CONTINUE
QJ=QJ*SIG
RETURN
200 Q2=CN(IAT,N)*(EN/400.)**AH(IAT,N)
IAT=IAT-1
Q1=CN(IAT,N)*(EN/400.)**AH(IAT,N)
QJ=Q2+(Q1-Q2)*(A3-A2)/(A1-A2)
SIG =45.*AP**.7*(1.+016*SIN(5.3-2.62* ALOG(AP)))
IF(EN.GT.2000.) GO TO 2002
SIG =SIG *(1-.62*TEXP(-EN/200.)*SIN(10.6/EN**.28))
2002 CONTINUE
QJ=QJ*SIG
RETURN
END
C
C*****
C
C      SUBROUTINE YIELDA(IZP,IAP,IZF,IAF,EJ,QJ)
C
C      PURPOSE
C      SUBROUTINE YIELDA IS BERTINI ALPHA PRODUCTION IN COLLISION WITH PROTONS
C
C      DESCRIPTION OF PARAMETERS
C      IZP - CHARGE OF PROJECTILE
C      IAP - MASS OF PROJECTILE
C      IZF - CHARGE OF FRAGMENT
C      IAF - MASS OF FRAGMENT
C      EJ - LAB ENERGY MEV/NUCLEON
C      QJ - OUTPUT FRAGMENTATION CROSS SECTION
C
C      USAGE
C      CALL YIELDA(IZP,IAP,IZF,IAF,EJ,QJ)
C
EJ=EJ/IAP
IF(IZF.EQ.2 ) GO TO 2
QJ=0.

```

```

RETURN
2 AP=IAP
AP3=AP**.33333
IF(IAP.LE.16) GO TO 16
IF(IAP.LT.27) GO TO 27
QJU=.009*EJ**.4
IF(EJ.LE.400.) GO TO 27
QJU=7.26E-4*EJ**.82
IF(EJ.LT.2700.) GO TO 27
QJU=.473
27 QJL=.055*EJ**.4
IF(EJ.LT.110.) GO TO 100
QJL=.36
IF(EJ.LT.460.) GO TO 100
QJL=3.6E-3*EJ**.75
IF(EJ.LT.900.) GO TO 100
QJL=.59
100 IF(IAP.LT.27) GO TO 110
QJ=QJL+(QJU-QJL)*(AP3-3.)
GO TO 155
110 CONTINUE
QJU=QJL
16 QJL=.162*EJ**.35
IF(EJ.LT.50.) GO TO 120
QJL=.637
IF(EJ.LT.300) GO TO 120
QJL=.321*EJ**.12
IF(EJ.LT.600.) GO TO 120
QJL=.692
120 CONTINUE
IF(IAP.LE.16) GO TO 130
QJ=QJL+(QJU-QJL)*(AP3-2.52)/.48
GO TO 155
130 CONTINUE
QJ=QJL*(16./AP)**.3
IF(IAP.LT.5) QJ=0.
155 SIG =45.*AP**.7*(1.+.016*SIN(5.3-2.62* ALOG(AP)))
IF(EJ.GT.2000.) GO TO 2000
SIG =SIG *(1.-.62*TEXP(-EJ/200.)*SIN(10.6/EJ**.28))
2000 CONTINUE
QJ=QJ*SIG
EJ=EJ*AP
RETURN
END
C
C*****
C
C      SUBROUTINE YIELDT(IZP,IAP,IZF,IAF,EJ,QJ)
C
C      PURPOSE
C      SUBROUTINE YIELDT IS BERTINI MASS 3 PRODUCTION IN COLLISION WITH PROTONS
C
C      DESCRIPTION OF PARAMETERS
C      IZP - CHARGE OF PROJECTILE
C      IAP - MASS OF PROJECTILE

```

```

C   IZF - CHARGE OF FRAGMENT
C   IAF - MASS OF FRAGMENT
C   EJ - LAB ENERGY MEV/NUCLEON
C   QJ - OUTPUT FRAGMENTATION CROSS SECTION
C
C   USAGE
C   CALL YIELDT(IZP,IAP,IZF,IAF,EJ,QJ)
C
C       DIMENSION A(3),F(3,3)
C
C       DATA F/.32,.025,.05,.57,.071,.11,2.,.4,.3/
C       DATA A/16.,27.,64./
C
C       ITYPE=0
C       AP=IAP
C       AP3=AP**.3333
C       QJ=0.
C       IF(IZF.GT.2.OR.IZF.LT.1) RETURN
C       CALL YELDA(IZP,IAP,2,4,EJ,QJA)
C       IF(IZF.EQ.1.AND.IAF.EQ.2)ITYPE=1
C       IF(IZF.EQ.1.AND.IAF.EQ.3)ITYPE=2
C       IF(IZF.EQ.2.AND.IAF.EQ.3) ITYPE=3
C       IF(ITYPE.EQ.0) RETURN
C       IF(IAP.LE.5) GO TO 5
C       IF(IAP.LE.16)GO TO 16
C       IF(IAP.LE.27.) GO TO 27
C       FAC=F(ITYPE,2)+(F(ITYPE,3)-F(ITYPE,2))*(AP3-3.)
C       QJ=FAC*QJA
C       RETURN
5  CONTINUE
C       IF(IAP.EQ.5) RETURN
C       IF(IAP.EQ.4.AND.ITYPE.GT.1)RETURN
C       IF(IAP.LT.3)RETURN
C       EN=EJ/AP
C       SIG =45.*AP**.7*(1.+0.016*SIN(5.3-2.62* ALOG(AP)))
C       IF(EN.GT.2000.) GO TO 2000
C       SIG =SIG *(1-.62*TEXP(-EN/200.)*SIN(10.6/EN**.28))
2000 CONTINUE
C       QJ=SIG/2.
C       RETURN
27  FAC=F(ITYPE,1)+(F(ITYPE,2)-F(ITYPE,1))*(AP3-2.52)/.48
C       QJ=FAC*QJA
C       RETURN
16  QJ=F(ITYPE,1)*QJA
C       RETURN
C       END
C
C ****
C
C   SUBROUTINE GEODA(E,AP,AT,AF,SIGT,SIG,ABR,ABL,SIGP,ABRP,ABLP)
C
C   PURPOSE
C   SUBROUTINE GEODA CALCULATES ABLATION AND ABRASION CROSS SEC.
C
C   DESCRIPTION OF PARAMETERS

```

```

C E - LAB ENERGY MEV/NUCLEON
C AP - MASS OF PROJECTILE
C AT - MASS OF TARGET
C AF - MASS OF FRAGMENT
C SIGT - ABSORPTION CROSS SECTION
C SIG - FRAGMENTATION CROSS SECTION
C ABR - OUTPUT; AVERAGE NUMBER OF ABRADED NUCLEONS WITH FSI
C ABL - OUTPUT; AVERAGE NUMBER OF ABLATED NUCLEONS WITH FSI
C ABRP - OUTPUT; AVERAGE NUMBER OF ABRADED NUCLEONS WITHOUT FSI
C ABLP - OUTPUT; AVERAGE NUMBER OF ABLATED NUCLEONS WITHOUT FSI
C
C USAGE
C CALL GEODA(E,AP,AT,AF,SIGT,SIG,ABR,ABL,SIGP,ABRP,ABLP)
C
C     RP = RADIUS (AP)
C     RT = RADIUS (AT)
C     BMAX=RP+RT
C     EG=E
C
C     FRAGMENTATION WITH FRICTIONAL SPECTATOR INTERACTION (F.S.I.)
C
C     CALL BSEACH(EG,AP,RP,RT,AF+.5,B2,ABR2,ABL2)
C     CALL BSEACH(EG,AP,RP,RT,AF-.5,B1,ABR1,ABL1)
C
C     SIG=10.*3.1415*(B2**2-B1**2)
C     SIGT=10.*3.1415*(BMAX-.504)**2
C     ABL=(ABL1+ABL2)/2.
C     ABR=(ABR1+ABR2)/2.
C
C     FRAGMENTATION WITHOUT F.S.I.
C
C     CALL BSEEK(EG,AP,RP,RT,AF+.5,B2,ABR2,ABL2)
C     CALL BSEEK(EG,AP,RP,RT,AF-.5,B1P,ABR1,ABL1)
C
C     SIGP IS FRAGMENTATION CROSS SECTION
C
C     SIGP=10.*3.1415*(B2**2-B1P**2)
C     SIGTP=10.*3.1415*(BMAX-.504)**2
C     ABLP=(ABL1+ABL2)/2.
C     ABRP=(ABR1+ABR2)/2.
C     IF(AF.EQ.1.)GO TO 17
C     IF(AF.EQ.5.) SIG=0.0
C     IF(AF.EQ.5.) SIGP=0.
C     IF(AF.EQ.8.)SIG=SIG/10.
C     IF(AF.EQ.8.) SIGP=SIGP/10.
C     IF(AF.EQ.9.)SIG=.5*SIG
C     IF(AF.EQ.9.) SIGP=.5*SIGP
C     RETURN
17 CONTINUE
C
C     CENTRAL COLLISION YIELD IF AF=1
C
C     SIG1=10.*3.1415*B1**2
C     SIG1P=10.*3.1415*B1P**2
C     ABL=ABL*SIG/(SIG+SIG1)

```

```

ABLP=ABLP*SIGP/(SIGP+SIG1P)
ABR=(ABR*SIG+AP*SIG1)/(SIG+SIG1)
ABRP=(ABRP*SIGP+AP*SIG1P)/(SIGP+SIG1P)
SIGP=SIGP+SIG1P
SIG=SIG+SIG1
200 FORMAT(1X,'AF ',F10.5,2X,'B1 ',F10.5,2X,'B2 ',F10.5)
      RETURN
      END
C
C*****
C
C      SUBROUTINE BSEARCH(E,AP,RP,RT,AF,B,ABR,ABL)
C
C      PURPOSE
C      SUBROUTINE BSEARCH USES A GEOMETRICAL APPROACH TO FIND ABR AND ABL
C      CALCULATES DELTAA AS A FUNCTION OF IMPACT PARAMETER
C      INCLUDES F.S.I.
C
C      DESCRIPTION OF PARAMETERS
C      E - LAB ENERGY MEV/NUCLEON
C      AP - MASS OF PROJECTILE
C      RT - RADIUS OF TARGET
C      RP - RADIUS OF PROJECTILE
C      AF - MASS OF FRAGMENT
C      B - OUTPUT; IMPACT PARAMETER
C      ABR - OUTPUT; ABRDED NUCLEONS
C      ABL - OUTPUT; ABLDED NUCLEONS
C
C      USAGE
C      CALL BSEARCH(E,AP,RP,RT,AF,B,ABR,ABL)
C
C          REAL RTT(5),ABRT(300,5,2),ABLT(300,5,2),BT(300,5,2)
C
C          DATA NUM,I NUM/0,0/
C
C          FSI=1.
C          ES=E
C
1 CONTINUE
IF(NUM.EQ.0) GO TO 9006
C
DO 9005 INNN=1,NUM
IFX=INNN
IF(RT.EQ.RTT(INNN)) GO TO 9001
9005 CONTINUE
C
9006 I NUM=I NUM+1
IF(I NUM.GT.5) I NUM=1
NUM=NUM+1
IF(NUM.GT.5) NUM=5
GO TO 9000
9001 INDEX=1.01+FSI
IAF=AF+.51
B=BT(IAF,IFX,INDEX)
ABR=ABRT(IAF,IFX,INDEX)
ABL=ABLT(IAF,IFX,INDEX)

```

```

      RETURN
9000 CONTINUE
      IF(AP.GT.300.)  WRITE(6,6969)
      IF(AP.GT.300.)  WRITE(6,6996)
      OFSI=FSI
      OAF=AF
      RTT(INUM)=RT
C
      DO 9002 IN=1,2
      FSI=IN-1
      UAF=AP-.5
C
      DO 9003 AFF=.5,UAF,1.
      AF=AFF
      ABLMIN=0.
      ABLMAX=0.
      ABRMIN=AP
      ABRMAX=0.
      BMAX=RT+RP
      BMIN=0.
      XAVE = 16.6/(ES**0.26)
      UN=RP/BMAX
      UM=RT/RP
      IIT=0
70  CONTINUE
      IF(IIT.EQ.13)GO TO 2000
      B=(BMAX+BMIN)/2.
      BTA=B/(RP+RT)
      IF(RT.LT.RP) GO TO 1000
      IF(B.LT.(RT-RP)) GO TO 10
      P=.125*TSQR(UM*UN)*(1./UM-2.)*((1.-BTA)/UN)**2
      +- .125*(.5*TSQR(UM*UN)*(1./UM-2.)+1.)*((1.-BTA)/UN)**3
      F=.75*TSQR(1.-UN)*((1.-BTA)/UN)**2-.125*(3.*TSQR(1.-UN)-1.)
      +*((1.-BTA)/UN)**3
      GO TO 20
10  CONTINUE
      P=-1.
      F=1.
      GO TO 20
1000 CONTINUE
      IF(B.LT.(RP-RT)) GO TO 1010
      P=.125*TSQR(UN*UM)*(1./UM-2.)*((1.-BTA)/UN)**2
      +- .125*(.5*TSQR(UN/UM)*(1./UM-2.)-(TSQR(1.-UM*UM)/UN-1.))
      +*TSQR((2.-UM)*UM)/UM**3)*((1.-BTA)/UN)**3
      F=.75*TSQR(1.-UN)*((1.-BTA)/UN)**2
      +- .125*(3.*TSQR(1.-UN)/UM-(1.-(1.-UM*UM)**1.5)*(1.-(1.-UM)
      +**2)**.5/UM**3)*((1.-BTA)/UN)**3
      GO TO 20
1010 CONTINUE
      P=(TSQR(1.-UM*UM)/UN-1.)*TSQR(1.-(BTA/UN)**2)
      F=(1.-(1.-UM*UM)**1.5)*TSQR(1.-(BTA/UN)**2)
20  ROT=ABS(B-RP)
      ROP=ABS(B-RT)
      IF(ROT.GE.RT) ROT=RT
      IF(ROP.GT.RP) ROP=RP

```

```

C
C CLT IS LONGITUDINAL CHORD IN TARGET
C CLP IS LONGITUDINAL CHORD IN PROJECTILE
C
CLT=2.*TSQR(RT*RT-ROT*ROT)
CLP=2.*TSQR(RP*RP-ROP*ROP)
ATTEN=1.-.5*TEXP(-CLT/XAVE)-.5*TEXP(-CLP/XAVE)

C
C ABL HERE IS DUE TO SURFACE DEFORMATION ONLY
C
FAB=1.-F
IF(FAB .LT. 1.E-12) FAB=0.
C EB IS THE BINDING PER NUCLEON FOR THE ABLATION STAGE
EB = 10.
ABL=4.*3.1415*RP*RP*(1.+P-FAB**.6667)*.95/EB
RO=ABS(B-RT)

C
C FUDGE IS A SEMI-EMPRICAL CORRECTION TO DEFORMATION ENERGY
C
FUDGE = 1 + 5*F
IF ( RT.LT.RP.AND.B.LT.(RP-RT))FUDGE = FUDGE + 25*F*F
IF(RO.LT.RP)GO TO 333
RO=RP
333 AEX=1.3*CLP
BP=(RP*RP+B*B-RT*RT)/(2.*B+1.E-12)
IF (BP.LT.0.) BP=0.
IF(BP.GE.RP)BP=RP-1.E-12
CT=2.*TSQR(RP*RP-BP*BP)
IF(CT.LT.1.5)CT=1.5

C
C AEX IS THE F.S.I. ENERGY CORRECTION
C
AEX =AEX*(1.+(CT-1.5)/3.)

C
C USE NEXT LINE IF DON'T WANT ANY FSI
C ABL=ABL*FUDGE+AEX*FSI*0.0
C
ABL=ABL*FUDGE+AEX*FSI

C
C AFP IS THE FINAL FRAGMENT MASS
C
AFP=AP-(F*AP+ABL)*ATTEN
IIT=IIT+1
IF(AF.GE.AFP) GO TO 21
BMAX=B
ABRMAX=AP*F*ATTEN
ABLMAX=ABL*ATTEN
GO TO 199
21 CONTINUE
BMIN=B
ABLMIN=ABL*ATTEN
ABRMIN=AP*F*ATTEN
199 CONTINUE
IF(ABS(AF-AFP).LT..0001) GO TO 2000
GO TO 70

```

```

2000 CONTINUE
ABL=(ABLMIN+ABLMAX)/2.
B=(BMAX+BMIN)/2.
ABR=(ABRMAX+ABRMIN)/2.
IAF=AF+.51
ABLT(IAF,INUM,IN)=ABL
ABRT(IAF,INUM,IN)=ABR
BT(IAF,INUM,IN)=B
9003 CONTINUE
C
9002 CONTINUE
C
FSI=OFSI
AF=OAF
GO TO 1
ENTRY BSEEK(E,AP,RP,RT,AF,B,ABR,ABL)
FSI=0.
ES=E
GO TO 1
6996 FORMAT('YOUR VALUE OF AP IS TOO LARGE.')
6969 FORMAT('THE BT,ABRT,ABLT ARRAYS ARE DIMENSION TO 300.')
END
C
C*****
C
SUBROUTINE YIELDH(AP,ZP,AT,ZT,AF,ZF,E,QJ,SOG,SIGT)
C
C PURPOSE
C SUBROUTINE YIELDH CALCULATES FRAGMENTATION CROSS SEC. FOR SPECIFIC FRAGMENT
C
C DESCRIPTION OF PARAMETERS
C AP - MASS OF PROJECTILE
C ZP - CHARGE OF PROJECTILE
C AT - MASS OF TARGET
C ZT - CHARGE OF TARGET
C AF - MASS OF FRAGMENT
C ZF - CHARGE OF FRAGMENT
C E - LAB ENERGY MEV/NUCLEON
C QJ - OUTPUT; FRAGMENTATION CROSS SECTION
C SOG - OUTPUT; UNNORMALIZED FRAGMENTATION CROSS SECTION WITH FSI
C SIGT - OUTPUT; UNNORMALIZED FRAGMENTATION CROSS SECTION WITHOUT FSI
C
C USAGE
C CALL YIELDH(AP,ZP,AT,ZT,AF,ZF,E,QJ,SOG,SIGT)
C
QJ=0.
SOG=0.
SOGP=0.
EL=E
IF(AF.LE.4.) GO TO 4
CALL LIMIT(AF,ZF,ITOP,IBOTTOM)
IF((ZF.LT.IBOTTOM).AND.(ZF.GT.ITOP)) RETURN
CALL GEOFR(AP,ZP,AT,AF,ZF,ITOP,IBOTTOM,FNOR)
CALL GEODA(EL,AP,AT,AF,SIGT,SOG,ABR,ABL,SOGP,ABRP,ABRL)
QJ=FNOR*(SOG+SOGP)/2.

```

```

SOG =QJ
RETURN
4 CONTINUE
IF(AP.EQ.1.) QJ=45.*AT**.7
IF(ZF*AF.EQ.ZP*AP) RETURN
IF(ZF*AF.GT.8.) RETURN
IF(ZF.GT.AF) RETURN
IF(ZF*AF.EQ.4.) RETURN
IMAX=AP-1
C
DO 10 IA=1,IMAX
AAF=IA
CALL LIMIT(AAF,ZF,ITOP,IBOTTOM)
C
DO 11 IZ=IBOTTOM,ITOP
ZZF=IZ
CALL GEOFR(AP,ZP,AT,AAF,ZZF,ITOP,IBOTTOM,FNOR)
CALL GEODA(EL,AP,AT,AAF,SIGT,SOOG,ABR,ABL,SOOGP,ABRP,ABLP)
SOG=SOG+SOOG*FNOR
SOGP=SOGP+SOOGP*FNOR
ZBR=ABR*ZP/AP
ZBRP=ABRP*ZP/AP
ZBL=ZP-ZZF-ZBR
ZBLP=ZP-ZZF-ZBRP
IAAL=ABL/4.
IAALP=ABLP/4.
IZAL=ZBL/2.
IZALP=ZBLP/2.
NAL=IAAL
NALP=IAALP
IF(IAAL.GT.IZAL) NAL=IZAL
IF(IAALP.GT.IZALP) NALP=IZALP
AN=ABL-NAL*4.
ANP=ABLP-NALP*4.
ZN=ZBL-NAL*2.
ZNP=ZBLP-NALP*2.
IF(AF.EQ.4.)GO TO 12
IF(AF.EQ.1.) GO TO 13
GO TO 11
12 QJ=QJ+(NAL*SOOG*FNOR+NALP*SOOGP*FNOR)/2.
GO TO 11
13 CONTINUE
IF(ZF.EQ.1.) GO TO 14
QJ=QJ+((AN-ZN+ABR-ZBR)*SOOG*FNOR+(ANP-ZNP+ABRP-ZBRP)*SOOGP*FNOR)/2
GO TO 11
14 QJ=QJ+((ZN+ZBR)*SOOG*FNOR+(ZNP+ZBRP)*SOOGP*FNOR)/2.
11 CONTINUE
C
10 CONTINUE
C
RETURN
END
C
*****
C

```

```

SUBROUTINE LIMIT(AF,ZF,ITOP,IBOTTOM)
C
C PURPOSE
C USING RUDSTAM FORMULAS, FOR A GIVEN FRAGMENT MASS AF,
C SUBROUTINE LIMIT CALCULATES LOWER AND UPPER BOUND OF
C FRAGMENTATION ISOTOPES
C
C DESCRIPTION OF PARAMETERS
C AF - MASS OF FRAGMENT
C ZF - CHARGE OF FRAGMENT
C ITOP - OUTPUT; UPPER BOUD OF ISOTOPE
C IBOTTOM - OUTPUT; LOWER BOUND OF ISOTOPE
C
C USAGE
C CALL LIMIT(AF,ZF,ITOP,IBOTTOM)
C
C     DATA S,T/.486,3.8E-4/
C
C     ITOP=IFIX(S*AF-T*AF**2)+2
C     IBOTTOM=IFIX(S*AF-T*AF**2)-2
C     IF(IBOTTOM.LT.1) IBOTTOM=1
C     RETURN
C     END
C
C ****
C
C SUBROUTINE GEOFR(AP,ZP,AT,AF,ZF,ITOP,IBOTTOM,FNOR)
C
C PURPOSE
C SUBROUTINE GEOFR CALCULATES FNOR (NORMALIZATION) FACTOR FOR
C RUDSTAM CHARGE DISTRIBUTION
C
C DESCRIPTION OF PARAMETERS
C AP - MASS OF PROJECTILE
C ZP - CHARGE OF PROJECTILE
C AT - MASS OF TARGET
C AF - MASS OF FRAGMENT
C ZF - CHARGE OF FRAGMENT
C ITOP - UPPER BOUND OF ISOTOPE
C IBOTTOM - LOWER BOUND OF ISOTOPE
C FNOR - OUTPUT; NORMALIZATION CONSTANT
C
C USAGE
C CALL GEOFR(AP,ZP,AT,AF,ZF,ITOP,IBOTTOM,FNOR)
C
C     DATA D,S,T/.45,.486,3.8E-4/
C
C     R=11.8*AF**(-D)
C     F1=TEXP(-R*(ABS(ZF-S*AF+T*AF**2)**1.5))
C     FN=0.
C
C     DO 10 I=IBOTTOM,ITOP
C     FI=TEXP(-R*(ABS(I-S*AF+T*AF**2)**1.5))
C     FN=FN+FI
C 10 CONTINUE

```

```

C
FNOR=F1/FN
IF(AF.LT.AP-1.) RETURN
FNOR=0.
IF(ZF.EQ.ZP) FNOR=0.5
IF(ZF.EQ.ZP-1.) FNOR=0.5
IF(AF.GE.AP) FNOR=0.
IF(AF.EQ.8..AND.ZF.EQ.4.) FNOR=0.
IF(AF.EQ.5.) FNOR=0.
IF(AF.EQ.9..AND.ZF.EQ.5.) FNOR=0.
RETURN
END

C
C*****
C
C FUNCTION CROS(AT,Z,A,ENG)
C
C PURPOSE
C FUNCTION CROS IS RUDSTOM FIVE PARAMETER FORMULA DESCRIBING
C CROSS SEC. FOR PRODUCTION OF FRAGMENTS FROM PROTON NUCLEI BOMBARDED
C WITH HEAVY IONS
C
C DESCRIPTION OF PARAMETERS
C AT - MASS OF TARGET
C Z - CHARGE OF FRAGMENT
C A - MASS OF FRAGMENT
C ENG - LAB ENERGY MEV/NUCLEON
C
C USAGE
C RESULT = CROS(AT,Z,A,ENG)
REAL K,L
C
DATA D,E,G,H,K,L/11.8,.45,.25,.0074,1.73,.0071/
C
V=3.8E-4
S=0.486
R=D*A**(-E)
IF(ENG.LT.2100.) P=20.*((ENG**(-.77)))
IF(ENG.GE.2100.) P=0.056
IF(ENG.LT.240.) F2=TEXP(K-L*ENG)
IF(ENG.GE.240.) F2=1.
X2=F2
F1=TEXP(-G+H*AT)
X6=ABS(Z-S*A+V*A**2)
X5=TEXP(P*A-R*(X6**1.5))
X1=F1
X3=P*D**.66666*AT**(-2*E/3)
X4=1.79*(TEXP(P*AT)*(1.-2*E/(3*P*AT))-1+2*E/3+2*E/(3*P*AT))
CROS=X1*X2*X3*X5/X4
RETURN
END

C*****
C
FUNCTION TSQR(Y)

```

```

C PURPOSE
C TO ELIMINATE OVER/UNDER FLOW OF CPU IF SQRT IS USED
C
C USAGE
C RESULT = TSQR(Y)
C
C X=Y
C IF(X .LT. 1.E-37) X=1.E-37
C IF(X .GT. 1.E+37) X=1.E+37
C TSQR=SQRT(X)
C RETURN
C END
C
C ****
C
C FUNCTION TEXP(X)
C
C PURPOSE
C TO ELIMINATE OVER/UNDER FLOW OF CPU IF EXP IS USED
C
C RESULT = TEXP(X)
C IF(X .LT.-80.) X=-80.
C IF(X .GT. 80.) X=80.
C TEXP =EXP(X)
C END
C
C ****
C
C FUNCTION RADIUS (A)
C
C PURPOSE
C GIVES RADIUS OF A NUCLEUS
C
C DESCRIPTION OF PARAMETERS
C A - MASS NUMBER OF A NUCLEUS
C
C USAGE
C RESULT = RADIUS (A)
C
C DIMENSION NA(23),RMS(23)
C
C DATA NA/1,2,3,4,6,7,9,10,11,12,13,14,15,16,17,18,19,20,22,
C +23,24,25,26/
C DATA RMS/0.85,2.095,1.976,1.671,2.57,2.41,2.519,2.45,2.42,
C +2.471,2.440,2.58,2.611,2.730,2.662,2.727,2.900,3.040,2.969,2.94,
C +3.075,3.11,3.06/
C FACT = SQRT (5./3.)
C IA = A + 0.4
C RADIUS = FACT * ( 0.84* A**(1./3.) + 0.55 )
C
C DO 1 I =1,23
C IF ( IA .EQ. NA(I)) GO TO 2
C GO TO 1
C 2 RADIUS = FACT*RMS(I)
C 1 CONTINUE

```

C
RETURN
END

Appendix B

Sample Case: 2.1 GeV/Nucleon Carbon Fragmenting in Lead Targets

Appendix B is the complete listing of an interactive session for ^{12}C nuclei with incident kinetic energies of 2.1 GeV/nucleon fragmenting in a ^{208}Pb target.

INPUT PROJ. ENERGY IN MEV/NUCLEON ?

2100.000

INPUT CHARGE AND MASS OF PROJ. ?

6.000000 12.00000

INPUT CHARGE AND MASS OF TARGET ?

82.00000 208.0000

CHARGE (ZF)	MASS (AF)	NUC.FRAG. CRS. (MB)	E1+E2 FRAG CRS (MB)	(NUC+E1+E2) FRAG CRS (MB)
6	11	92.437592	48.158577	140.59618
6	10	0.77374035	0.00000000E+00	0.77374035
6	9	0.88362647E-02	0.00000000E+00	0.88362647E-02
6	8	0.60364164E-05	0.00000000E+00	0.60364164E-05
		-----	-----	-----
		93.220177	48.158577	TOTAL = 141.37875
<hr/>				
CHARGE (ZF)	MASS (AF)	NUC.FRAG. CRS. (MB)	E1+E2 FRAG CRS (MB)	(NUC+E1+E2) FRAG CRS (MB)
5	11	92.437592	72.237869	164.67546
5	10	119.35381	0.00000000E+00	119.35381
5	9	9.9387589	0.00000000E+00	9.9387589
5	8	0.41971810E-01	0.00000000E+00	0.41971810E-01
5	7	0.86885029E-02	0.00000000E+00	0.86885029E-02
5	6	0.10429365E-04	0.00000000E+00	0.10429365E-04
		-----	-----	-----
		221.78084	72.237869	TOTAL = 294.01868
<hr/>				
CHARGE (ZF)	MASS (AF)	NUC.FRAG. CRS. (MB)	E1+E2 FRAG CRS (MB)	(NUC+E1+E2) FRAG CRS (MB)
4	11	0.00000000E+00	0.00000000E+00	0.00000000E+00
4	10	7.2157054	0.00000000E+00	7.2157054
4	9	42.538204	0.00000000E+00	42.538204
4	8	9.0558434	0.00000000E+00	9.0558434
4	7	19.652256	0.00000000E+00	19.652256
4	6	0.21810415	0.00000000E+00	0.21810415
4	5	0.00000000E+00	0.00000000E+00	0.00000000E+00
4	4	0.00000000E+00	0.00000000E+00	0.00000000E+00
		-----	-----	-----
		78.680115	0.00000000E+00	TOTAL = 78.680115
<hr/>				

CHARGE (ZF)	MASS (AF)	NUC.FRAG. CRS. (MB)	E1+E2 FRAG CRS (MB)	(NUC+E1+E2) FRAG CRS (MB)
3	11	0.00000000E+00	0.00000000E+00	0.00000000E+00
3	10	0.55146748E-02	0.00000000E+00	0.55146748E-02
3	9	0.11067543	0.00000000E+00	0.11067543
3	8	0.27827829	0.00000000E+00	0.27827829
3	7	66.122002	0.00000000E+00	66.122002
3	6	79.498459	0.00000000E+00	79.498459
3	5	0.00000000E+00	0.00000000E+00	0.00000000E+00
3	4	0.00000000E+00	0.00000000E+00	0.00000000E+00
3	3	0.00000000E+00	0.00000000E+00	0.00000000E+00
3	2	0.00000000E+00	0.00000000E+00	0.00000000E+00
		-----	-----	-----
		146.01494	0.00000000E+00	TOTAL = 146.01494
<hr/>				
CHARGE (ZF)	MASS (AF)	NUC.FRAG. CRS. (MB)	E1+E2 FRAG CRS (MB)	(NUC+E1+E2) FRAG CRS (MB)
2	5	0.00000000E+00	0.00000000E+00	0.00000000E+00
2	4	254.08287	0.00000000E+00	254.08287
2	7	0.71365029E-01	0.00000000E+00	0.71365029E-01
2	6	1.0207902	0.00000000E+00	1.0207902
2	3	0.00000000E+00	0.00000000E+00	0.00000000E+00
2	2	0.00000000E+00	0.00000000E+00	0.00000000E+00
2	9	0.14907217E-04	0.00000000E+00	0.14907217E-04
2	8	0.87753448E-04	0.00000000E+00	0.87753448E-04
2	1	0.00000000E+00	0.00000000E+00	0.00000000E+00
		-----	-----	-----
		255.17514	0.00000000E+00	TOTAL = 255.17514
<hr/>				
CHARGE (ZF)	MASS (AF)	NUC.FRAG. CRS. (MB)	E1+E2 FRAG CRS (MB)	(NUC+E1+E2) FRAG CRS (MB)
1	5	0.00000000E+00	0.00000000E+00	0.00000000E+00
1	4	0.00000000E+00	0.00000000E+00	0.00000000E+00
1	1	11947.960	0.00000000E+00	11947.960
1	3	0.00000000E+00	0.00000000E+00	0.00000000E+00
1	2	0.00000000E+00	0.00000000E+00	0.00000000E+00
1	7	0.29637001E-05	0.00000000E+00	0.29637001E-05
1	6	0.92565700E-04	0.00000000E+00	0.92565700E-04
		-----	-----	-----
		11947.960	0.00000000E+00	TOTAL = 11947.960

REPORT DOCUMENTATION PAGE			Form Approved OMB No. 0704-0188
<p>Public reporting burden for this collection of information is estimated to average 1 hour per response, including the time for reviewing instructions, searching existing data sources, gathering and maintaining the data needed, and completing and reviewing the collection of information. Send comments regarding this burden estimate or any other aspect of this collection of information, including suggestions for reducing this burden, to Washington Headquarters Services, Directorate for Information Operations and Reports, 1215 Jefferson Davis Highway, Suite 1204, Arlington, VA 22202-4302, and to the Office of Management and Budget, Paperwork Reduction Project (0704-0188), Washington, DC 20503.</p>			
1. AGENCY USE ONLY (Leave blank)	2. REPORT DATE	3. REPORT TYPE AND DATES COVERED	
	May 1993	Technical Paper	
4. TITLE AND SUBTITLE HZEFRG1: An Energy-Dependent Semiempirical Nuclear Fragmentation Model		5. FUNDING NUMBERS WU 593-42-21-01	
6. AUTHOR(S) Lawrence W. Townsend, John W. Wilson, Ram K. Tripathi, John W. Norbury, Francis F. Badavi, and Ferdous Khan			
7. PERFORMING ORGANIZATION NAME(S) AND ADDRESS(ES) NASA Langley Research Center Hampton, VA 23681-0001		8. PERFORMING ORGANIZATION REPORT NUMBER L-17161	
9. SPONSORING/MONITORING AGENCY NAME(S) AND ADDRESS(ES) National Aeronautics and Space Administration Washington, DC 20546-0001		10. SPONSORING/MONITORING AGENCY REPORT NUMBER NASA TP-3310	
11. SUPPLEMENTARY NOTES Townsend and Wilson: Langley Research Center, Hampton, VA; Tripathi: ViGYAN, Inc., Hampton, VA; Norbury: Rider College, Lawrenceville, NJ; Badavi: Christopher Newport University, Newport News, VA; Khan: Old Dominion University, Norfolk, VA.			
12a. DISTRIBUTION/AVAILABILITY STATEMENT Unclassified–Unlimited Subject Category 73		12b. DISTRIBUTION CODE	
13. ABSTRACT (Maximum 200 words) Methods for calculating cross sections for the breakup of high-energy heavy ions by the combined nuclear and coulomb fields of the interacting nuclei are presented. The nuclear breakup contributions are estimated with an abrasion-ablation model of heavy ion fragmentation that includes an energy-dependent, mean free path. The electromagnetic dissociation contributions arising from the interacting coulomb fields are estimated by using Weizsäcker-Williams theory extended to include electric dipole and electric quadrupole contributions. The complete computer code that implements the model is included as an appendix. Extensive comparisons of cross section predictions with available experimental data are made.			
14. SUBJECT TERMS Nuclear reactions; Nuclear fragmentation model; Electromagnetic dissociation model		15. NUMBER OF PAGES 63	
		16. PRICE CODE A04	
17. SECURITY CLASSIFICATION OF REPORT Unclassified	18. SECURITY CLASSIFICATION OF THIS PAGE Unclassified	19. SECURITY CLASSIFICATION OF ABSTRACT	20. LIMITATION OF ABSTRACT